

# Insulin Delivery Using Dynamic Covalent Boronic Acid/Ester-Controlled Release

Łukasz Banach,\* George T. Williams, and John S. Fossey\*

The number of people affected by diabetes mellitus increases globally year on year. Elevated blood glucose levels may result from a lack of insulin to manage these levels and can, over a prolonged period, lead to serious repercussions. Diabetes mellitus patients must monitor and control their blood-glucose levels with invasive testing and often alongside administration of intravenous doses of insulin, which can often lead to suboptimal compliance. To mitigate these issues, “closed-loop” insulin delivery systems are deemed to be among superior options for rapid relief from the demanding and troublesome necessity of self-directed care. The reversible dynamic covalent chemistry of boronic acid derivatives and their competitive affinity to 1,2- and 1,3-diols (such as those present in saccharides) allows for the design and preparation of responsive self-regulated insulin delivery materials which respond to elevated and changing glucose levels. A range of meritorious and noteworthy contributions in the domain of boron-mediated insulin delivery materials is surveyed, and providing a multidisciplinary context in the realisation of the ambitious goal of ultimately addressing the desire to furnish glucose-responsive insulin delivery materials through innovative synthesis and rigorous testing is targeted.

for adequate regulation of blood glucose, requires frequent monitoring of blood glucose levels by finger-prick tests and the subsequent administration of insulin by injection.<sup>[2]</sup> Such a regime is demanding and can lead to poor compliance, resulting in imbalanced blood glucose, in turn resulting in further complications and increased cost of treatment.<sup>[2a,3]</sup> Insulin delivery materials are one strategy envisioned to overcome the burden of such a frequent and invasive regime.<sup>[4]</sup> While not completely removing the need for invasive interventions, materials that function as insulin reservoirs may act as an “artificial pancreas,” discharging insulin inside a patient’s body in response to elevated glucose levels then ceasing release under normoglycemic conditions, i.e., closed-loop systems.<sup>[5]</sup> While such systems must be replenished at regular intervals, they remove the worry of monitoring and reactive treatment scenarios. The development of such systems has seen increased attention in recent years, as the best hope for a rapid increase in quality of

## 1. Introduction

Diabetes mellitus is a chronic disease that, if not treated well, leads to serious health degeneration which can manifest in loss of sight, stroke, heart attack and other severe consequences. The number of people suffering from diabetes mellitus is increasing, and the search for improved diabetes treatments and management strategies has never been more urgent.<sup>[1]</sup> The most common management strategy in therapy for patients with type 1 diabetes, those whose pancreas is not producing enough insulin

life lies with advanced management strategies in the intervening years before a true cure for diabetes is hopefully realised. The intrinsic ability of boronic acid derivatives to reversibly react with 1,2 and 1,3-diols to form boronic esters, enables boronic acid derivatives to reversibly and covalently bind with saccharides, making them among the most promising platforms for the innovation and discovery of materials capable of responding to fluctuations in blood glucose levels. Recent advances in combining functional and soft materials research with the reversible covalent supramolecular chemistry of boronic acid derivatives, offer the potential for the realisation of a closed-loop insulin delivery without the need of external accoutrements.

Alongside the herculean effort put into the development of new drugs, parallel research into materials capable of controlled release, in order to find the more effective administration methods is also ongoing;<sup>[6]</sup> the mechanism delivery of a drug cannot be underestimated in realising its full potential and efficacy.<sup>[7]</sup> Optimal delivery regimes can mitigate disadvantages such as short lifetimes of biologically active substances due to metabolic transformations, low cellular uptake or poor drug distribution.<sup>[8]</sup> Drug delivery materials aim to overcome these problems, typically by encapsulating a drug in order to store, protect, distribute and subsequently release it. The potential of the relatively new area of controlled release is evidenced by an increasing number of drug delivery systems approved for clinical use,<sup>[9]</sup> utilising

Ł. Banach<sup>[†]</sup>, G. T. Williams, J. S. Fossey  
School of Chemistry  
University of Birmingham  
Edgbaston, Birmingham, West Midlands B15 2TT, UK  
E-mail: lukasz.banach@amu.edu.pl; j.s.fossey@bham.ac.uk

 The ORCID identification number(s) for the author(s) of this article can be found under <https://doi.org/10.1002/adtp.202100118>

<sup>[†]</sup>Present address: Centre for Advanced Technologies, Adam Mickiewicz University, Poznań 61–614, Poland

© 2021 The Authors. *Advanced Therapeutics* published by Wiley-VCH GmbH. This is an open access article under the terms of the Creative Commons Attribution License, which permits use, distribution and reproduction in any medium, provided the original work is properly cited.

DOI: 10.1002/adtp.202100118

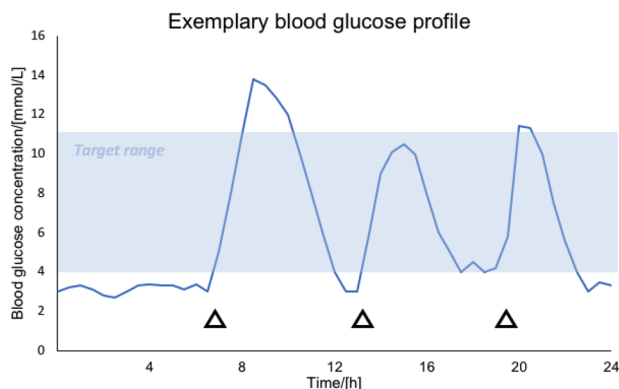
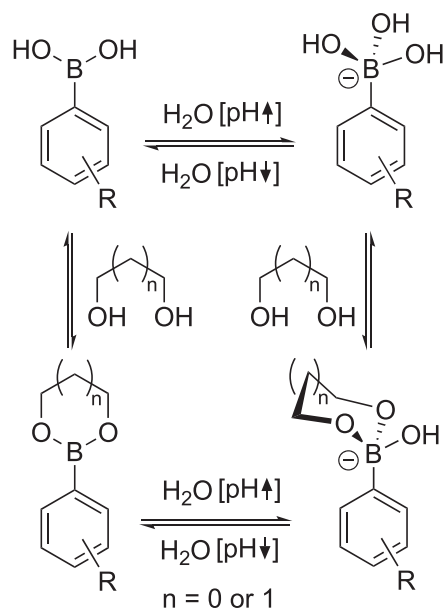


**Figure 1.** Exemplary blood glucose profile chart. Blue region denotes “extended target range” of blood glucose concentration [mmol L<sup>-1</sup>], while fasting 4–7 mmol L<sup>-1</sup> is recommended, 2 h after meals up to 11 mmol L<sup>-1</sup>. Symbol Δ denotes meal intake.<sup>[13]</sup>

materials that range from hydrogels to gated porous nanoparticles, with numerous release mechanisms and supporting mathematical models having been explored.<sup>[10]</sup> Beyond diffusion-mediated release are the designed, responsive drug-delivery materials that release their cargo in response to specific stimuli, to control and cease liberation of a payload in response to the drug delivery environment. An obvious trigger for such materials in the treatment of diabetes is an elevated level of the saccharide, glucose, in the blood. Blood glucose levels change over the course of a day, and there is a clear correlation with meal intake, often requiring diabetics to inject themselves with insulin shortly after meals, often preceded by invasive monitoring.<sup>[2a,11]</sup> Not only is this inconvenient, error could lead to mistakes resulting in hypoglycemia with serious medical consequences.<sup>[1c,12]</sup> An ideal smart glucose-responsive insulin-delivery material would release its cargo in such way to maintain healthy blood glucose levels between  $4 \times 10^{-3}$  and  $11 \times 10^{-3}$  M, avoiding high-glucose spikes while not attenuating glucose levels too much (**Figure 1**).<sup>[13]</sup>

Reports dating back to the 1950s first revealed the ability of aryl boronic acid derivatives to reversibly form cyclic boronic esters upon complexation with 1,2- or 1,3-diols.<sup>[14]</sup> This reversibility makes aryl boronic ester derivatives ideal candidates for the construction of saccharide responsive materials, where the diol motifs within the saccharide become competitive binders for the integral boronic acids.<sup>[15]</sup> The planar sp<sup>2</sup> hybridised boron of an aryl boronic acid is a Lewis acidic center that in an aqueous environment is coordinated by water, which in turn facilitates liberation of a proton generating the corresponding boronate anion. While the formation of neutral boronic esters is indeed possible, boronate anions are more prone to diol complexation than their neutral counterparts at physiological pH (**Scheme 1**). The pH of the aqueous media and the pK<sub>a</sub> of the boronic acid play a significant role in the propensity for boronate ester formation, namely if the pH is below the pK<sub>a</sub> then boronate ester formation is disfavored.<sup>[16]</sup>

The diol-binding properties of aryl boronic acids may be tuned through the modification of the electronic properties of their aryl ring or by employing ligating pendant substituents *ortho* to the boron-containing substituent, such as an *N,N*-dimethylaminomethyl group (Wulff-type complexes),<sup>[17]</sup> which



**Scheme 1.** pH-Dependent equilibria of aryl boronic acid and boronate derivatives in aqueous media: boronic acid derivatives tend to undergo condensation reactions with 1,2- and 1,3-diols to form the corresponding boronic/boronate esters.

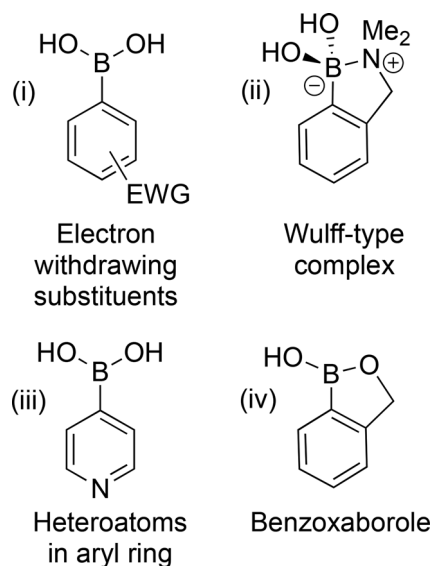


**Figure 2.** Boronic acid derivatives with superior diol-binding properties, exhibiting the ability to undergo diol complexation at physiological pH. i) Aryl boronic acids featuring electron withdrawing groups, which increase the Lewis acidity of the boron. ii) Wulff-type complexes featuring an amino-group capable of coordinating the boron. iii) Aryl boronic acids featuring heteroatoms within the aromatic ring. iv) Benzoxaboroles which offer increased propensity to form boronate anions.

have a pK<sub>a</sub> significantly lower than their phenyl-derived analogs (**Figure 2**).<sup>[18]</sup> This tunability makes boronic acid derivatives versatile components for the development of saccharide responsive materials.<sup>[19]</sup> While nature provides a wide range of biomolecules that can be used to create drug delivery systems with stimuli selectivity (i.e., enzymes),<sup>[20]</sup> there are some drawbacks. The

possibility for an immunogenic response, coupled with their low stability (tendency for denaturation), makes the storage and processing of such materials problematic. On the other hand, synthetic chemical (as opposed to biopolymer-derived) materials confer advantages ready for exploitation.<sup>[21]</sup> These systems can be free of such limitations but rarely offer such exquisite selectivity profiles. While aryl boronic acid derivatives may often present some synthetic challenges,<sup>[22]</sup> they form a large component of the efforts toward selective, responsive, delivery materials research,<sup>[23]</sup> as this review aims to demonstrate.

Owing to the fast moving and rapidly expanding research base in the area of boron-diol-mediated controlled release, this review surveys contributions primarily made over the past five years. The focus is on insulin delivery systems that make use of the dynamic reversible covalent chemistry of principally aryl boronic acid derivatives targeted toward the treatment of diabetes mellitus.

## 2. Diabetes Mellitus

Diabetes mellitus, often referred to as diabetes, is a chronic disease characterised by high blood glucose levels (i.e., hyperglycemia), which is defined as a blood glucose concentration at  $>2.0 \text{ g L}^{-1}$  (or  $11.1 \times 10^{-3} \text{ M}$ ) over a prolonged time.<sup>[12,24]</sup> Diabetes is a global condition which is increasing in prevalence; 422 million people were affected in 2016 which is predicted to rise to 642 million in the year 2040.<sup>[25]</sup> Diabetes, together with cancer and cardiovascular diseases, is a major endangerment to human health and is of growing significance. In general, elevated glucose levels in diabetic patients are the result of either insufficient production of insulin (type 1 diabetes) or ineffective response to insulin (type 2 diabetes).<sup>[26]</sup>

Insulin was first isolated and identified by Banting and Best in 1922.<sup>[27]</sup> It is a peptidic hormone consisting of 51 amino acids arranged into two polypeptide chains which are connected by two disulphide bridges. In the presence of zinc ions it often adopts a hexameric form.<sup>[28]</sup> Insulin is secreted by  $\beta$ -cells in pancreas regions known as the Islets of Langerhans.<sup>[29]</sup> The main function of insulin is the regulation of metabolism of carbohydrates and lipids, but it also suppresses protein breakdown and influences other physiological processes.<sup>[30]</sup> This gives it applications outside of diabetes treatment, e.g., in wound healing, treating poisoning with calcium channel blockers or in anti-ageing therapy.<sup>[31]</sup> Increased secretion of insulin is a natural response to elevated blood glucose levels, which triggers cells in the body (particularly in the liver and muscles) to uptake and store glucose in the form of glycogen.<sup>[32]</sup> It is the disruption of this process that results in diabetes.

There are two main types of diabetes. Type 1 diabetes, known also as Juvenile Diabetes, has its onset primarily in children and is a result of autoimmune damage of  $\beta$ -cells in the Islets of Langerhans that leads to insulin deficiency.<sup>[2a]</sup> Conversely, type 2 diabetes afflicts mainly adults and is a state of systemic resistance to insulin, despite its normal production by  $\beta$ -cells.<sup>[33]</sup> A third type of diabetes is gestational diabetes, which is a transient resistance to insulin developing at times during pregnancy.<sup>[34]</sup> Moreover, cases are known where diabetes and insulin deficiency can arise as a result of disease (e.g., pancreatic cancer), infection or side effects of used medication.<sup>[1b]</sup>

A persistent state of elevated blood glucose levels leads to a series of severe complications, including cardiovascular disease, nephropathy, ketoacidosis, stroke, nerve damage and retinopathy.<sup>[12]</sup> Diabetes is also responsible for elevation of oxidative stress, thus generated reactive oxygen species contribute to these secondary diabetic complications.<sup>[35]</sup> People suffering from type 1 diabetes are treated almost exclusively with exogenous insulin, while type 2 diabetics may be prescribed small molecule drugs and advised to make lifestyle changes.<sup>[33]</sup> However, advanced type 2 diabetes can lead to insulin deficiency and insulin has to be introduced to the therapeutic regime.<sup>[36]</sup>

As discussed, current diabetes treatment requires patients to monitor their blood sugar concentration, most often by finger prick tests, calculate required insulin dosage and self-administer by subcutaneous injection several times a day (so called “open loop” treatment). Multiple types of insulin injections a day are often required for effective treatment. For mealtimes rapid acting insulins (aspart, glulisine, and lispro) or intermediate acting insulins (neutral protamine, Hagedorn, or Lente) are used, while long acting insulins (glargine or detemir) are applied in order to meet the required basal level of insulin throughout the day.<sup>[11,37]</sup> In order to achieve best therapeutic outcomes this strict regime has to be carefully followed.<sup>[36]</sup> High patient burden results from the need for multiple doses each day, the need to match insulin doses to carbohydrate counts at mealtimes, and also the timing of insulin administration at meals (rapid-acting insulins are recommended 15 min before a meal).<sup>[38]</sup> High levels of insulin can lead to hypoglycemia that can result in coma or even death.<sup>[39]</sup> Furthermore, frequent insulin injections and blood glucose self-monitoring can be inconvenient in social situations and cause physical pain, skin necrosis, local infections and nerve damage, further reducing patient compliance.<sup>[1b,24]</sup>

These drawbacks attracted the attention of scientists working on diabetes treatment and inspired different research approaches from engineering of insulin<sup>[40]</sup> toward designing other means of delivery. An alternative approach is the use of a continuous subcutaneous insulin infusion pump. As well as the high cost of such devices it has been shown that incidents of insulin pump malfunction increases frequency of ketoacidosis.<sup>[41]</sup> Originally, these pumps consisted of an insulin reservoir and pump which was worn either on a belt or kept in a pocket, with a tube running into an injection site; this tube could be over a meter in length, presenting obvious inconvenience.<sup>[42]</sup> Recent developments include patch pumps. These are adhesive reservoir and pump combinations that sit near the subcutaneous delivery site, removing inconvenience and offering greater discretion, making them more popular in patient surveys.<sup>[43]</sup> Alternative noninvasive routes, such as nasal,<sup>[44]</sup> oral,<sup>[45]</sup> pulmonary,<sup>[46]</sup> and transdermal insulin delivery systems<sup>[47]</sup> have gained attention. However, the intrinsic properties of insulin, such as its poor permeation of biological membranes, high molecular weight and ease of deactivation, limits these noninvasive administration methods. Nevertheless, such an approach would still have to rely on active monitoring of blood glucose levels by the patient in order to determine whether insulin is required. Therefore, further work into the development of self-regulating insulin release strategies is required.

Oral delivery of drugs is preferable to either subcutaneous or intravenous administration; its ease and lack of invasiveness prevents the need for trained personnel, and patient preference across a range of other disease treatments tends toward oral administration being preferred.<sup>[48]</sup> Unfortunately, the peptidic nature of insulin means that it is metabolised by the digestive track if ingested unprotected, and has a poor diffusion rate through the mucosal layer.<sup>[49]</sup> A recent review by Xiao et al. outlines the strides that have been taken toward making these technologies a reality. While orally available insulin would begin to address the inconvenience of regular injections, patients would still be required to maintain vigilance of their blood glucose levels, and as such we believe that the future of transformative care is in the development of closed-loop delivery materials.

In an attempt to develop external “closed-loop” insulin delivery systems, there have been attempts to combine continuous glucose monitoring (CGM) and insulin pump technologies. These systems use a CGM to automatically detect blood glucose level (BGL) fluctuations, and an algorithm then alters insulin administration via an insulin pump in response. One early effort to produce such systems was the “Medtronic MiniMed 640G with Smart guard.” This device would predict hypoglycemic events and suspend insulin delivery, significantly reducing these events compared to the control group.<sup>[50]</sup> The first commercially available closed-loop system capable of reacting to both hyper- and hypoglycemic events was the Medtronic 670G.<sup>[50b,51]</sup> This, and all other systems currently commercially available, are known as hybrid closed-loop systems. This means that they still require the patient to manually enter carbohydrate levels that they plan to consume. Unfortunately, the expense of these systems has rendered their use minimal in clinical practice. Indeed, the expense of such systems has led to a movement toward the use of home-made or do-it-yourself artificial pancreas-type systems, with guides and software available online.<sup>[52]</sup> True closed-loop systems have yet to be made commercially available. Indeed, the nature of the subcutaneous delivery system means that a long road may need to be followed to realise a true artificial pancreas. Researchers have made many efforts to minimise the issues through the use of insulin releasing materials, which removes the requirement for the external pump and the CGM.

Such insulin releasing constructs are often called “intelligent” or “smart” with their ultimate goal being to serve as an artificial or pseudo pancreas. That is a system composed of insulin loaded into an appropriate abiotic carrier that would be regulated by endogenous feedback mechanism in which this hormone would be released as a response to a rise in blood glucose levels (“closed-loop”). Despite ruling out the necessity for frequent insulin injections and invasive monitoring, this type of material would also benefit diabetic patients by making the therapy truly adjusted to their blood glucose level in real time. However, reaching this long-standing goal represents a great challenge. Materials for “closed-loop” diabetes insulin replacement therapy must be sensitive specifically to glucose, with both a quick response to elevation in blood glucose levels and the ability to promptly cease insulin release to prevent overdose. As diabetes therapy is a life-long process, the desired system must be convenient and practical in application over the years, and possess physiological properties like good clearance kinetics, without triggering inflamma-

tion and immune response. These and other requirements must be met to develop functional and applicable glucose-responsive insulin delivery system.

### 3. General Modes of Operation in Glucose-Responsive Materials for Insulin Release

Efforts toward creating such synthetic pancreas are underway, and have been for about the last forty years.<sup>[53]</sup> Development of smart insulin delivery materials has also become a strategic priority of Juvenile Diabetes Research Fund (JDRF) and other institutions supporting this cause.<sup>[54]</sup> Generally, three different approaches have been used in the development of these materials in regard to glucose sensing that later induces insulin release.<sup>[20]</sup> One common strategy is incorporation of an enzyme–glucose oxidase (GOx) into pH-responsive material. GOx catalyze oxidation of glucose with molecular oxygen in water to produce gluconic acid and H<sub>2</sub>O<sub>2</sub>.<sup>[55]</sup> As GOx converts glucose into gluconic acid it induces a change in the pH of microenvironment of the material, causing a structural change of the GOx-incorporated carrier allowing for insulin release.<sup>[56]</sup> While GOx is very selective for glucose, its activity is strongly dependent on its microenvironment. Accumulation of hydrogen peroxide and depletion of oxygen are an effect of GOx’s activity, such changes can intern have a deleterious effect on the efficiency of GOx.<sup>[55]</sup> This has been mitigated by incorporation of other components capable of transforming of hydrogen peroxide back into oxygen and water, i.e., other enzyme–catalases or nanoparticles of cerium or manganese oxides.<sup>[55c,57]</sup> Gu and co-workers turned GOx induced hypoxia into a factor further strengthening the responsiveness of insulin releasing material. They modified water soluble hyaluronic acid with 2-nitroimidazole units which were responsible for hydrophobic properties of overall amphiphilic vesicle forming material. That is until GOx consumed oxygen for reaction with glucose yielding conditions in with bio-reduction took place transforming mentioned moieties into hydrophilic 2-aminoimidazole units leading to dissociation and liberation of insulin.<sup>[58]</sup> There are also examples of drug delivery platforms using both GOx and boronates together.<sup>[20]</sup> However, instead of being dependent on pH changes, the cargo is released due to irreversible oxidation of boronates to alcohols or phenols by H<sub>2</sub>O<sub>2</sub>, produced in the reaction of GOx with glucose. As boronates in these types of materials serve as linking units holding the material’s network together, their oxidation causes breakage of the link and the overall structure, consequently discharging an insulin cargo. Since this is not a dynamic or reversible transformation, these types of materials are outside of the scope of the present review. Another approach for endowing an insulin delivery material with glucose sensitivity is the use of concanavalin A (ConA), a plant lectin protein possessing capacity for binding glucose with high affinity.<sup>[59]</sup> ConA is known to form tetramers that are capable of binding four glucose molecules. Hence, ConA often serves as an exquisite recognition motif in glucose sensitive materials for insulin delivery where it can be deployed as a crosslinker of molecules with pendant saccharide units such that competitive glucose binding disrupts the network causing cargo liberation.<sup>[60]</sup> ConA can also bind saccharide-modified insulin that is later detached due to substitution with glucose. That is the mode of operation of the first reported system for

glucose-sensitive insulin release.<sup>[53]</sup> Despite high sensitivity for glucose GOx- and ConA-based materials for insulin release display some disadvantages. One such disadvantage being the fact that these proteins show immunogenic properties.<sup>[61]</sup> Moreover, preparation and processing of GOx- or ConA-containing materials is limited in respect of possible protein denaturing. Long-term storage difficulties due to instability of GOx and ConA also can be an issue. GOx and ConA based insulin release systems have been expertly reviewed elsewhere, to where readers are directed for more details.<sup>[4a,20,62]</sup> Arylboronic acids, a class of compounds capable of reversibly binding to glucose and other saccharides, are free of these limitations and synthetically tractable yet are relatively underutilised in a clinical setting, however they are emerging as a class of compounds subject to intense research in the challenging area of “closed-loop” responsive/controlled insulin therapy and are thus the subject of this review.<sup>[16,62e,63]</sup> These systems, when compared to protein/enzyme based materials, offer greater potential for versatile design. Their preparation can be conducted in a wider range of conditions as they are more stable, thus are also easier to process and store. Versatile design of materials based on the chemistry of arylboronic acids is exemplified by the fact that they are known in forms of gels,<sup>[64]</sup> vesicles,<sup>[65]</sup> and nanoparticles<sup>[66]</sup> amongst other materials and particles.<sup>[67]</sup>

#### 4. Boronic Acid Materials for Glucose-Responsive Insulin Release

The potential of arylboronic acids in the preparation of materials for insulin delivery was first recognised in 1991 by Kataoka and co-workers who obtained a polymer based gel that undergoes a gel–sol transition upon treatment with glucose.<sup>[68]</sup> Soon after, the concept of utilising the glucose-responsiveness of arylboronic acid containing co-polymers for triggered insulin releasing gels was realised concurrently by them and Seo Young and co-workers.<sup>[69]</sup> These pioneering findings established the foundation for further research in the area of arylboronic acid-based glucose-responsive materials for controlled insulin release. Subsequent efforts probed aspects, including adjusting operational pH,<sup>[70]</sup> endowing materials with thermo-responsiveness<sup>[71]</sup> or using formulations other than gels.<sup>[72]</sup> It is worth noting that the conducted studies often employed modified versions of insulin, e.g., labeled with fluorescein, for ease of determination of release process, or insulin functionalised with saccharide moieties in systems where its release was based on competition with glucose.<sup>[73]</sup> Herein we offer a detailed account of recent advances within this field, focusing not only on the physiochemical and biological efficacy of these systems, but also the syntheses of glucose-responsive materials in a variety of forms.

#### 5. Gels and Polymer Network Materials

Gels are essentially amorphous materials often composed of inter-spaced chains thus forming a network structure with “jelly-like” mechanical properties. Among them are hydrogels which are systems capable of retaining relatively large amounts of water without dispersing in aqueous environment.<sup>[74]</sup> Such materials have been studied for use as drug delivery reservoirs, owing to their

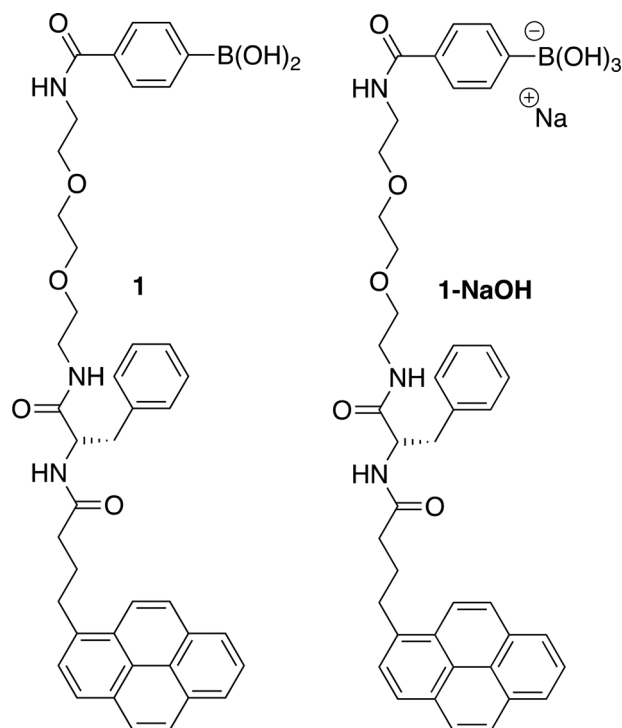


**Figure 3.** Gelators **1** and **1-NaOH** for obtaining low molecular weight hydrogels as synthesised by Das and co-workers,<sup>[76]</sup> featuring a carbamoylphenylboronic acid unit to imbue it with glucose sensitivity, and a pyrene group to enable  $\pi$ -stacking and acts as a fluorescent reporter.

high biocompatibility, adjustable pore size and ease of synthesis. However, they also face challenges when considering nonspecific release of compounds and administration. Since diabetes is a long-term disease it is essential that gels used for this purpose are injectable, rather than requiring a more invasive implantation protocol.<sup>[75]</sup>

The first low molecular weight hydrogel displaying glucose-responsive release of insulin, as well as glucose sensing properties, was obtained by Das and co-workers.<sup>[76]</sup> The authors believed that hydrogels would be more susceptible to external stimuli than polymeric gels.<sup>[77]</sup> The authors carefully designed a gelator molecule taking into account hydrogen bonding and hydrophilic-lipophilic balance while maintaining glucose sensitivity. Compound **1** (**Figure 3**) utilised a pyrene unit as both a reporter moiety and a platform for  $\pi$ – $\pi$  stacking interactions, amides were incorporated to enable hydrogen bonding, as both types of interactions facilitate the gelation processes. A spacer derived from 1,8-diamino-3,6-dioxaoctane was integrated to provide appropriate hydrophilicity to the structure. Finally, a 4-carbamoylphenylboronic acid derived fragment is utilised as the glucose sensitive unit. The authors found that **1** shows water imbibing properties forming hydrogels in a pH range from 8 to 12, which is unfortunately above the physiologically most relevant pH value (7.4). Not discouraged, Das and co-workers prepared the corresponding sodium salt **1-NaOH** (**Figure 1**), and found that it presented efficient hydrogelation ability at pH 7.4 with a minimum gelation concentration of 5 mg mL<sup>-1</sup> (6.6  $\mu$ mol mL<sup>-1</sup>).

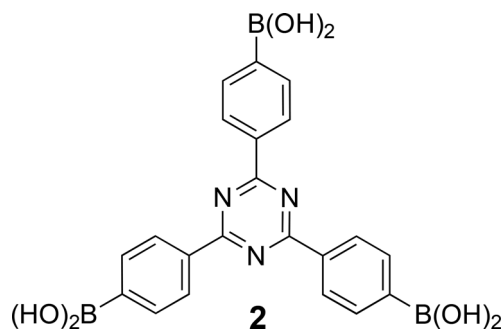


**Figure 4.** Tris-boronic acid gelator as synthesised by Sarkar and Dastidar,<sup>[64b]</sup> with a rigid structure to enable the formation of “honeycomb” gels.

The obtained hydrogel and its response to glucose was thoroughly characterised by transmission electron microscopy (TEM) and scanning electron microscopy (SEM), as well as a series of FTIR, UV-vis, fluorescence and circular dichroism (CD) spectroscopic studies. All this allowed the authors to characterise the entangled fibrillary structure of a hydrogel network with  $\alpha$ -helical aggregates, as well as to investigate key interactions for gel formation to be hydrogen bonding between the carbonyl and amide NH and also  $\pi$ - $\pi$  stacking of pyrene. Fluorescence studies of **1-NaOH** were conducted in dilute ( $0.05 \text{ mg mL}^{-1}$ ) and concentrated ( $0.5 \text{ mg mL}^{-1}$ ) solutions, and showed that binding glucose causes increase in emission intensity even for minute quantities of analyte, with saturation of  $0.6 \times 10^{-3}$  and  $1.2 \times 10^{-3} \text{ M}$  of glucose respectively. Authors found that upon contact with glucose, the gel's fibers increased in diameter with macroscale swelling of the hydrogel reaching 500% within 10 h in  $12 \times 10^{-3} \text{ M}$  glucose solution. The authors thus investigated the insulin loading capacity for the hydrogel obtained from **1-NaOH** at minimum gelation concentration, which was found to be about 3%, but the authors noted that this could be improved by increasing gelator concentration. Release studies were conducted using hydrogels with an insulin content of 1%. In phosphate-buffered saline (PBS) without glucose  $\approx 10\%$  of insulin was released within 60 h, with a plateau being reached after 16 h. At normoglycemic glucose concentration ( $6 \times 10^{-3} \text{ M}$ ) about 60% of insulin was released in 60 h, however a plateau is not reached in that time. On exposure to hyperglycemic glucose concentrations ( $12 \times 10^{-3}$  and  $18 \times 10^{-3} \text{ M}$ ),  $\approx 80\%$  of insulin was released within 60 h reaching plateau after 48 h and showing more rapid rate than for normoglycemic glucose concentration. The storage/release of large structures such as insulin may change their structure, rendering them inactive; however investigations using CD proved that the released insulin remains in an active form. Moreover, authors found that gels obtained by them show good thixotropic properties (making them suitable injectable materials), and cell viability studies using HeLa cells in MTT-based assays proved good biocompatibility of studied material.

Recently, Sarkar and Dastidar reported a tris-boronic acid (**2**) (**Figure 4**), able to form hydrogels in DMSO/water (1:9 v/v) mixture.<sup>[64b]</sup> This compound was designed to utilise the ability of boronic groups to dimerise (or oligomerise) through hydrogen bonding. The tris-boronic acid drove self-assembly into honeycomb structure, forming a network that was able to occlude sol-

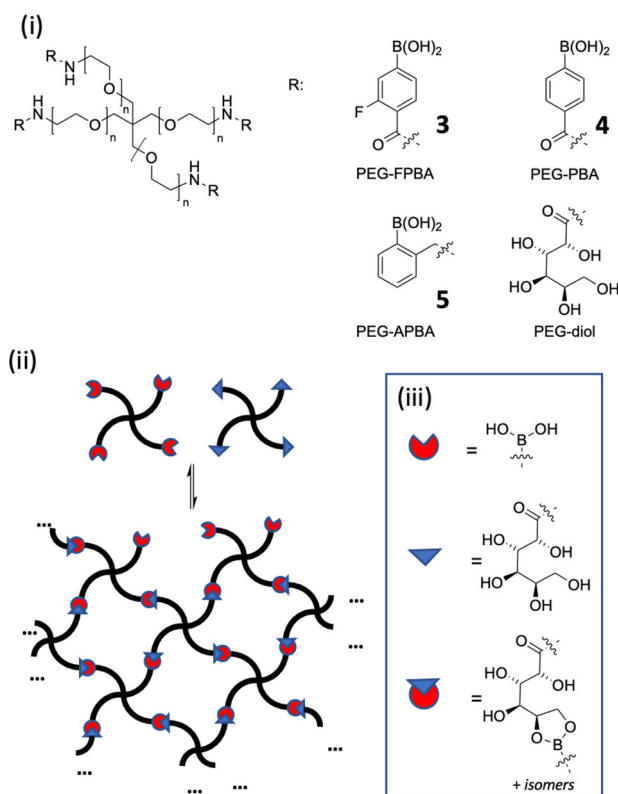


**Figure 5.** Illustration of Anderson and co-workers' hydrogel network.<sup>[78]</sup> i) The structure of the boronic acid and sugar based four-armed peg building blocks. ii) A schematic representation of the peg-diol interactions that forms the hydrogel network. iii) Key: Red cut out circles represent boronic acid groups. Blue triangles represent diol containing saccharide units. Blue triangles in red cut out circles indicate boronic acid complexed with diol within the saccharide unit.

vent molecules, resulting in a gel. The authors demonstrated that insulin can be entrapped in the hydrogel structure, and subsequently investigated its glucose-dependent release at physiological pH (7.4). On exposure to  $5 \times 10^{-3} \text{ M}$  glucose  $\approx 40\%$  of insulin was released, while at  $10 \times 10^{-3} \text{ M}$  it was almost 60% and at  $20 \times 10^{-3} \text{ M}$  glucose about 75% of entrapped insulin was released after 30 h. Analysis using CD indicated the structure of the insulin was conserved.

Anderson and co-workers presented an approach utilizing dynamic covalent chemistry in the preparation of hydrogels from macromonomers derived from four-arm polyethylene glycol amine (PEG-NH<sub>2</sub>).<sup>[78]</sup> Amino-groups in starting substrate were functionalised either with a saccharide unit (containing diols) or with an arylboronic acid unit (**Figure 5**). Boronic acid derived structures included 4-carbamoyl-3-fluorophenylboronic acid (**3**), 4-carbamoylphenylboronic acid (**4**) and 2-aminomethylboronic acid (**5**) (**Figure 5**). The authors envisioned hydrogels obtained from these components would exhibit shear-thinning and self-healing properties along with pH- and saccharide-responsiveness, due to the dynamic nature of the boronic acid-diol bonds. Among the obtained materials, the material based on **3** showed optimal mechanical properties and pH-response, therefore it was used for further investigations related to protein encapsulation and release. Three model proteins were chosen:

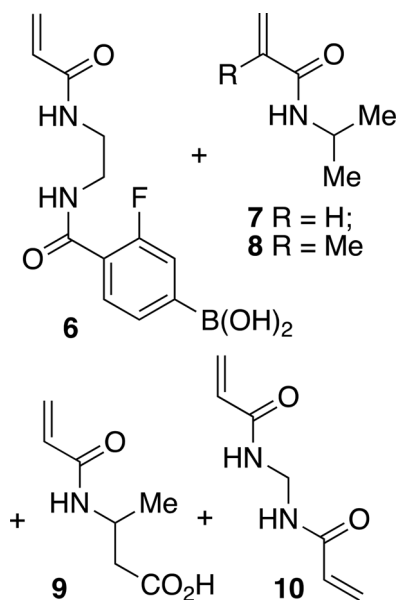


**Figure 6.** Acrylamide monomers used for terpolymer synthesis: 4-(2-Acrylamidoethylcarbamoyl)-3-fluorophenylboronic (**6**) to yield glucose responsiveness, 2-carboxyisopropylacrylamide (**7**) to maintain solubility, *N*-isopropylacrylamide (**8**) or *N*-isopropylmethacrylamide (**9**) used to imbue the material with temperature responsiveness, and *N,N'*-methylenebisacrylamide (**10**) to act as a crosslinker.

insulin labeled with fluorescein isothiocyanate (FITC), bovine serum albumin-FITC and Alexa Fluor-conjugated immunoglobulin G. Release of all proteins was tested first without glucose stimuli in single cargo loaded hydrogels. Results showed that full release of insulin was achieved within 150 h, while the two other proteins only displayed partial release. As insulin is the smallest among tested cargos, the authors concluded that this was due to the “mesh size” of the hydrogel network being too large, hence not displaying a high degree of glucose dependent controlled release.

In recent years Matsumoto et al. published follow-on results of their investigation on fully synthetic co-polymeric gels based on *N*-substituted poly(acrylamide) and its derivatives bearing fluoro-substituted arylboronic acid functionality.<sup>[70,79]</sup> In one contribution, the authors concentrated on a phenomenon of “skin layer” formation<sup>[80]</sup> on a surface of glucose-responsive hydrogels when glucose concentration decreases in the medium.<sup>[79a]</sup> That phenomenon is essentially gel dehydration in the surface region resulting from a change in counterionic osmotic pressure upon transformation of the negatively charged borate to neutral species which occurs as concentration decreases in the bulk hydrogel. Matsumoto et al. sought a chance for using this process to improve control over insulin release, hoping to use this effect to give the ability to cease insulin release as glucose concentration diminishes. Owing to its influence on this process, the effect of temperature was a key consideration in the selection of monomers for this gel-forming terpolymer synthesis (**Figure 6**). The authors sought to include a maximal amount of 4-(2-acrylamidoethylcarbamoyl)-3-fluorophenylboronic (**6**) acid in order to minimise temperature dependent gel-hydration/dehydration, while com-

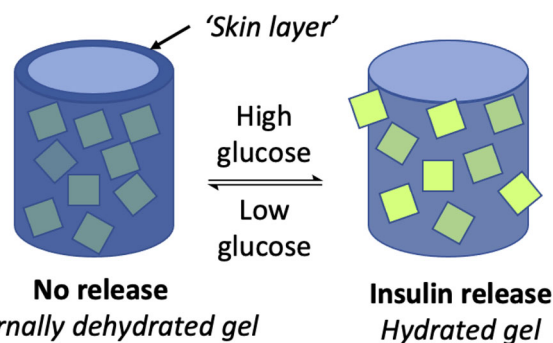


**Figure 7.** A pictographic representation of the glucose triggered insulin releasing hydrogel designed by Matsumoto et al.<sup>[79b]</sup> The external surface of the gel would react to changing glucose concentrations while the bulk remains unchanged. This enabled the surface to dehydrate, forming a “skin layer” at low glucose concentrations, decreasing the mesh size and retaining the encapsulated insulin. At high glucose concentrations the outer layer is hydrated, enabling insulin release.

pensating decreased solubility of the gel by introducing 2-carboxyisopropylacrylamide (**7**). Thermosensitive *N*-isopropylacrylamide (**8**) or *N*-isopropylmethacrylamide (**9**) were used alternatively as the main component of the polymer chain while *N,N'*-methylenebisacrylamide served as a crosslinker (**10**) (**Figure 6**).

A series of terpolymer gels were obtained. The size of the materials in different glucose concentrations ( $2.78 \times 10^{-3}$  to  $55.5 \times 10^{-3}$  M) at temperatures ranging from 30 to 45 °C was probed. The authors noted that increasing the concentration of the boronic acid functionality yielded a proportional increase in hydration upon contact with glucose solution. It was also found that increasing the proportion of carboxylic acid bearing monomer improved swelling at higher temperatures, enabled gelation even at high boronic acid concentration. The ability of these gels to control insulin release was studied at temperatures between 35 and 40 °C. Surprisingly, the best material in the series was the one with the least significant scale of glucose-dependent hydration changes. This was composed of 20% of boronic acid functionalised monomer **6** and 1% of monomer **7**, with the main component being **8**. The experiments consisted of treating the studied materials with different glucose concentrations at discreet time points, and simultaneously monitoring insulin release, a plot of which gave a series of peaks alternating in shape (symmetric and nonsymmetric). For the above-mentioned material, insulin release reflected the glucose treatment profile at applied temperatures and discharge of the cargo was proportional to and efficiently shut off with change and removal of the stimuli. The authors rationalised the results in terms of “mesh size” the internal and surface of studied gels changing in response to stimuli.

Additionally, Matsumoto et al. utilised a hydrogel based on **6**, **9**, with **10** serving as a crosslinker in preparation of an electronics-free insulin delivery device confined within a single catheter, which was proven to function as an artificial pancreas in vivo.<sup>[79b]</sup> Insulin release was controlled by glucose concentration and skin layer formation served to shut off cargo discharge (**Figure 7**). Injections of fructose or aspartame did not cause a significant effect on blood glucose levels in mice implanted with insulin-loaded

devices showing glucose-specificity of studied material. In vivo studies on mice proved effective control of glucose concentration levels and high durability of the device, which was functioning for at least three weeks.

The established boronic acid-based hydrogel system of Matsumoto et al. was also employed as constituent of a microneedle array patch for glucose responsive transdermal insulin delivery.<sup>[81]</sup> Thus achieving the first example of an enzyme-free self-regulated system that can serve as an “on-skin pancreas.” A glucose-responsive hydrogel was blended with silk fibroin to form a semi-interpenetrated network providing the appropriate mechanical properties of microneedles. The authors found that the presence of silk fibroin does not impair the glucose-responsiveness of boronic acid-based hydrogel. In vitro studies at 37 °C proved that insulin release from this microneedle array is glucose-dependent and occurs promptly, mirroring the glucose concentration profile. Further improvements to the needle-patch system involved developing a fabrication method of a gel-silk fibroin hybrid material using a two-layer strategy, yielding a deformation resistant structure.<sup>[82]</sup> Matsumoto et al. took another step forward in regard of hydrogel composition, improving the formulation to decrease the effect of temperature on mesh size (and consequently insulin release), while maintaining high glucose responsivity,<sup>[83]</sup> by replacing **9** with **8** and decreasing its overall content. Moreover, the percentage of **6** was increased and *N*-hydroxyethylacrylamide was introduced to make up for increased hydrophobicity and prevent the network loosening due to crosslink formation with boronic groups. As a result, the authors obtained a hydrogel material with glucose responsive insulin release properties that were insensitive to temperature change within a 28 to 39 °C range.

The utility of this new formulation was demonstrated by Matsumoto et al. in another electronics-free insulin delivery device.<sup>[84]</sup> The authors combined their glucose-sensitive gel with bundled hemodialysis hollow fibers, they covered the bundle with a thin layer of PEG leaving open ends, and connected one end to an insulin reservoir, and the other to a cellulose dialysis membrane. Such a device was subcutaneously implanted into rats and its effect was studied within groups of healthy and diabetic rodents. The obtained results showed that glucose levels were well normalised and fluctuations were mitigated. In using a rat model, the authors demonstrated scalability of their approach since rats are about ten times larger than the previously used mice.<sup>[79b]</sup>

Gu and co-workers recently reported a microneedle patch for transdermal insulin delivery in response to elevated glucose levels.<sup>[85]</sup> The authors based their device on a polymeric matrix constructed of three different monomers: *N*-vinylpyrrolidone (**11**), 2-(dimethylamino)ethyl acrylate (**12**) and 3-(acrylamido)phenylboronic acid (**13**). These were mixed together with ethylene glycol dimethacrylate (crosslinker, **14**) (**Figure 8**) insulin (20 wt%) and photoinitiator (1 mol%, Irgacure 2959) in a microneedle mold, followed by UV irradiation causing photopolymerisation, yielding a set of polymeric needles loaded with insulin. The UV-curable polymer base was later laid out and after photopolymerisation the microneedle patch could be de-molded. The authors also prepared reference microneedle patches, which were also loaded with insulin but lacked **12** and **13**. The boronic acid part of **13** is responsible for binding glucose, forming a

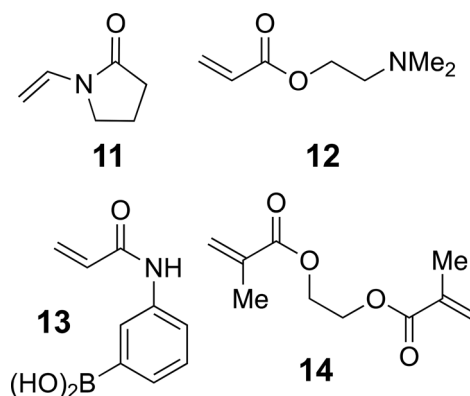
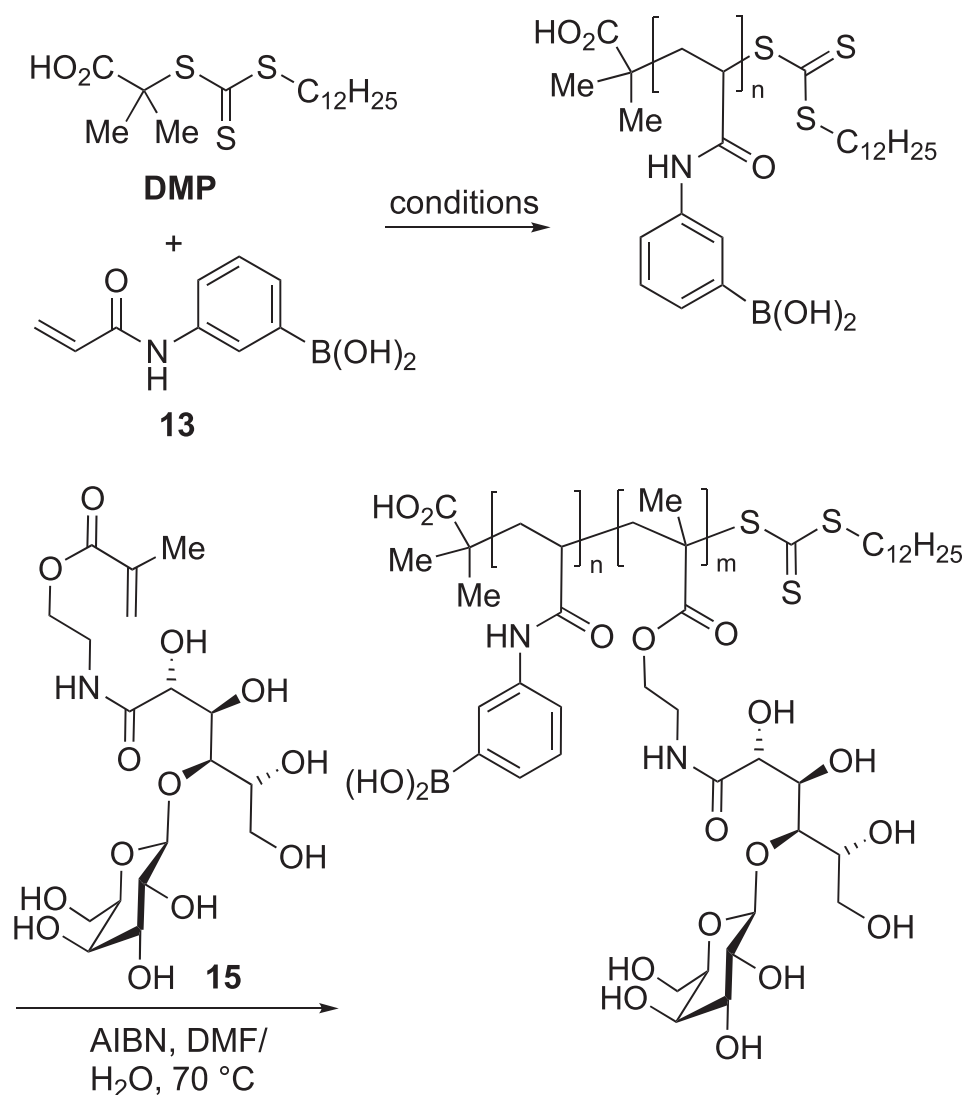


**Figure 8.** Monomers *N*-vinylpyrrolidone (**11**), 2-(dimethylamino)ethyl acrylate (**12**), 3-(acrylamido)phenylboronic acid (**13**) (to imbue the material with glucose responsiveness) and ethylene glycol dimethacrylate crosslinker (**14**) used by Gu and co-workers in preparation polymeric matrix for microneedle path releasing insulin in response to glucose.<sup>[85]</sup>

boronate complex under hyperglycemic conditions. This in turn increases the negative charge density, causing polymer swelling and repulsion of negatively charged insulin, initiating its release. Monomer **12** introduces a tertiary amine functionality that is easily protonated, forming areas of positive charge, which increase the affinity of the polymer to insulin, preventing its release under normoglycemic conditions. In vitro experiments revealed glucose binding by microneedles to proportionally increase across the normoglycemic ( $5.5 \times 10^{-3}$  M) to hyperglycemic ( $22 \times 10^{-3}$  M) range. Insulin release profiles for different glucose concentrations were presented, and the ability of the materials to switch cargo release on and off in response to glucose was demonstrated. Insulin loaded microneedles proved to work well in vivo, as demonstrated using mice and minipigs animal models. A patch of about 5 cm<sup>2</sup> enabled effective regulation of the plasma glucose levels of 25 kg minipigs for over 20 h, during which time minipigs were subject to glucose tolerance tests.

The concept of incorporating saccharide units into the hydrogel structure was explored by several other groups. Wu and co-workers used reversible addition-fragmentation chain transfer (RAFT) polymerisation in order to obtain block co-polymer comprised of **13** and 2-lactobionamidoethyl methacrylate (**15**), (**Scheme 2**). However, the obtained material showed limited glucose responsiveness.<sup>[86]</sup> Ju and co-workers prepared a cellulose/4-vinylphenylboronic acid composite bio-hydrogel by electron beam irradiation, which they investigated for glucose triggered insulin release at pH 9.0, 28 °C. The release profiles for normoglycemic ( $5.5 \times 10^{-3}$  M) and hyperglycemic ( $16.5 \times 10^{-3}$  M) were very similar in range of slightly over 20 h, thus were not suitable for a glucose responsive insulin release system.<sup>[87]</sup> Maynard and co-workers prepared a hydrogel based on a trehalose functionalised polymer derived from polystyrene and eight-arm PEG-NH<sub>2</sub>, functionalised with boronic acid units via reductive amination with 4-formylphenylboronic acid.<sup>[88]</sup> Trehalose was chosen because of its weak affinity to boronic acids, which was anticipated to provide high glucose-sensitivity to the hydrogel. Another reason for selecting trehalose was its abundance of hydroxyl groups which have been observed to aid hydrogel formation. The authors obtained a hydrogel loaded





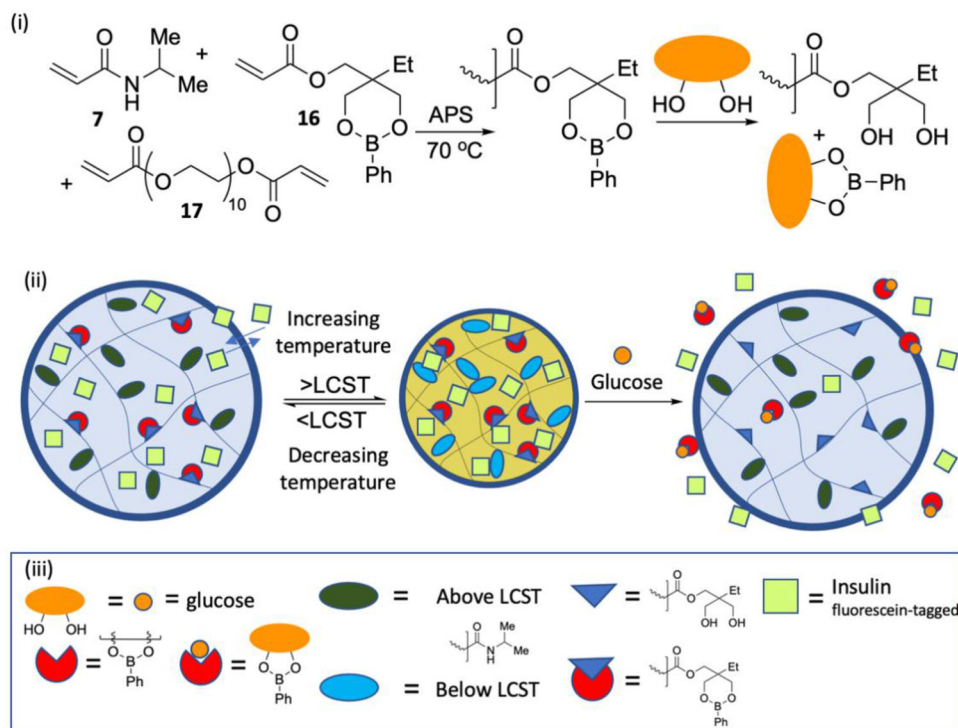
**Scheme 2.** Synthetic procedure developed by Ju et al.,<sup>[86]</sup> using RAFT to generate a block co-polymer containing both 3-acrylamidophenylboronic acid 13 and 2-lactobionamidoethyl methacrylate (15), which offered limited glucose responsiveness (conditions: AIBN, DMP, DMF/H<sub>2</sub>O, 70 °C).

with FITC-insulin by mixing the three components together. Although after 2 h, without glucose stimulation, over 60% of insulin was released, applying a  $27.8 \times 10^{-3}$  M concentration of glucose resulted in complete release.

The use of hydrogels as multifunctional materials in various applications requires endowing them with multiple physicochemical properties. Zhang and co-workers addressed this need with their nanofilamentous virus-based dynamic hydrogel incorporating boronate esters to give them glucose sensitivity.<sup>[89]</sup> The authors functionalised the rod-like M13 virus with 4-((3-((2,5-dioxopyrrolidin-1-yl)oxy)-3-oxopropyl)carbamoyl)phenylboronic acid in an active ester approach. This bioconjugate was then coupled with poly(vinyl alcohol) (PVA) giving an injectable and self-healing hydrogel. This hydrogel could be structured by shear-induced orientation of virus nanofibers. Also, gelation by diffusion of diol-containing material engendered a chiral liquid crystal phase into the hydrogel leading to unique internal chiral

structures. Insulin loading took place at the hydrogel formation step through mixing three components together (bioconjugate, insulin, and PVA). Insulin release studies showed that after 120 h,  $\approx 85\%$  of the cargo was discharged in medium with no glucose while for glucose concentration of  $33.3 \times 10^{-3}$  M, cumulative release after the same time was  $\approx 95\%$ .

Recent work by Zhang and co-workers showed an example of a multifunctional glucose and thermally responsive microgel with high salt tolerance.<sup>[90]</sup> The authors synthesised a random copolymer using 7 and (2-phenylboronic esters-1,3-dioxane-5-ethyl)methyl acrylate (16) as monomers, endowing thermo-responsiveness and the other in glucose-responsiveness respectively, with PEG diacrylate used as a crosslinker (17) (Scheme 3). Three microgels varying in monomer ratio were prepared via radical initiated polymerisation. FITC-tagged insulin was loaded through diffusion. Analysis of insulin release against varying temperature, concentrations of phosphate buffer



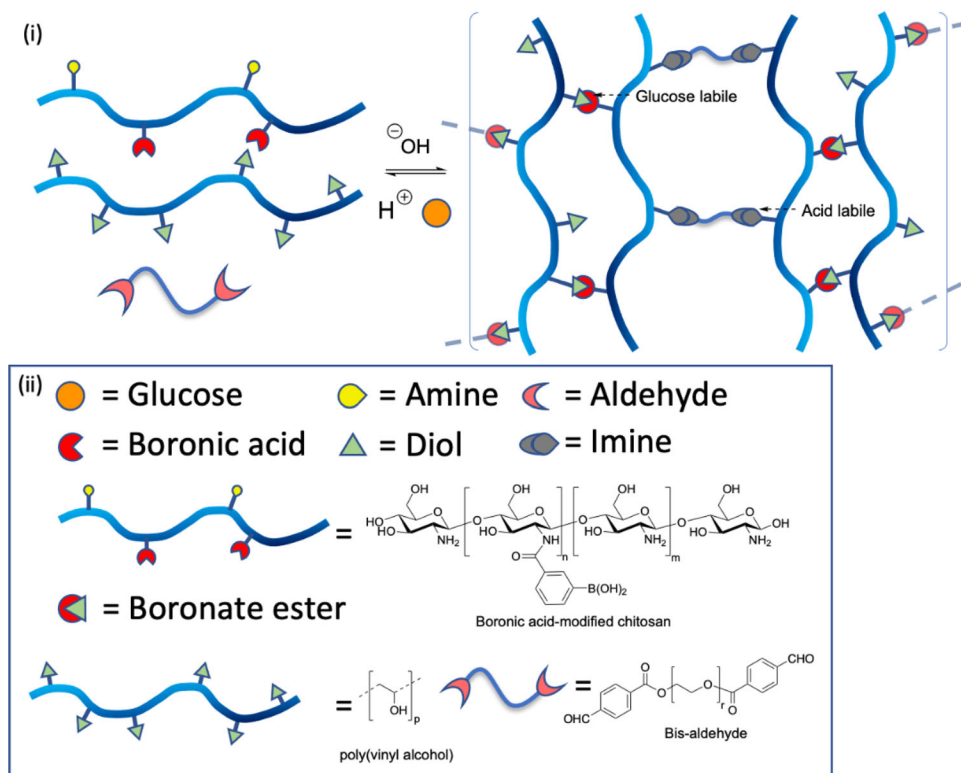
**Scheme 3.** A pictographic representation of the glucose responsive microgel as developed by Zhang and co-workers.<sup>[90]</sup> i) Radical initiated polymerisation of acrylamide monomers. ii) Schematic of the materials response to temperature and the presence of glucose. iii) Key: Orange circle/oval represents glucose. Green oval represents bulk polymer above its lower critical solution temperature (LCST). Blue triangle represents diol-containing monomeric unit. Pale green square represents fluorescein-tagged insulin. Red cut out circle represents boronic acid unit. Orange circle within the red cut out circle represents glucose complexed to the boronic acid. Pale blue oval represents bulk polymer below its LCST. Blue triangle within red cut out circle represents boronic acid unit bound to the diol containing monomeric unit.

and concentrations of glucose demonstrated that while changes of first two factors within physiological range do not exert significant effects, altering glucose concentrations adequately influence insulin release. The extent of this effect was proportional to boron-containing monomer (**16**) incorporation.

Zhao et al. sought to take advantage of insulin's tissue regenerative ability in the design of a bioactive dressings for diabetic wound healing. They synthesised a three-component hydrogel comprising of boronic acid-modified chitosan, PVA, and benzaldehyde capped PEG.<sup>[91]</sup> Bis-aldehyde formed crosslinks between chitosan derived chains that were complexing PVA by boronate ester formation (**Scheme 4**). The authors found that hydrogel formation could occur in the presence of insulin and live cells could also be incorporated. The obtained material was shown to release insulin in response to glucose (at  $16.6 \times 10^{-3}$  M) and lowering pH (from 7.4 to 6.4), with cumulative discharge in response to these stimuli after 34 h being 43% and 33%, respectively. This process was influenced by changing the ratio of the hydrogel monomers components. The authors tested their insulin- and fibroblasts-loaded hydrogel topically on the wounds of diabetic mice. They were shown to reduce blood glucose levels and improve the healing process compared to controls over an 18-day experimental time course.

Chitosan was also incorporated into an insulin-releasing hydrogel by Yu and co-workers.<sup>[92]</sup> The authors sought to use chitosan to imbue the material with biodegradability, as well as to

lower the  $pK_a$  of the boronic acid moiety through the interactions of chitosan amine groups with the boronic acid groups. Another benefit of the incorporation of chitosan units was improved mechanical properties, better protecting loaded insulin against mechanical deformations at the site of implantation. The authors synthesised a set of materials by radical polymerisation of acrylamide, **13**, maleic acid grafted chitosan and poly(ethylene glycol) diacrylate crosslinker, with varied monomer ratios. Investigation into the mechanical properties of the hydrogel samples confirmed that the chitosan was responsible for both an increased stiffness of the hydrogel and an increased storage modulus. Increasing the proportion of chitosan also increased the hydrogel's swelling in response to glucose. However, the authors noticed that their materials were swelling more in PBS solution than in glucose solution, and swelling was smaller in  $22.2 \times 10^{-3}$  M glucose than in  $5.5 \times 10^{-3}$  M glucose. This was hypothesised to be due to the 2:1 boronic acid to glucose binding that was essentially forming additional crosslinks. Only at concentrations of  $55 \times 10^{-3}$  M of glucose did the hydrogel swell more than in the control experiments. To further evidence this theory, the authors conducted experiments with fructose, as the fructose boronic acid binding is 1:1. This resulted in the hydrogels swelling two to four times more than the equivalent glucose concentrations. Following this investigation, insulin was loaded into hydrogels by the swelling-diffusion method. Insulin solution was added to a vial with a dried sample of the hydrogel and the vial was



**Scheme 4.** Glucose responsive PVA based hydrogel for diabetic wound healing as developed by Zhao et al.<sup>[91]</sup> i) Schematic representation of the effects of pH and glucose on the hydrogel material, outlining the acid sensitive imine bonds and the glucose sensitive boronate esters. ii) Key: Orange circles represent glucose. Yellow pear-shape represents amines present on chitosan. Pink sickle-shapes represent aldehydes present on bis-aldehyde crosslinker. Red cut out circle represents boronic acid unit. Pale green triangle represents diol unit on PVA chains. Grey sickle pear-shape bound unit represent imine bonds. Thick blue lines represent polymeric chains.

incubated at 25 °C for 48 h. The hydrogel was then washed with distilled water. Optimal loading capacity was observed for the material with intermediate chitosan content. In vitro tests for insulin release in response to glucose were conducted, showing differentiation in cargo liberation in response to different glucose concentrations. In the case of the hydrogel with the highest chitosan content, insulin release was most effective in absence of glucose. However, all other tested materials liberated their payload in correlation with increasing glucose concentrations.

Zhao and co-workers developed a glucose-responsive hydrogel for diabetes therapy that releases insulin and liraglutide, chosen since a combination of these has greater potential for preventing diabetic nephropathy.<sup>[93]</sup> The authors based their material on poly( $\gamma$ -glutamic acid) which they modified through amide formation with 3-aminophenylboronic acid (24). Boronic esters formed between boronic acid and diol units of konjac glucomannan, a polysaccharide consisting of glucose and mannose, resulting in the formation of a hydrogel network. Insulin and liraglutide were loaded into this network. In vitro experiments showed that release of both cargos was influenced by glucose. However, it was observed that insulin discharge was slightly more glucose sensitive than liraglutide. Cumulative insulin release for glucose concentrations of  $0 \times 10^{-3}$ ,  $22.2 \times 10^{-3}$ , and  $66.6 \times 10^{-3}$  M, in otherwise physiological conditions, was 60%, 70%, and 80% within 72 h, respectively. For liraglutide cumulative release under these same conditions varied from  $\approx 71\%$  to about 82%. The material

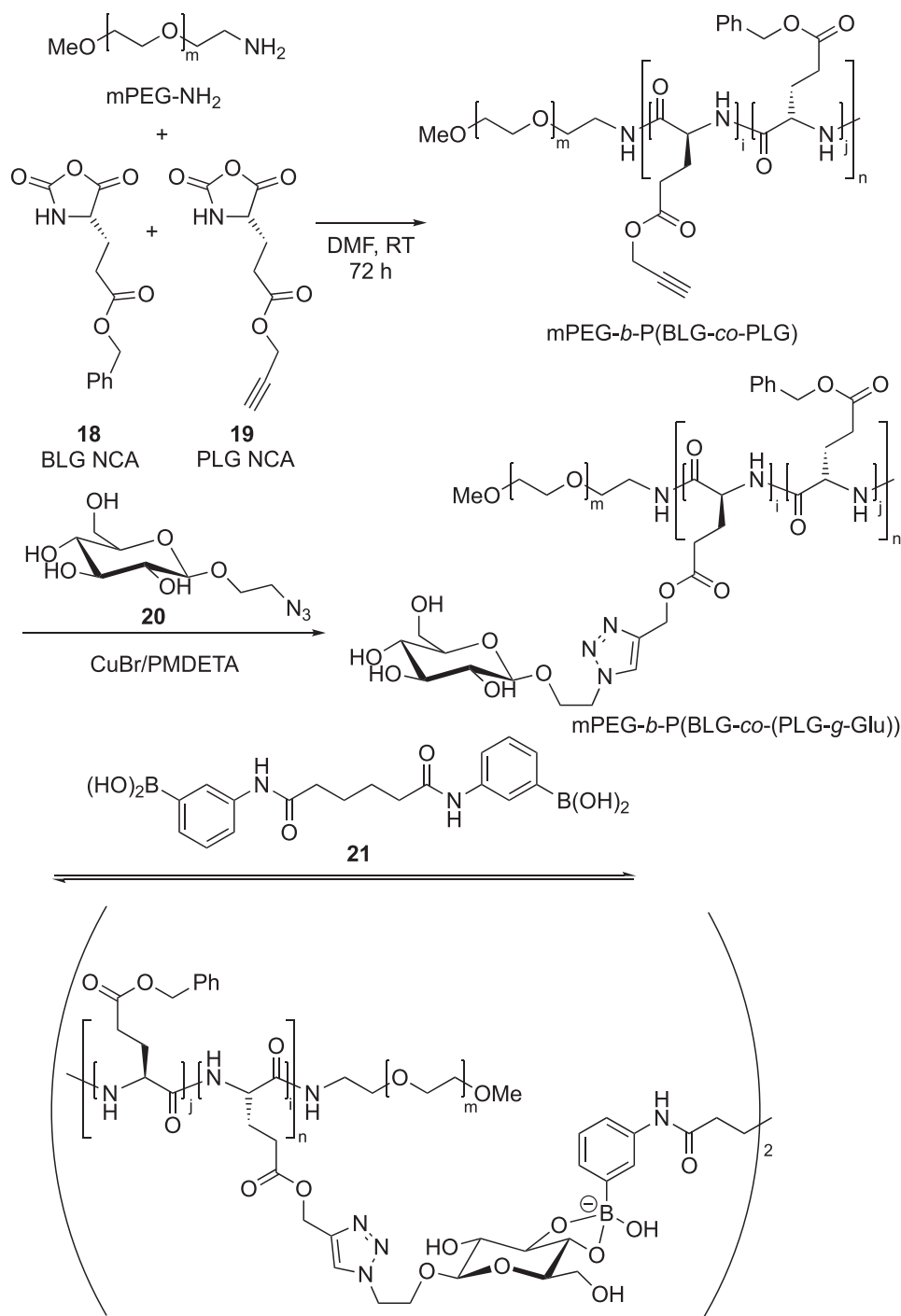
was also demonstrated to undergo “on-off” release cycling in response to varying glucose concentration. Diabetic rats were used to perform in vivo test over 42 days, therapeutic administration took place once every three days and provided good blood glucose normalisation. Moreover, the authors have also confirmed that development of nephropathy in studied rats was prevented.

## 6. Nano Objects/Nano Materials

Nanomaterial encompasses materials composed of particles in the range of 1 to 1000 nm. This size range is accompanied with unique properties, e.g., a relatively high surface area and surface tension.<sup>[94]</sup> Nanotechnology materials offer advantages when considering the design of an artificial pancreas such as increased permeability across mucosal membranes, and the ability to form novel insulin formulations.<sup>[62c]</sup> However, it should be noted that such nano-objects can suffer from low loading capacity or levels, which may ultimately require more frequent treatment.

## 7. Nanogels

Hydrogels can be prepared in the form of nanoscale objects,<sup>[95]</sup> which when compared to larger formulation bulk hydrogels have advantages such as faster response to external stimuli.<sup>[96]</sup> Chen and co-workers recently reported an insulin-releasing polypeptide nanogel with a bis-boronic acid crosslinker endowing it with



**Scheme 5.** The synthesis the terpolymer reported by Chen and co-workers,<sup>[97]</sup> via ring opening polymerisation of  $\gamma$ -benzyl-L-glutamate *N*-carboxyanhydride (**18**) and  $\gamma$ -propargyl-L-glutamate *N*-carboxyanhydride (**19**), with subsequent addition of  $\alpha$ -D-glucopyranoside (**20**) units with copper(I)-catalyzed alkyne-azide cycloaddition (CuAAC), which is then crosslinked with bisboronic acid (**21**) to yield a glucose responsive material.

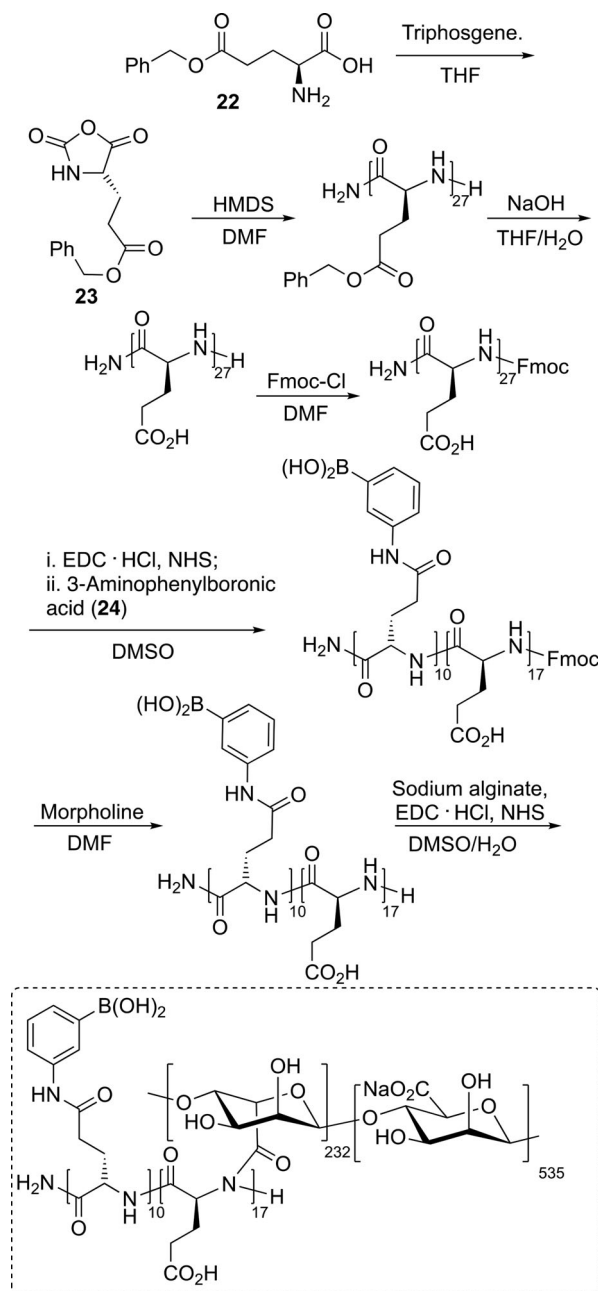
glucose-sensitivity.<sup>[97]</sup> The authors prepared their material utilizing amino-terminated methoxy-PEG initiated ring opening polymerisation (ROP) of  $\gamma$ -benzyl-L-glutamate *N*-carboxyanhydride (**18**) and  $\gamma$ -propargyl-L-glutamate *N*-carboxyanhydride (**19**) (Scheme 5), obtaining first a block terpolymer with PEG and polypeptide blocks. Following this,  $\alpha$ -D-glucopyranoside (**20**)

units were appended to the polymer by copper(I)-catalyzed alkyne-azide cycloaddition. Finally, a bis-boronic acid (**21**) was used as a crosslinker binding to the saccharide motif appended to the polymer chains (Scheme 5). The material was shown, by dynamic light scattering (DLS) and TEM analyses, to be a spherical nanogel with low polydispersity (PDI = 0.12). This

nanogel exhibited glucose-dependent swelling. For glucose concentrations in the range of  $0 \times 10^{-3}$  to  $5.5 \times 10^{-3}$  M, only a slight increase in particle size was observed, while in a range of  $5.5$  to  $16.6 \times 10^{-3}$  M, network expansion was much more significant, a promising result considering the physiological and pathophysiological glucose concentrations in diabetes. Therefore, the authors loaded insulin into their nanogel with a loading capacity of 9.5% and an efficiency of 47.5%. The authors noted that loading insulin increased the particle size. Insulin release as a function of glucose concentration was studied at pH 7.4 and 37 °C, with increased release observed with increasing glucose concentrations between 0 to  $16.6 \times 10^{-3}$  M. In all cases a burst release of over 50% of the insulin was observed in first 2 h, which was attributed to partial entrapment of insulin on the nanogel's surface. Analysis of the released hormone showed that discharged insulin did not suffer from structural changes. Chen and co-workers also performed cytotoxicity and hemotoxicity analyses of the studied nanogel showing very good results in both cases.

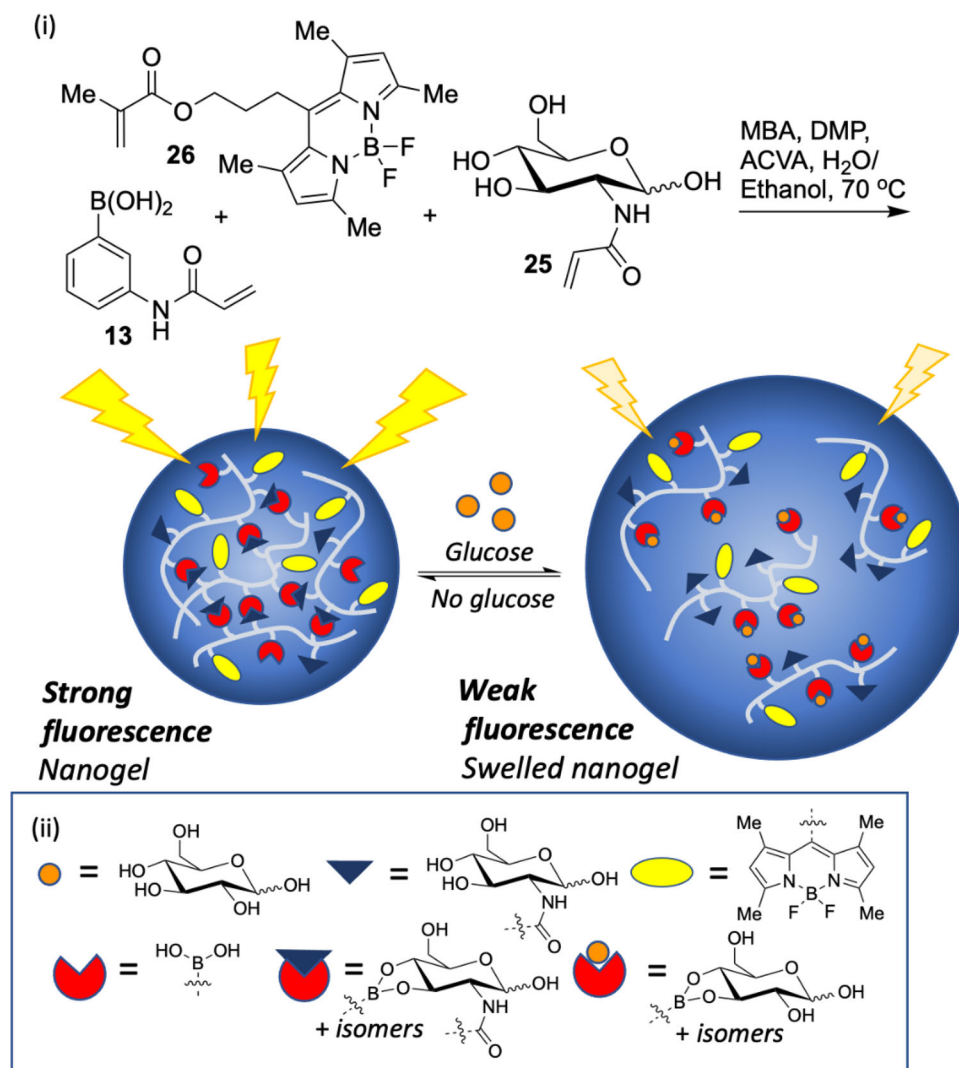
Kim and co-workers also focused their attention on hydrogel preparation using L-glutamic acid derivatives but they addressed the challenge of increasing bio-compatibility.<sup>[98]</sup>  $\gamma$ -Benzyl-L-glutamic acid (**22**) was converted to (**23**), and **23** was treated with hexamethyldisilazide in order to perform controlled polymerisation (Scheme 6). The obtained product was subjected to benzyl-deprotection and subsequent amino-group protection, before an amide-coupling with 3-aminophenylboronic acid (**24**) was performed. The resulting product had 37.5% of its carboxylic groups functionalised. After cleaving amino-protecting fluorenylmethoxycarbonyl group the obtained compound was grafted on to sodium alginate (Scheme 5). The obtained material (SA-PGGA) was able to form a nanogel by itself. Kim and co-workers utilised glycol chitosan (GCh) to form a double-layered nanogel (GCh/SA-PGGA), with GCh serving as the outer layer. This material showed glucose concentration-dependent swelling properties. Insulin-loaded GCh/SA-PGGA material was prepared by an isotropic gelation and electrostatic interactions. The release of insulin in solutions ranging in glucose concentration from  $0 \times 10^{-3}$  to  $55.5 \times 10^{-3}$  M was studied, showing burst release within the first 5 h for each concentration, with cumulative release varying from 40% to 80% within 60 h. Biocompatibility and hemotoxicity of GCh/SA-PGGA were also investigated, showing promising results. Finally, Kim and co-workers studied the material in vivo. Insulin loaded-GCh/SA-PGGA was able to effectively lower blood glucose levels in mice. The authors have shown that GCh/SA-PGGA has the potential to lower the frequency of insulin injections, as a single dose of insulin loaded-GCh/SA-PGGA performed as well as two injections of free insulin which totaled 150% the insulin loaded into the nanogel.

The effective combination of glucose-responsive cargo delivery and glucose-sensing nanogel platform was achieved by Guo and Zhang.<sup>[99]</sup> The authors utilised RAFT to build a polymer using **13**, 2-(acrylamido)glucose (**25**), methacrylate ester with a boron-dipyrromethene moiety (**26**) and *N,N'*-ethylenbisacrylamide as crosslinker (Scheme 7). A set of three polymers of varying boronic acid concentration were prepared, and the resulting nanogels were characterised by DLS. The particle size ranged from about 178 to 249 nm, with increased boronic acid incorporation resulting in larger sizes. The obtained hydrogels were



**Scheme 6.** The synthetic route toward the GCh/SA-PGGA double-layered hydrogel reported by Kim and co-workers.<sup>[98]</sup>  $\gamma$ -Benzyl-L-glutamic acid (**22**) was converted to (**23**) through reaction with phosgene, which was subsequently polymerised using hexamethyldisilazane. After benzyl deprotection of the acid and Fmoc protection of the amine, 3-aminophenylboronic acid (**24**) is coupled to 37.5% of the free acid groups. Following Fmoc deprotection, the compound was bound to sodium alginate, before being fabricated into a dual layered hydrogel with chitosan.

also studied using UV-vis and fluorescence spectroscopies in solutions of glucose with concentrations from  $0 \times 10^{-3}$  to  $22.2 \times 10^{-3}$  M with  $2.78 \times 10^{-3}$  M increments. Glucose concentration-dependent changes in fluorescence of the BODIPY-derived fluorophore and UV-vis absorption were observed. Insulin release studies showed that the boronic acid content in the nanogel was



**Scheme 7.** The glucose responsive nano-gel formulated by Guo and Zhang.<sup>[99]</sup> i) Glucose responsive increase in nanogel size, accompanied by a fluorescence decrease. ii) Key: Orange circles represent glucose. Blue triangles represent 2-(acrylamido)glucose units. Red cut out circle represents boronic acid units. Red cut out circles with orange circles represent boronic acid units complexed to glucose. Red cut out circles with blue triangles represent boronic acid units complexed 2-(acrylamido)glucose units. Yellow ovals represent BODIPY units.

inversely proportional to cumulative release. Moreover, for the nanogel with medium boronic acid content showed a significant discrepancy in total cumulative release for  $5.5 \times 10^{-3}$  M glucose and  $16.6 \times 10^{-3}$  M glucose as the results were  $\approx 25\%$  and  $55\%$ , respectively. Alternating pulsatile glucose concentration changes from  $16.6 \times 10^{-3}$  to  $0 \times 10^{-3}$  M exerted on the nanogel demonstrated the “on-off” release capabilities of this platform. CD analysis of the released insulin confirmed that it does not suffer from structural changes, and cell viability studies confirmed good biocompatibility of the nanogels.

Lu and co-workers developed a glucose-responsive nanogel for insulin delivery through the emulsion precipitation polymerisation method using *N,N*-diethylacrylamine and 4-vinylphenylboronic acid.<sup>[100]</sup> Insulin release studies showed that within 50 h, a glucose solution of  $5.5 \times 10^{-3}$  M causes about 85% cumulative insulin release, while at  $16.6 \times 10^{-3}$  M glucose this release reaches almost 100%. The authors also demonstrated

that alternating glucose solution concentration changes insulin release with fluctuations of  $16.6 \times 10^{-3}$  to  $8.4 \times 10^{-3}$  M and then back to  $16.6 \times 10^{-3}$  M again. The gradient of the insulin release curve flattens at lower glucose concentrations, and increases again with the concentration.

Huang and co-workers prepared glucose-responsive core-shell hydrogels via one-pot thiol-ene copolymerisation under DMAP catalysis.<sup>[101]</sup> The authors used PEG methyl ether acrylate, 4-(5-(acryloyloxy)methyl)-5-methyl-1,3,2-dioxaborinan-2-yl)benzyl acrylate and pentaerythritol tetra(3-mercaptopropionate) as monomers. The nanogel was designed to be prone to decomposition through competitive transesterification of the boronate with glucose, as well as by the oxidation of the C–B bond by  $H_2O_2$  that was to be produced by GOx, which was encapsulated alongside insulin. Glucose-responsive insulin release was investigated at 37 °C using solutions of pH 7.4 and glucose concentrations of  $0 \times 10^{-3}$ ,  $5.5 \times 10^{-3}$ , and  $22.2 \times 10^{-3}$  M.

Over 30 h, up to 60% of insulin was released in response to a glucose solution of  $22.2 \times 10^{-3}$  M, while for  $5.5 \times 10^{-3}$  and  $0 \times 10^{-3}$  M solutions about 35% and 15% of the insulin was released respectively. In vivo studies on diabetic mice were also performed, showing stabilisation of blood glucose for 9 h.

## 8. Nanoparticles

Siddiqui et al. functionalised chitosan with boronic acid units by reductive amination using 4-formylphenylboronic acid, and studied the resulting materials for glucose-responsiveness and insulin release.<sup>[102]</sup> During the insulin release studies the glucose concentrations used were  $5.5 \times 10^{-3}$ ,  $16.6 \times 10^{-3}$  and  $27.7 \times 10^{-3}$  M at 37 °C in phosphate buffered solutions; over 45 min each concentration yielded similar results, indicating a lack of suitability for use in treating diabetes.

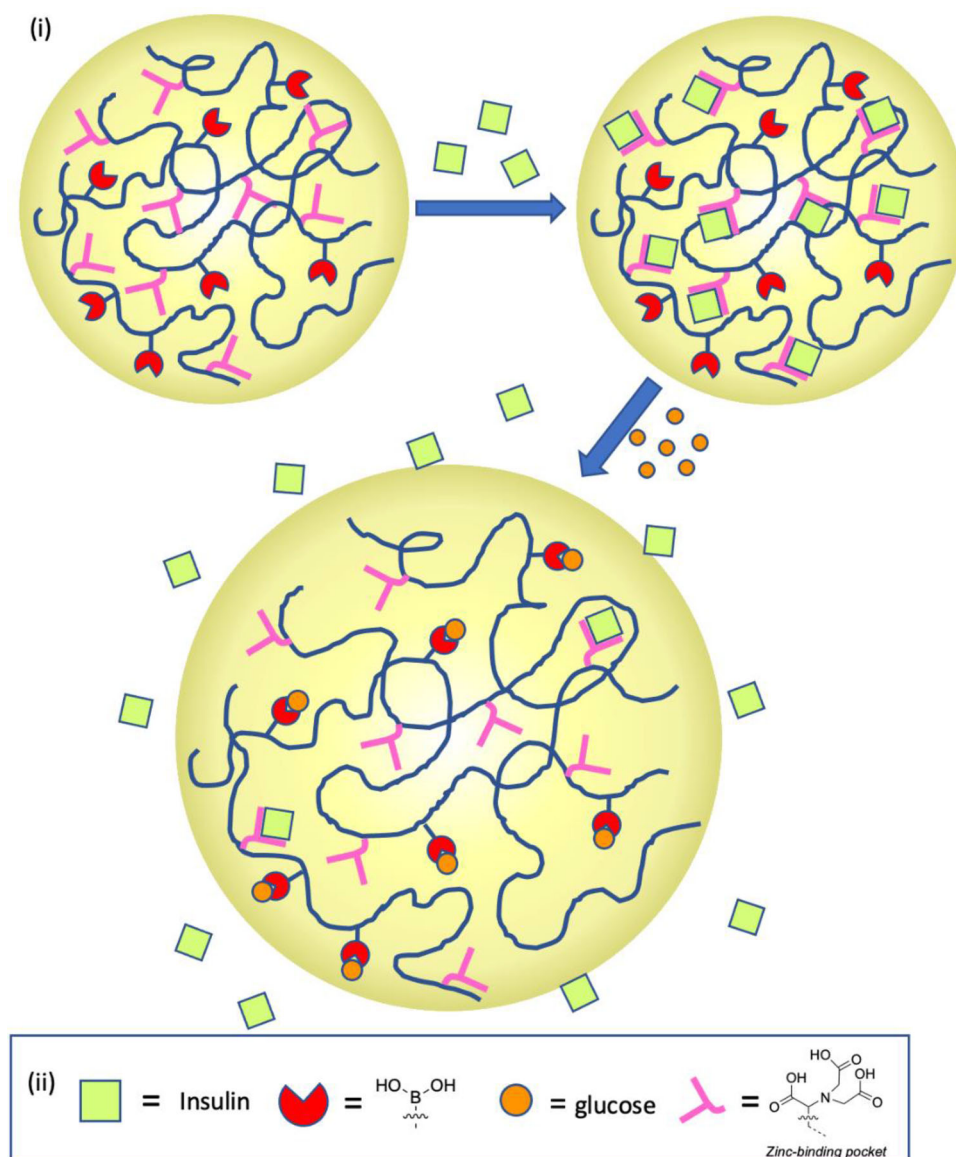
Another chitosan-derived delivery system based on glucose boronate formation was developed by Chai and co-workers.<sup>[103]</sup> The authors produced two-component nanocarriers composed of poly(3-methacrylamidophenylboronic acid) and thiolated-chitosan, a product of amide-coupling between chitosan and *N*-acetyl-L-cysteine. These two constituents were able to form nanoparticles thanks to boronic acid-diol binding, with disulphide bridges conferring structural integrity. The authors obtained a series of three types of nanoparticles with different ratios of components, as well as nanoparticles consisting of poly(3-methacrylamidophenylboronic acid) and nonthiolated-chitosan for comparison purposes. Insulin was successfully loaded into the assemblies (with a capacity of up to 18%) and its release in response to glucose in was studied in physiologically relevant conditions (pH 7.4 and 37 °C). Disulphide crosslinks proved to be crucial in controlling insulin release, for those particles without the disulphide 60% of cumulative release was reached within 14 h without glucose, which was reduced to below 20% by the thiolated-chitosan. In glucose-containing media, insulin release was characterised by a burst in the initial stages, with differences in the cumulative release for normoglycemic ( $5.5 \times 10^{-3}$  M) and hyperglycemic ( $16.6 \times 10^{-3}$  M) of about 25% to almost 100% respectively. Moreover, authors showed that under hyperglycemic conditions with increased boronic acid unit content, the intensity of insulin release decreased, while preserving the same cumulative value over 14 h. CD spectra of released insulin showed that it was not distorted, hence its activity should be preserved. The authors also demonstrated good biocompatibility of studied the materials.

Chitosan-based materials were further explored by Jiang and co-workers who developed an oral delivery system for insulin.<sup>[104]</sup> The authors envisioned that functionalizing chitosan with L-valine would enhance absorption in the small intestine, while grafting chitosan with boronic acids will endow resulting material with glucose responsive properties. In the synthetic procedure chitosan was first alkylated with chloroacetic acid, followed by amide coupling between the newly introduced carboxylic groups, 3-aminophenylboronic acid (**24**) and L-valine. Insulin could be loaded into this material with an efficiency of 67% and a capacity of 9.8%. Studies of cargo release revealed burst discharge profiles in initial stages. Moreover, in all studied conditions cumulative release reached a plateau after 12 h. The authors also found that in acidic conditions (pH 1.2) release

is least efficient and does not exceed 20% with no glucose present, indicating the potential for the protection of cargo from stomach acid. Experiments at pH 6.8, still without glucose stimuli, revealed cumulative insulin release of 50%, which was essentially the same as for  $5 \times 10^{-3}$  M glucose solution at pH 7.4 (55%). Further increasing the glucose concentration to  $10 \times 10^{-3}$  and  $20 \times 10^{-3}$  M resulted in 68% and 92% of cumulative insulin release respectively. CD spectral analysis showed that discharged insulin does not differ in its secondary structure from a standard sample. The studied material was found to be of good biocompatibility and confocal laser scanning microscopy showed that insulin loaded nanoparticles are being internalised by HT-29 cells (FITC-labeled insulin was used).

The affinity of different saccharides to boronic acids varies,<sup>[105]</sup> for monoboronic acids fructose is generally the strongest binder due to the favorable orientation of hydroxyl groups in its highly present furanose form,<sup>[106]</sup> and this is a potential problem in saccharide-mediated release systems. Billa and co-workers decided to take a deeper look at this issue while working on boronic acid-functionalised chitosan nanoparticles for insulin delivery.<sup>[107]</sup> The authors used reductive amination to conjugate chitosan with 2-formyl-thienylboronic acid or 4-formylphenylboronic acid, allowing them to obtain two series of materials with different ratios of functionalisation. These materials were used in a curcumin displacement assay to evaluate their affinity to glucose and fructose. Comparison of results showed that thienylboronic acid functionalised chitosan (at 1:1 ratio) displayed slightly better selectivity for glucose over fructose. The authors ascribed this to favorable orientation of boronic acid groups and secondary interactions (e.g., C-H... $\pi$ ). Insulin was loaded into both types of material and its release was studied. Cargo discharge was monitored throughout 60 min either in deionised water,  $0.11 \times 10^{-6}$  M fructose solution and glucose solutions with concentrations ranging from  $5.5 \times 10^{-3}$  to  $16.6 \times 10^{-3}$  M. These studies also showed that material bearing thienylboronic acid had better glucose-selectivity when compared to the phenylboronic acid analog, however in glucose concentrations of  $11.1 \times 10^{-3}$  M or higher the cumulative insulin release reached the same level for both materials.

Ma and co-workers prepared a glucose-sensitive nanogel by thermally initiated precipitation polymerisation.<sup>[108]</sup> In the synthesis process **13**, methacrylic acid and ethylene glycol methacrylate as crosslinker were mixed together with 2,2'-azobisisobutyronitrile radical initiator in acetonitrile at 60 °C. The authors obtained a set of nanogels varying in monomer ratio, including one with no boronic acid component. Nanogels incorporating **13** swelled in glucose solutions, proportional to the inclusion of boronic acid units. Insulin was loaded into the studied nanogels by the immersion method with a loading capacity of 14.8%. Insulin release was studied in PBS at 37 °C and showed to proceed with an initial burst. At glucose concentrations of  $10 \times 10^{-3}$  M about 60% insulin was released, while at  $50 \times 10^{-3}$  M cumulative release slightly exceeded 70%, in both cases within 70 h. The authors performed an in vivo study using diabetic rats which showed sustained insulin release, which was compared to free insulin and insulin loaded-poly(methacrylic acid) and was able to stabilise blood glucose levels over time. Although adverse effects relating to blood-clotting were observed, the material exhibited acceptable cytocompatibility and low hemotoxicity,



**Scheme 8.** The glucose sensitive nanogel reported by Ma and co-workers.<sup>[110]</sup> i) A pictographic representation of the nanogel displaying increased insulin loading, with subsequent glucose triggered insulin release; ii) Key: Pale green square represents insulin. Red cut out circle represents boronic acid units. Orange circle represents glucose. Pink Y-shapes represent nitrilotriacetic zinc binding units. Blue lines indicate polymer chains.

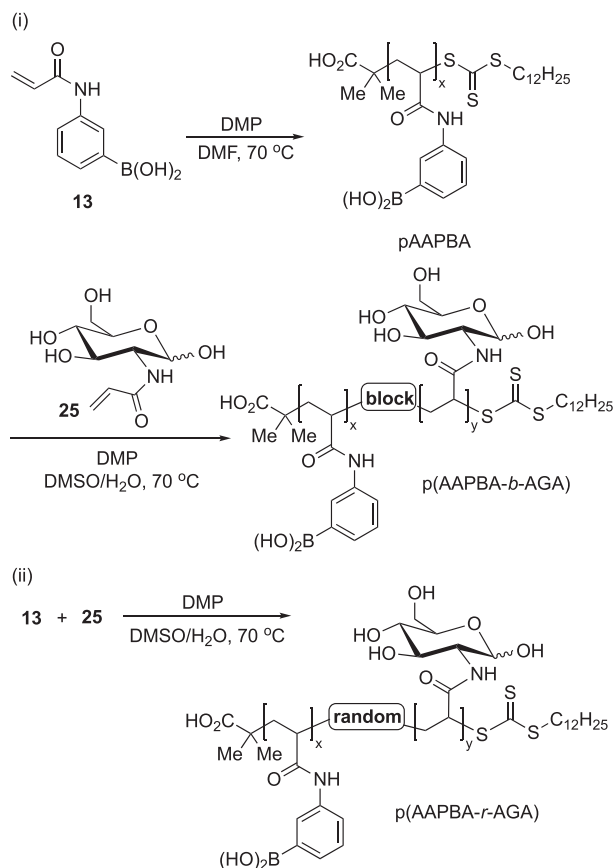
further underpinned the merit of future work on these systems. Moreover, the authors demonstrated that insulin loaded into their nanocarriers was protected from simulated gastric or intestinal fluid. The authors performed *in vivo* studies on diabetic rats in order to verify performance of their delivery system as in oral administration route and was shown to effectively reduce blood glucose concentration.

Ma and co-workers, inspired by inherent affinity of insulin to zinc ions,<sup>[109]</sup> used this phenomenon to improve the loading capacity of a glucose-sensitive nanogel (Scheme 8).<sup>[110]</sup> In order to do so the authors incorporated nitrilotriacetic units into a polyacrylamide derived structure. While 3-carbamoylphenylboronic acid units endowed the material with glucose-responsiveness, the zinc ions chelated by nitrilotriacetic fragment could bind to in-

sulin through its histidine imidazole rings. The authors showed that this modification allowed for an increase of insulin loading capacity from 11.0% to 18.3%. Cargo release was studied in different solutions of pH 7.4 at 37 °C varying with glucose concentration from  $0 \times 10^{-3}$  to  $111 \times 10^{-3}$  M and cumulative release was observed ranging from about 20% to almost 80% over 60 h. Although burst release was observed for the nanogel, the authors also demonstrated that their material is capable of on-off cargo discharge, and offers good biodegradability and biocompatibility.

Zhang and co-workers showed how important polymer structure is in formation of glucose-responsive nanoparticles for insulin delivery by contrasting random and block copolymers of constructed from monomers 13 and 25.<sup>[66b]</sup> Both random and block copolymers were obtained using RAFT polymerisation.





**Scheme 9.** The synthetic procedure toward developing nanoparticles featuring different distributions of functional groups as reported by Zhang and co-workers to demonstrate the importance of this distribution.<sup>[66b]</sup> i) **13** was first polymerised using RAFT polymerisation in DMF, and the obtained polymer was subsequently used as a macro-raft agent in DMSO/H<sub>2</sub>O to build a **25** block. ii) Random polymers were obtained by performing RAFT polymerisation in DMSO/H<sub>2</sub>O with a mixture of each monomer at defined ratios.

In the case of block copolymers, **13** was polymerised first and used subsequently as a macroRAFT agent upon which to build a block of poly(2-acrylamido-D-glucose) (**Scheme 9i**). Random copolymers were obtained by performing RAFT polymerisation in a mixture of both monomers at specific ratios (**Scheme 9ii**). A total of six copolymers were obtained, three block and three random. Synthesised copolymers were assembled into nanoparticles using the nanoprecipitation method, which was assisted by complexation of boronic acid and glucosamide units. TEM and DLS served to investigate size and morphology of the nanoparticles, revealing spherical shaped assemblies. It was noted that those nanoparticles comprised of block copolymers were smaller than those built of random copolymers. This was thought to be due to a higher content of boronate linkages in random copolymer-based materials. This was further supported with result of <sup>11</sup>B NMR spectroscopic analysis, which showed higher ratio of ester to acid signals in the random copolymer sample. Nanoparticles of both copolymers exhibited glucose-triggered swelling, proportional to increased boronic acid content. Insulin was successfully encapsulated in the studied nanoparticles, with those derived

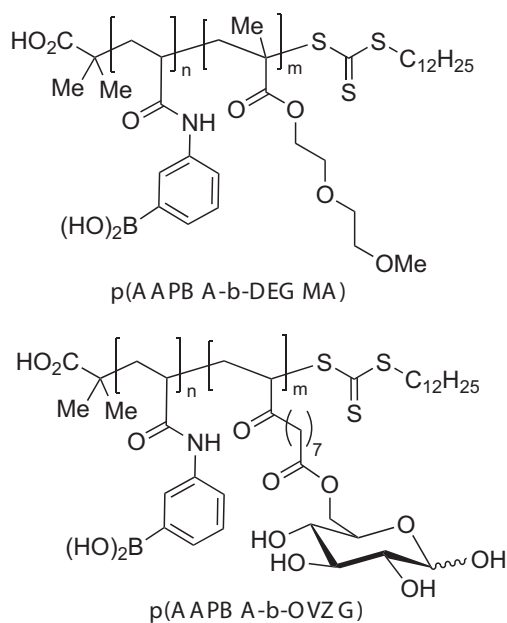
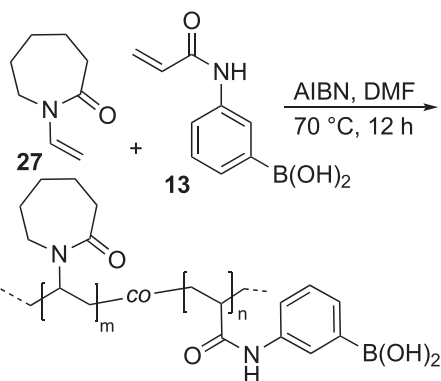


**Figure 9.** Two amphiphilic copolymers reported by Zhu and co-workers synthesised using RAFT polymerisation,<sup>[111]</sup> derived either from either **13** and diethylene glycol monomethyl ether methacrylate (**p(AAPBA-b-DEGMA)**) or 6-O-vinylazeloil-D-galactose (**p(AAPBA-b-OVZG)**).

from block copolymers having higher encapsulation efficiency (3% to 5%, with highest value being  $64.9 \pm 3.6\%$ ) and loading capacity (about 2%, with highest value being  $12.9 \pm 1.4\%$ ) than corresponding random copolymer nanoparticles. While loading capacity increased with the content of boronic acid units, encapsulation efficiency showed the opposite trend. Insulin release was studied in solutions of pH 7.4 varying in glucose concentration of either  $0 \times 10^{-3}$ ,  $5.5 \times 10^{-3}$  or  $16.6 \times 10^{-3}$  M at 37 °C. Cargo discharge was the most effective for materials with the least boronic acid content and random copolymer nanoparticles were showing quicker release. Both types of nanoparticles showed good biocompatibility.

Another glucose-responsive insulin delivery system based on a block copolymeric structure was obtained by Zhu and co-workers.<sup>[111]</sup> Amphiphilic copolymers were obtained using RAFT methods with **13** and diethylene glycol monomethyl ether methacrylate or 6-O-vinylazeloil-D-galactose as monomers (**Figure 9**). In both cases a series of five materials varying in monomer ratio were produced. Particles containing diethylene glycol monomethyl ether pendant units displayed both temperature and pH responsiveness. Increasing the temperature from 12 to 47 °C caused a 60% decrease in size, an effect that was reduced as boronic acid content increased. On the contrary, pH-dependent size change of nanoparticles was more pronounced for materials richer in boronic acids, causing up to 30% swelling with pH increase from 5 to 9.5. Both types of particles, grafted with D-galactose and diethylene glycol monomethyl ether, were successfully loaded with insulin and its release upon glucose stimulation was investigated. The material with saccharide pendant units showed better differentiation of discharge rate at different glucose concentrations and offered a more sustained payload release. Following toxicity studies both types of nanoparticle



**Scheme 10.** Radical-initiated polymerisation of **13** and *N*-vinyl- $\epsilon$ -caprolactam (**27**) yielding random copolymers capable of forming nanoparticles, as reported by Zhu and co-workers.<sup>[115]</sup>

were shown to be biocompatible. Importantly, the authors also performed *in vivo* evaluation of their systems on diabetic mice, showing that both insulin delivery platforms work well in lowering and stabilising blood glucose levels, with the system including *D*-galactose units exerting this effect for twice as long. Wu and co-workers also worked on a similar material built of two polyvinyl-type blocks: a hydrophilic one appended with galactose units and a hydrophobic part including boronic acid groups,<sup>[112]</sup> and obtained similar results.

The challenge of achieving glucose-stimulated insulin release was also tackled by Chang and co-workers who developed nanoparticles derived from 3-aminophenylboronic acid **24** and formaldehyde.<sup>[113]</sup> By use of an extended Stöber method<sup>[114]</sup> the authors prepared nanoparticles loaded with insulin. TEM imaging demonstrated swelling behavior upon contact with glucose and cell viability studies revealed good biocompatibility of this material in concentrations below  $20 \mu\text{g mL}^{-1}$ . Insulin release was also found to be glucose concentration-dependent. The authors found that for glucose concentrations up to  $7 \times 10^{-3}$  M cargo release was negligible, and that total discharged insulin after 90 min increases with increased glucose above this point. Furthermore, the authors shown that for  $5 \times 10^{-3}$  M glucose solutions, insulin release reaches a plateau at about 15% cumulative release within 60 min whereas at  $15 \times 10^{-3}$  M glucose the release increases to over 80% at about 180 min, at which time a plateau in payload release was not reached. While, insulin release under hyperglycemic was rapid, *in vivo* studies may be needed to verify appropriateness of release kinetics. Chang and co-workers also performed rhodamine 6G encapsulation in the same polymer nanoparticle formulation and showed that the obtained nanoparticles can serve as glucose sensors in concentrations ranging from  $0 \times 10^{-3}$  to  $10 \times 10^{-3}$  M.

Zhu and co-workers prepared a series of random copolymers using **13** and *N*-vinylcaprolactam and studied their potential as insulin delivery materials (Scheme 10).<sup>[115]</sup> In aqueous media they obtained copolymers formed nanoparticles with temperature-, pH- and glucose-responsiveness that was investigated by monitoring hydrodynamic diameter in response to stimuli. While an increased content of boronic acid lowered the degree of thermo-response, it increased pH- and glucose-induced swelling. Moreover, a higher ratio of boronic acid to *N*-vinyl- $\epsilon$ -

caprolactam units results in a higher insulin loading/entrapment capacity, although this occurred at the expense of lower loading efficiency. Insulin release studies were performed at pH 7.0 at 37 °C over 120 min with glucose concentrations varying from  $0 \times 10^{-3}$  to  $16.6 \times 10^{-3}$  M. The authors observed that while glucose had some impact on the discharge of insulin, release without stimuli amounted to between 60% and 90% for different polymers, with only slight increases on exposure to glucose. CD spectroscopic analysis was used to demonstrate retention of insulin's structure post-release. Both *in vitro* and *in vivo* toxicity studies were performed giving good results. Finally, the authors performed *in vivo* studies with insulin loaded nanoparticles in rats and found them able to stabilise blood glucose levels with similar efficacy to a control group treated with insulin injection.

Wu and co-workers have also used **13** and *N*-vinyl- $\epsilon$ -caprolactam (**27**) to obtain a glucose responsive material for insulin delivery, using a diblock copolymer synthesised using RAFT methods.<sup>[116]</sup> The authors prepared a set of copolymers varying ratios of **13** and **27** from 1:0 to 1:5. All the polymers formed had similar molecular weights with a  $M_n$  in range of  $4.5 \times 10^4$  to  $6.4 \times 10^4$ , and were very close in polydispersity (PDI between 1.20 and 1.23). The authors showed that these polymers self-assemble into nanoparticles in aqueous media. Measuring hydrodynamic diameters the authors noted that increasing the content of caprolactam units resulted in the formation of larger nanoparticles. Moreover, nanoparticles also increased in diameter with increasing pH, attributed to boronate anion formation. Seeing that nanoparticle size increase was significant at pH 8.0 the authors concluded that copolymerisation lowered the  $pK_a$  of the boronic acid. Investigation of nanoparticle diameter in different glucose concentrations further supported that hypothesis. For all copolymers of **13** and **27**, nanoparticle size increased significantly with respect to glucose concentration, while the size of the purely poly(3-acrylamidophenylboronic acid) (from **13**) particles were essentially the same. Moreover, caprolactam units endowed the nanoparticles with temperature-sensitivity, gradually reducing in size as the temperature was increased from 12 to 42 °C. During insulin loading studies the authors noted that the composition of the copolymeric nanoparticles, i.e., ratio of monomers, had virtually no effect on loading capacity and encapsulation efficiency. Insulin release experiments revealed that at physiological conditions when no glucose was present  $\approx 35\%$ – $60\%$  of the insulin was discharged, depending on copolymer composition, with cumulative release increasing with increased caprolactam content. The presence of glucose furthered the insulin release, at  $16.6 \times 10^{-3}$  M glucose depending on copolymer composition  $\approx 60\%$ – $85\%$  of insulin was released. Toxicity investigations conducted gave rise to no concerns and *in vivo* studies on diabetic mice demonstrated that their glucose-responsive insulin delivery platform was capable of lowering blood glucose in a similar fashion to insulin injections.

Li and co-workers focused their efforts on developing orally administered glucose-responsive nanocarriers for insulin delivery.<sup>[117]</sup> The authors synthesised a set of three random copolymers using *D*-gluconamidoethyl methacrylate and **13** as monomers in ratios 1:1, 1:2, and 1:3 (Figure 10). Higher boronic acid content within the polymer yielded larger nanoparticles, with sizes ranging from  $131.1 \pm 3.1$  nm to  $191.5 \pm 2.3$  nm. With the increase of boronic acid units in copolymers both insulin

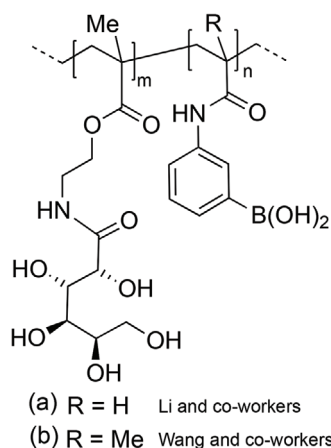


**Figure 10.** Random copolymers of i) D-gluconamidoethyl methacrylate and **13** as reported by Li and co-workers.<sup>[117]</sup> ii) D-Gluconamidoethyl methacrylate and 3-methacrylamidephenylboronic acid as reported by Wang and co-workers.<sup>[118]</sup>

loading capacity and encapsulation efficiency increased. All three types of particles displayed swelling in response to glucose, with concurrent release of insulin. Within the first two and a half hours, burst release was observed, thought to be due to the release of insulin adsorbed on the surface of nanoparticles. Importantly, the higher the content of boronic acid units in polymer nanoparticles, the lower the total cumulative release of insulin, and differences between normo- and hyperglycemic conditions were significant. CD spectroscopy was used to verify the integrity of released insulin and in vitro studies proved that it stimulated glucose transporter type 4. Cell viability studies also gave promising biocompatibility results. This prompted the researchers to further investigate their platform in vivo. Rats were orally administered with nanoparticles loaded with different amounts of insulin, control experiments whereby insulin or cargo-free nanoparticles were administered orally were performed. The obtained results indicated that in normoglycemic conditions studied nanoparticles do not release insulin. Also, insulin loaded nanoparticles were demonstrated to lower and stabilise blood glucose levels to different degrees, depending on their insulin content.

Similar materials were obtained by Wang and co-workers who copolymerised D-gluconamidoethyl methacrylate and 3-methacrylamidephenylboronic acid (**13**).<sup>[118]</sup> A series of three random copolymer differing in component ratio were obtained. All were able to form nanoparticles and encapsulate insulin, their loading capacity and efficiency increased with boronic acid content. Glucose stimulated insulin release was characterised by burst discharge in initial stages but differences between cumulative insulin release in normo- and hyperglycemic conditions were significant.

Polyamidoamine-based materials were developed by Liu and co-workers who prepared a nanoscale dendritic material for glucose-responsive insulin delivery (**Figure 11**).<sup>[119]</sup> A boronic acid moiety was grafted onto a polymer by amide formation between 3-aminophenylboronic acid (**24**) and carboxylic acid groups of a poly-L-aspartic acid block. The diameter of particles formed from the dendritic material was determined by

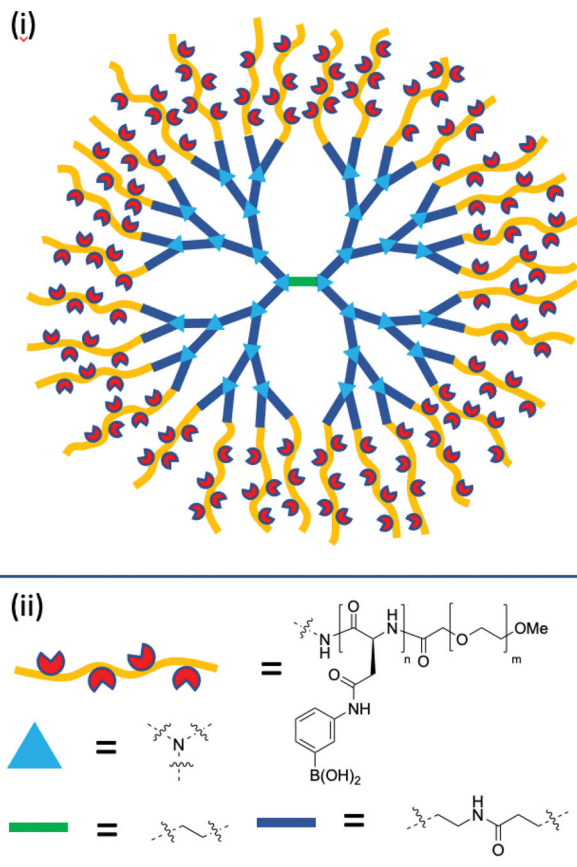
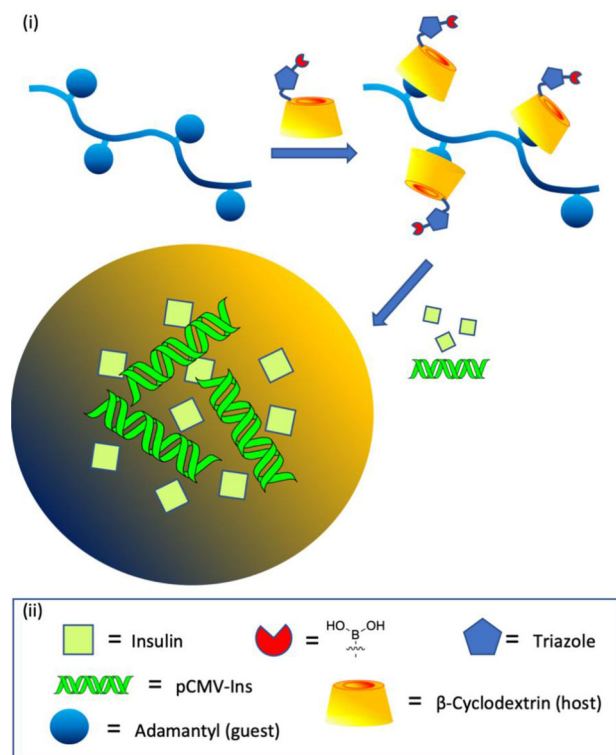


**Figure 11.** The nanoscale dendritic material reported by Liu and co-workers for glucose responsive insulin delivery.<sup>[119]</sup> i) A pictographic representation of the material; ii) Key: Yellow lines featuring red cut out circles represent the boronic acid units bound to a poly-L-aspartic acid block. The blue triangles represent amines acting as three-way linker between repeating polyamidoamine units. Green line represents an ethylene unit. Blue lines represent repeating polyamidoamine units.

TEM to be in the range of 80 to 150 nm. Initial studies of glucose-responsiveness by DLS confirmed that particle size increases upon treatment with glucose. Investigation of insulin release in response to various glucose solutions revealed a glucose concentration-dependent release. In vivo studies on diabetic mice revealed that the tested delivery material had a similar effect to free insulin in stabilising blood glucose.

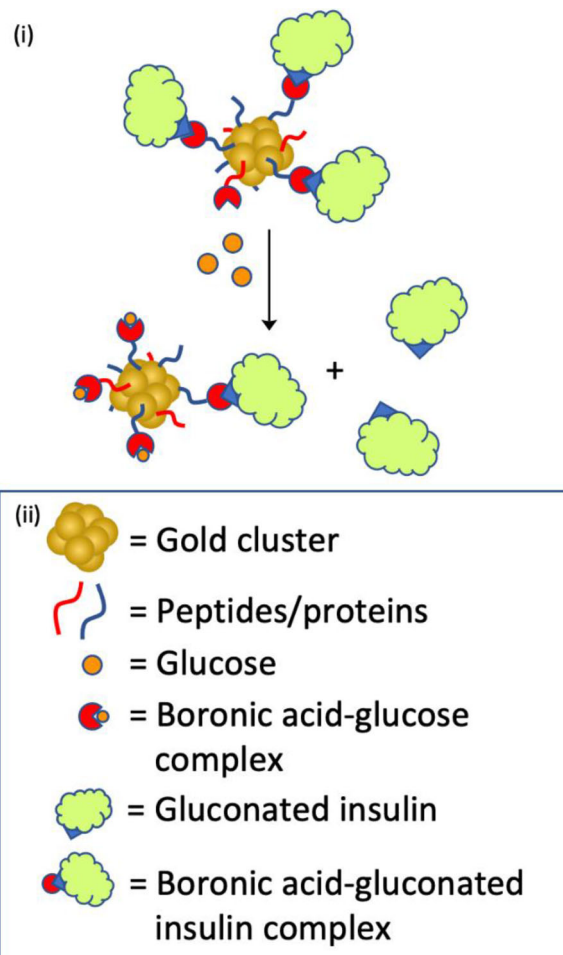
Combination of drug and gene therapy is gaining increasing attention in cancer treatment,<sup>[120]</sup> but Liu and co-workers demonstrated that a similar approach can also be applied in diabetes.<sup>[121]</sup> The authors synthesised nanoclusters composed of polyethyleneimine grafted with adamantyl units, and  $\beta$ -cyclodextrin with pendant 4-carbamoyl-3-fluorophenylboronic acid (**3**) moieties. Noncovalent complexation between the  $\beta$ -cyclodextrin cavity and adamantyl groups enabled the formation of assemblies capable of encapsulating insulin and plasmids containing full length clone DNA of human insulin (**Scheme 11**). These nanoclusters were characterised by TEM, SEM, and DLS. Insulin could be loaded into the nanoassemblies with an efficiency of 84.4% and with a loading capacity of 8.4%. The nanoclusters were able to effectively condense plasmid DNA, as



**Scheme 11.** Liu and co-workers' supramolecular combination insulin and clone DNA delivery system.<sup>[121]</sup> i) A pictographic representation of the host-guest driven formation of nanoclusters that encapsulate insulin and pCMV-Ins. ii) Key: Pale green squares represent insulin. Red cut out circles represent boronic acid units. Blue pentagons represent triazole rings. Lime green double helices represent pMV-Ins. Golden hollow cones represent  $\beta$ -cyclodextrins. Blue spheres represent adamantyl units.

measured by complete condensation of the plasmid DNA at a polyimine nitrogen to DNA phosphorus ratio of  $N/P = 4$ , compared to a ratio of  $N/P = 10$  for nonboronic acid containing nanoclusters. The authors attributed this to the intrinsic affinity of boronic acids to oligophosphates.<sup>[122]</sup> Both insulin release and gene transfection were investigated at 0 and  $27.7 \times 10^{-3}$  M glucose, showing dependence of response on the presence of the glucose stimuli. Insulin secretion of HepG2 cells doubled upon treatment with these nanoclusters, indicating the effectiveness of the gene delivery aspect of this multifunctional tool.

Lei and co-workers developed glucose-responsive materials for insulin delivery based on gold nanoclusters.<sup>[123]</sup> The authors took advantage of the small size of gold nanoclusters (below 5 nm), and their ease of surface modification.<sup>[124]</sup> In their first contribution<sup>[123a]</sup> gold nanoparticles were functionalised with amine groups (using thiol-containing peptides) that were later used for amide formation with 4-carboxyphenylboronic acid or 4-carboxy-3-fluorophenylboronic acid, yielding two distinct materials. This was followed by complexation of gluconic acid-modified insulin with free boronic acid groups. TEM imaging revealed that these insulin delivery systems consisted of spherical gold nanocluster aggregates with a diameter of about 11 nm, and three to six nanoclusters within a complex. The authors reported an insulin loading capacity of their materials of  $951 \pm 174 \mu\text{mol}$  of insulin per gram of gold

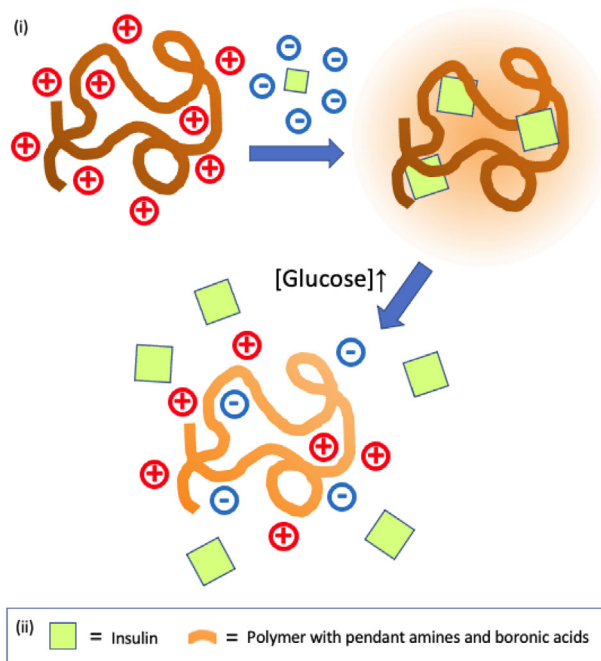


**Scheme 12.** Gold nanocluster-based glucose responsive materials as reported by Lei and co-workers.<sup>[123]</sup> i) A pictographic representation of boronic acid units bound to gold nanoclusters via peptides, and complexed to gluconated insulin. On exposure of the system to glucose the gluconated insulin is released. ii) Key: Aggregated gold spheres represent a gold nanocluster. Red or blue lines represent peptides/proteins. Orange circles represent glucose. Red cut out circles with orange circles represent boronic acid units complexed to glucose. Pale green cloud shapes represent insulin gluconated (grafting the insulin with diols). Pale green cloud shapes with blue triangles represent boronic acid units complexed to the gluconated insulin.

nanoclusters. In vitro insulin release tests at 0, 5.5 and  $22.2 \times 10^{-3}$  M glucose concentrations demonstrated that both materials exhibit glucose concentration-dependent cargo discharge. Slightly better results were obtained for a material containing a fluoro-boronic acid derivative which was attributed to the lower  $pK_a$  of the boronic acid unit in this material. Streptozotocin (STZ)-induced type 1 diabetic mice were used for in vivo testing and both materials were shown to be capable of stabilising blood glucose levels under  $11 \times 10^{-3}$  M for about 20 h without causing hypoglycemia. In their second contribution,<sup>[123b]</sup> the authors prepared gold nanoclusters in the presence of bovine serum albumin (**Scheme 12**) and treated the free amine groups with glutaraldehyde, followed by glycine, to enrich the carboxylic group content Amide coupling with

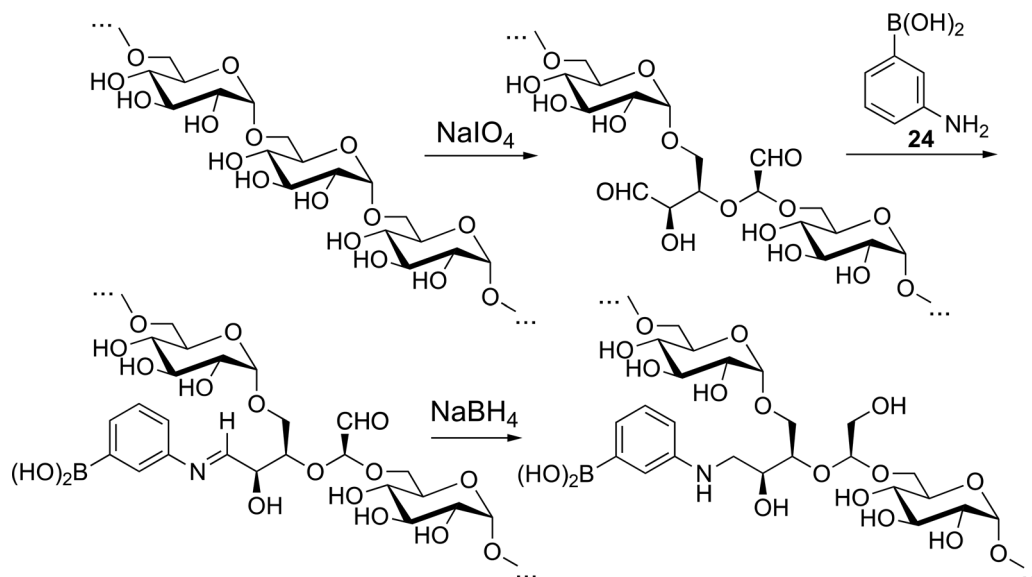
4-aminophenylboronic acid served to graft a glucose-responsive moiety to the surface of the nanoclusters at higher concentrations. This was followed by boronic ester mediated complexation of gluconic acid-modified insulin. TEM imaging of this material revealed that cluster complexes were also formed, with a diameter of about 23 nm with three to eight clusters within a complex. The insulin loading capacity was even higher than for previously reported materials at  $1297.5 \pm 211.1 \mu\text{mol}$  of insulin per gram of gold nanoclusters. In vitro insulin release experiments confirmed glucose concentration-dependent release cargo. Circular dichroism spectroscopic analysis confirmed the integrity of the liberated gluconic acid-modified insulin. The authors investigated the ability of their delivery platform to stabilise blood glucose levels in STZ-induced type 1 diabetic mice. Blood glucose levels were maintained at under  $11 \times 10^{-3} \text{ M}$  for about 20 h. Further increases in blood glucose concentration were slow and it took four days to reach  $20 \times 10^{-3} \text{ M}$ , and hypoglycemia was avoided when using the studied material. Lei and co-workers went on to incorporate their functional nanoclusters into microneedle patches composed of gelatine and starch.<sup>[125]</sup> Such a system performed well for transdermal insulin delivery, the microneedle patches gradually dissolved, liberating loaded insulin nanoclusters which were able to release insulin in response to elevated glucose concentrations. The authors have demonstrated that blood glucose in STZ-induced type 1 diabetic mice can be held within a normoglycemic region for two days by use of these microneedle patches.

Electrostatic interactions for insulin retention and release have been utilised recently by Gu and co-workers.<sup>[126]</sup> The authors synthesised a polyacrylamide-type polymer with pendant primary amine groups. They then coupled about 60% of these amino groups with either 4-carboxy-3-fluorophenylboronic acid or 4-carboxyphenylboronic acid to obtain materials that at pH 7.4 in aqueous solution had a positive net charge, enabling them to bind negatively charged insulin (**Scheme 13**). The cargo release mechanism was based upon creating a negatively charged boronate upon glucose binding, repelling the insulin. Glucose binding experiments revealed that fluoro-boronic acid functionalised material was significantly more efficient, binding approximately twice as much glucose for a given concentration (ranging from 5.5 to  $22.2 \times 10^{-3} \text{ M}$ ). Further insulin release investigations confirmed the glucose concentration-dependence, kinetics and “on-off” capability of this process, with the fluoro-functionalised boronic acid once again being shown to be the most effective. STZ-induced diabetic mice were treated with both types of material, as well as reference substances, to evaluate their influence on blood glucose. The fluoro-boronic acid-derived material stabilised blood glucose levels within the normoglycemic range for about 8.5 h while boronic acid derived material lacking fluorination exerted such effect for only 2 h, which underperformed against the 3 h stabilisation provided by free insulin. The authors went on to evaluate the fluoro-boronic acid derived material in a diabetic Göttingen mini pig model, displaying promising results with no hypoglycemia. Gu and co-workers further extended this concept,<sup>[127]</sup> with the aim to endow their material with biodegradability properties and ensure low and steady basal insulin release. They modified the original polyacrylamide polymer structure to one centered on poly(L-lysine). In order to transform poly(L-lysine) into glucose responsive material that



**Scheme 13.** The polyacrylamide-type polymer containing pendant amino groups, coupled with boronic acid groups, reported by Gu and co-workers<sup>[126]</sup> to be capable of electrostatically binding insulin, with subsequent glucose triggered release. i) A pictographic representation of the electrostatic binding of insulin to the cationic material, with subsequent release as the boronate ester formation that results from glucose complexation neutralises the overall cationic charge. ii) Key: Pale green squares represent insulin. Orange lines represent bulk polymer.

could serve to release insulin the authors functionalised a fraction of the free primary amine groups through amide formation with 4-carboxy-3-fluorophenylboronic acid. The authors thus prepared 35% and 60% boronic acid functionalised materials and insulin loading efficiency was over 90%. The obtained materials employed the same release principle as the aforementioned polyacrylamine material. Coulombic forces between positively charged protonated amine groups and negatively charged insulin were responsible for binding and holding cargo within material, a positive entropy change resulting from anion expulsion was ascribed as an additional insulin retention driving. The insulin liberation process relied upon boronate ester formation upon glucose binding to the boronic acid groups resulting in the formation of negatively charged boronate units thus decreasing effective positive charge and corresponding insulin retention capability resulting in its enhanced release. The authors noted that higher a content of boronic acid units resulted in a material that was more sensitive to glucose giving a more intense release of insulin. The phenomenon was rationalised to be a result of lowering the proportion of positively charged ammonium sites (since a greater proportion of amines were correspondingly converted to lining amide functionalities), and a higher proportion of boronic acid residues were available to bind glucose and accommodate a corresponding boronate-ester negative charge. The authors also demonstrated that the higher the ratio of polymer to loaded insulin, the more strongly insulin is held. This was ascribed to a higher polymer to insulin ratio containing a greater density



**Scheme 14.** The synthetic route toward a nanomaterial developed by Zang and co-workers for nasal insulin delivery.<sup>[128]</sup> Dextran is oxidised with sodium periodate, before undergoing reductive amination with 3-aminophenylboronic acid and sodium borohydride. Different materials were prepared by varying the amounts of 3-aminophenylboronic acid.

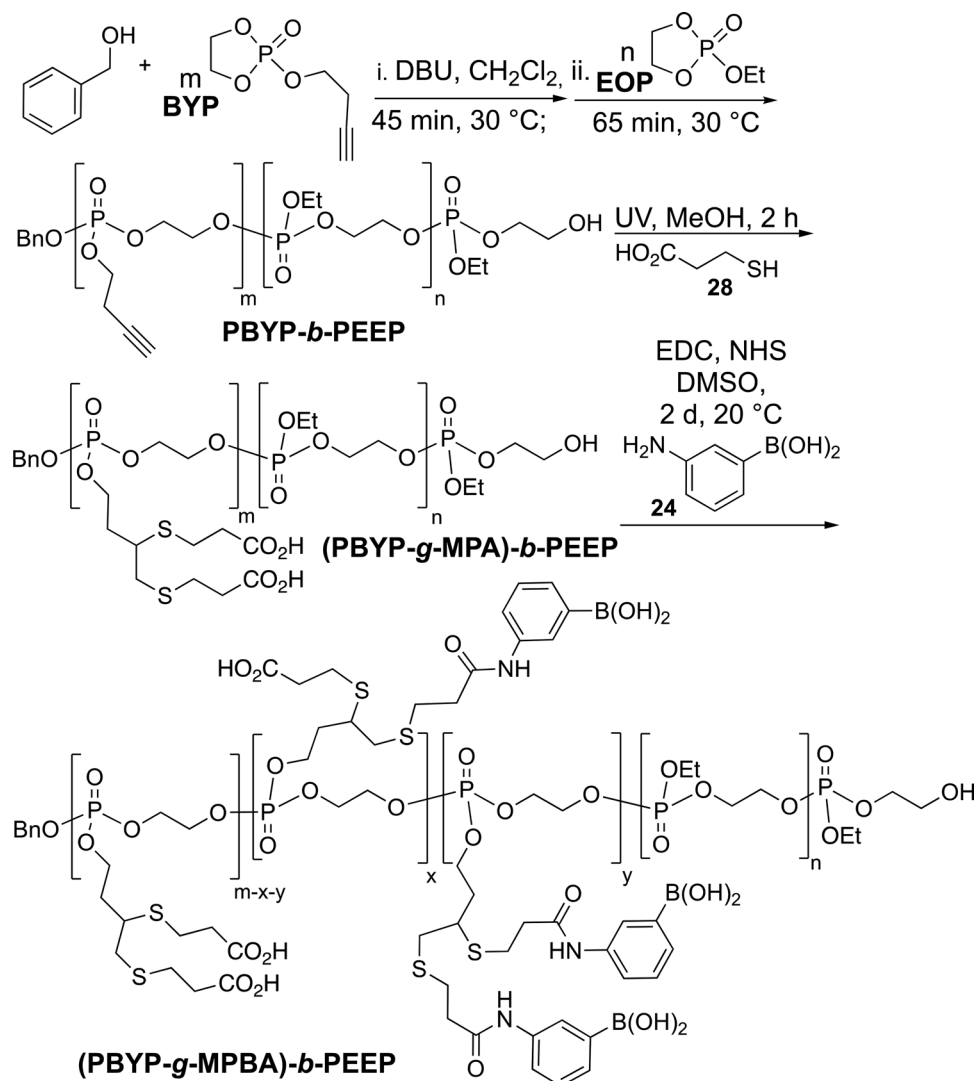
positively charged centers. The molecular weight of the polymer was also of significant impact to the glucose-responsiveness of insulin release, shorter polymer chains were characterised by faster payload release. In vivo testing of blood glucose management was performed in STZ-induced type 1 diabetic mice using recombinant human insulin. The obtained results showed that materials with 35% and 60% boronic acid unit incorporation and a 2:1 polymer to insulin weight ratio worked almost equally well for blood glucose stabilisation, maintaining normoglycemic levels for 20 h. Intraperitoneal glucose tolerance tests revealed that the material with 60% functionalisation by boronic acid units and 2:1 polymer to insulin ratio allowed for most effective plasma insulin increase and blood glucose normalisation.

Wang and co-workers have dedicated their efforts to the preparation of poly(acrylamido phenylboronic acid)/sodium alginate nanoparticles that were able to encapsulate insulin and release it in response to glucose.<sup>[128]</sup> Their particles were proven to dissipate and release entrapped insulin upon action of glucose which competes with the material-stabilising interactions between the alginate's diol units that serve to form boronic ester crosslinks in the absence of glucose. In vivo experiments using diabetic mice showed that insulin loaded particles stabilise blood glucose levels for about 8 h while insulin injection offer equivalent stabilisation for only 2.5 h. Superior results were obtained when GOx and insulin were encapsulated and normoglycemic conditions were maintained for 15 h.

The dynamic chemistry reversibly covalent chemistry of boronic acid derivatives with 1,2- and 1,3-diols was utilised by Zhang in co-workers to develop insulin-delivery materials for nasal administration.<sup>[128]</sup> The authors designed a nanomaterial decorated with boronic acid functionality, such that a high affinity for glycosylated mucin, an essential component of mucus, would manifest and increase residence time in nasal cavity. It is noteworthy that in this case boronic acid derivatives were not used for their glucose-responsive potential, but rather

to enhance its bioadhesion and improve endocytosis. The authors built their nanoparticles about dextran which they oxidised with sodium periodate and then reductively aminated with 3-aminophenylboronic acid **24** (Scheme 14). Different types of materials were prepared varying the ratio of oxidised dextran to **24** from 1:2 to 1:4. The authors noted that the higher proportion of boronic acid units the higher the insulin loading capacity (18.6% to 22.5%). The authors performed insulin release test in PBS buffer (pH 7.4) at 37 °C and found that the higher the content of boronic acid unit, the lower the insulin release (53% to 46% release over 36 h respectively). In both cases this was attributed to hydrophobic interactions between insulin and boronic acid units present in the material. It is feasible that boronate ester mediated crosslinking may be partially responsible for observed results. To study the mucoadhesive properties of their nanoparticles, i.e., interactions with mucin, the authors used turbidimetric measurements and differential scanning calorimetry (DSC). The results confirmed mucin absorption by the tested materials. Further cell viability studies showed good biocompatibility of the nanoparticles and in vivo experiments on diabetic rats were conducted. Where blood glucose levels were indeed lowered after nasal administration of insulin-loaded nanoparticles. The degree of this effect varied from about 20% to 50%, with better results being obtained for material with lowest boronic acid content.

Ni and co-workers developed a glucose responsive insulin delivery system based on diblock polyphosphoester grafted with boronic acid units.<sup>[129]</sup> The authors reasoned that the advantages of polyphosphoesters, such as biocompatibility, biodegradability, facile synthesis and functionalisation at low cost, make polyphosphoesters ideal candidates for creating insulin-release platforms.<sup>[130]</sup> Preparation of their final material consisted of three steps, the first being ring opening polymerisation leading to a diblock polyphosphoester, this was followed by double (*click*) reaction of 3-mercaptopropionic acid (**28**) with an alkyne, the free carboxylic acid groups of which were amide-coupled with

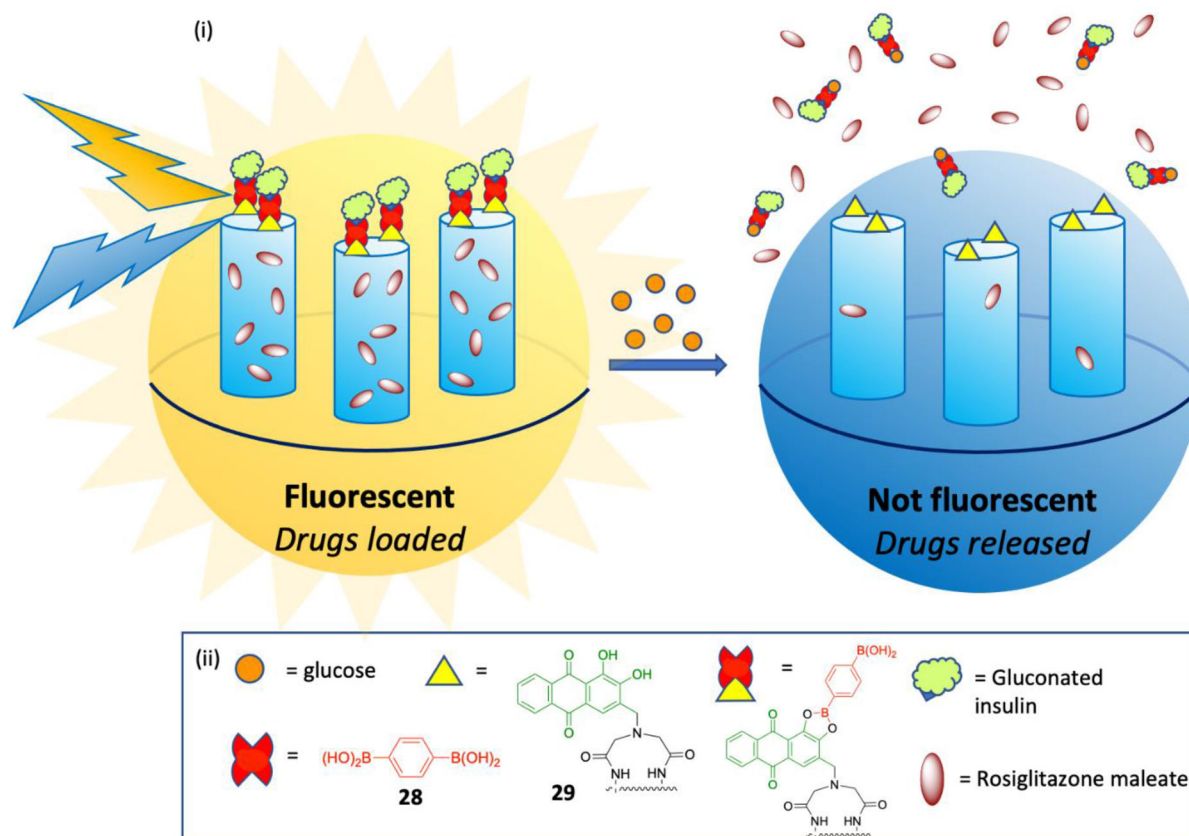


**Scheme 15.** The synthetic route toward the diblock polyphosphoester based glucose responsive insulin delivery system reported by Ni and co-workers.<sup>[129]</sup> Ring opening polymerisation yielded the diblock polyphosphoester (PBYP-*b*-PEEP), which was subsequently thiolated with **28** giving (PBYP-*g*-MPA)-*b*-PEEP. To imbue the material with glucose responsiveness, 3-aminophenylboronic acid **24** was bound through amide coupling to the free acid groups to yield (PBYP-*g*-MPBA)-*b*-PEEP.

**24 (Scheme 15).** This boronic acid-grafted material was able to self-assemble into nanoparticles of  $\approx 114$  nm diameter in aqueous media, as confirmed by DLS. Further studies showed that in the presence of glucose the nanoparticles exhibited swelling, attributed to the boronate ester formation between the saccharide and boronic units within the hydrophobic core of the functionalised polyphosphoester. The resulting boronate ester formation gives rise to a negative charge, with repulsive forces causing the observed increase in size. The authors loaded insulin into their platform using a dialysis method at pH 7.4 in phosphate buffer. In vitro insulin release experiments were carried out over 46.5 h with different glucose concentrations under physiologically relevant conditions. In the absence of glucose 20.4% of the totally entrapped insulin was released. As glucose concentration was increased to  $5.5 \times 10^{-3}$  M,  $11.1 \times 10^{-3}$  M,  $27.7 \times 10^{-3}$  M, and  $55.5 \times 10^{-3}$  M cumulative insulin release was measured at 24.5%,

37.9%, 64.5%, and 86.9%, respectively. CD spectroscopic measurements confirmed the integrity of the insulin discharged from the nanoparticles.

Gated porous silica nanoparticles have been deployed as insulin retention and release platforms. He and co-workers utilised them for simultaneous drug delivery and monitoring thereof.<sup>[131]</sup> In order to obtain the envisioned material, the authors functionalised the surface of porous silica nanoparticles with 3-aminopropyltriethoxysilane, to which alizarin complexone (**29**) was amide-coupled. Next, rosiglitazone maleate (an insulin-sensitizing drug) was loaded into the particles while gluconated insulin was linked to the surface through ditopic interactions between benzene-1,4-diboronic acid (**30**), thus serving as a gate for the cargo-filled pores. Exposure to glucose resulted in competitive displacement of the boronate assembly from the particles, accompanied by dissociation of gluconated insulin, opening the pores,



**Scheme 16.** Gated porous silica nanoparticles developed as a glucose responsive insulin release material by He and co-workers.<sup>[131]</sup> i) A pictographic representation of the rosiglitazone maleate loaded porous silica nanoparticles. Bound to the bisboronic acid, alizarin complexone (**29**) is fluorescent, and the other end of the bisboronic acid (**28**) binds to the gluconated insulin to “cap” the pores. As the system is exposed to glucose, the alizarin unit is displaced by glucose, turning off the fluorescence and releasing both the gluconated insulin and the previously encapsulated rosiglitazone maleate. ii) Key: Orange circles represent glucose. Yellow triangles represent alizarin complexone unit. Red dual cut out figures of eight represent bisboronic acid units. Red dual cut out figures of eight with a yellow triangle represent bisboronic acid unit bound on one side to alizarin. Pale green cloud shapes with blue triangles represent insulin gluconated (grafting the insulin with diols). Burgundy ovals represent rosiglitazone maleate.

allowing for rosiglitazone maleate release, as well as loss of spectral emission of the alizarin unit (**Scheme 16**). These events were correlated proportionally to glucose concentration, enabling real-time fluorescence monitoring of glucose-responsive cargo release. In addition to studying this system in physiologically relevant conditions the authors also used human serum as a medium to better evidence the potential of this material for application in a real-world setting. A claim further bolstered by the material's biocompatibility and low hemolytic activity.

Another example of insulin retention and controlled release from gated silica nanoparticles was reported by Lin and co-workers.<sup>[132]</sup> The authors prepared silica amine-functionalised nanoparticles that were amide-coupled to 4-carboxyphenylboronic acid. This material was loaded with insulin, and sodium alginate was then deposited to serve as a gatekeeper, blocking the channels. Boronate formation between boronic acid residues and 1,2-diol moieties from sodium alginate served well to ensure low level of insulin release without the presence of glucose; after 8 h about 8% of the loaded insulin was discharged. At glucose concentrations of  $11.1 \times 10^{-3}$  and  $27.7 \times 10^{-3}$  M cumulative insulin release after 8 h reached  $\approx 29\%$  and  $39\%$  respectively (**Scheme 17**). Moreover, with alternating glu-

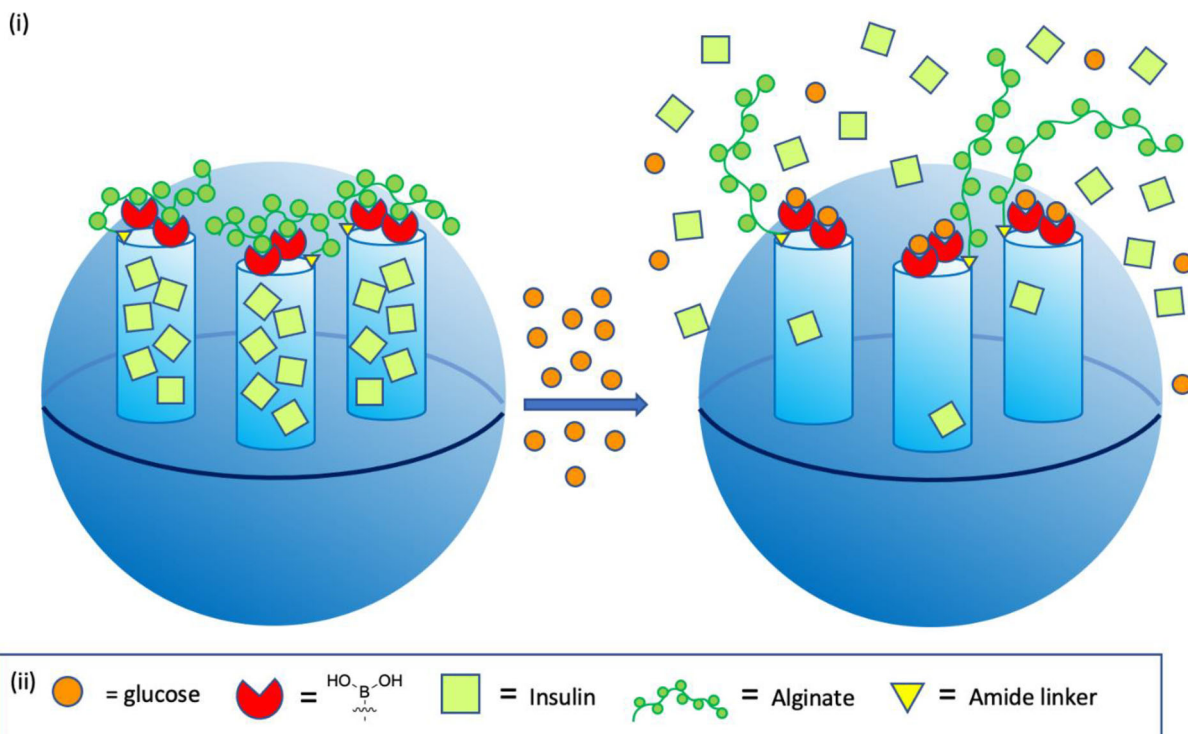
cose concentration the authors observed an alternating release profile, demonstrating the ability of the particles to perform “on-off” release cycles in this regime. CD spectroscopic analysis confirmed the integrity of the released insulin. Cell viability and hemolysis assays proved the nanoparticles to be nontoxic, and they were taken forward to in vivo studies. Experiments on diabetic mice provided evidence that a single dose of insulin loaded gated nanoparticle was able to stabilise blood glucose level for 12 h. The authors also proved that their material alleviated lipid metabolism disorder and organ damage of diabetic mice after treatment.

## 9. Gel-Particle Hybrids

Gel-particle hybrid materials display a number of properties desired in controllable drug delivery, e.g., decrease in burst release, injectability resulting from shear thinning, rapid stimuli responsiveness and better control of the discharge process.<sup>[133]</sup> These potential advantages have underpinned and inspired developments in insulin delivery systems.

To protect insulin loaded into nanoparticles from degradation in the gastrointestinal tract, Jiang and co-workers protected





**Scheme 17.** Porous gated silica nanoparticles as a glucose responsive insulin release system, as reported by Lin and co-workers.<sup>[132]</sup> i) A pictographic representation of the alginate capped pores in silica nanoparticles releasing their loaded insulin in response to glucose. The glucose complexes the boronic acids, displacing the alginate, removing the “cap” and enabling the insulin to diffuse out. ii) Key: Orange circles represent glucose. Red cut out circles represent boronic acid units. Pale green squares represent insulin. Green chains represent alginate polymers. Yellow triangles represent amides that link the alginate to the particle.

them in a hydrogel.<sup>[134]</sup> The authors prepared insulin loaded glucose-responsive nanocarriers by copolymerisation of 4-vinylphenylboronic acid, acrylic acid, folic acid conjugated poly(ethylene glycol) acrylate and ethylene glycol dimethacrylate in the presence of insulin. A further coating of hyaluronic acid and divinyl sulfone crosslinker was applied. The authors showed that the obtained nanoparticles are capable of insulin retention and release at different rates depending upon applied glucose concentrations. Moreover, in a comparative study between hydrogel coated and noncoated nanoparticles the hydrogel coating was shown to decrease insulin release in acidic conditions (pH 1.2) and give a more sustained release profile at close to neutral conditions (pH 6.8). CD spectroscopy corroborated the integrity of the released cargo, and cell viability studies gave good results. The authors tested their platform in vivo using diabetic rats. Over a 10 h study, hydrogel coated nanoparticles loaded with insulin were able to effectively lower and stabilise blood glucose levels more effectively than injection of insulin, even at loadings 15 times lower than the injected insulin. The authors also observed that nanoparticles without a hydrogel coating were unable to lower blood glucose as effectively, thought to be due to degradation in gastrointestinal tract.

Wang and co-workers developed an injectable hydrogel-particle hybrid with impressive blood glucose level-stabilising properties.<sup>[135]</sup> First, poly(lactic-co-glycolic) and porous microspheres were obtained via a modified water-in-oil-in-water double emulsion method<sup>[136]</sup> followed by amide coupling between

surface carboxylic acid groups and 3-aminophenylboronic acid (24). Insulin loading capacity was determined to be  $35.6\% \pm 4.5\%$  while the efficiency of this process was  $45.8\% \pm 2.9\%$ . These insulin loaded particles were embedded in a dopamine-modified hyaluronic acid hydrogel. Thanks to the presence of catechol-type diol units, a dense hydrogel layer was formed at the nanoparticle surface that positively influenced the properties of the drug releasing platform. This material was shown to be injectable and to display good bio-adhesion, attributed to dopamine moieties in hydrogel structure. In vitro studies of insulin release were performed in physiologically relevant conditions (37 °C and pH 7.4). Under normoglycemic conditions the investigated material discharged only about 7% of the loaded insulin over 24 h ( $5.5 \times 10^{-3}$  M glucose). For a hyperglycemic glucose concentration of  $16.6 \times 10^{-3}$  M  $\approx 11\%$  of the loaded insulin was released within the same time frame. Very high glucose concentrations ( $27.7 \times 10^{-3}$  and  $55.5 \times 10^{-3}$  M) were required to elicit 32% and 77% cumulative release, respectively and “on-off” insulin release was demonstrated (Figure 12). CD spectroscopic investigation evidenced the integrity of released insulin. In vitro cytotoxicity and in vivo studies confirmed the investigated material to have good biocompatibility. In vivo studies and appropriate control were conducted with diabetic mice. While injection of an insulin solution offered a fast-acting reduction in blood glucose level to a healthy level, within one day this level returns to the same as that of the control experiments. Whereas administering insulin that is loaded into the described microporous-gel healthy blood glucose levels

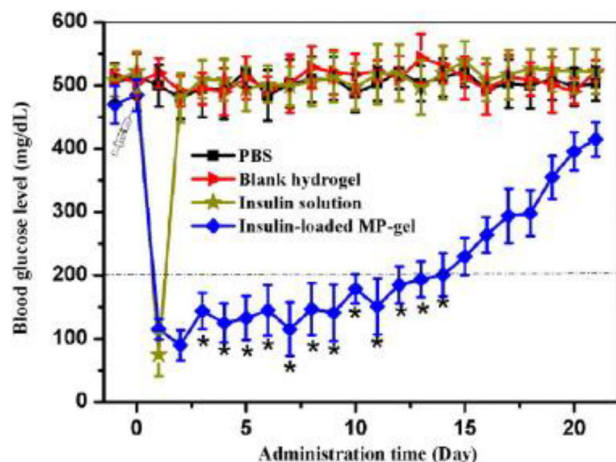


**Figure 12.** Results of in vivo studies on blood glucose levels in STZ-induced diabetic mice treated with microparticle–hydrogel hybrid system (MP–gel) loaded with insulin and other reference substances administered by a single abdominal subcutaneous injection. Values represent mean  $\pm$  standard deviation ( $n = 5$  per group). \* $p < 0.05$ . Reproduced with permission.<sup>[135]</sup> 2017, Elsevier.

were maintained for fourteen days. Notably glucose levels in the treated group did not reach the level of the control group over the course of the 21-day study.<sup>[135]</sup>

A dual glucose-sensing and glucose-mediated insulin-delivery nanoparticle–gel material was reported by Zhou and co-workers.<sup>[137]</sup> The authors hypothesised that upconversion carbon quantum dots could serve as a fluorescent probe for glucose sensing when anchored in a glucose-responsive hydrogel network which undergoes volume phase transition upon external stimuli, simultaneously discharging encapsulated cargo. One step radical copolymerisation of 4-vinylphenylboronic acid, acrylamide and *N,N'*-methylenebisacrylamide in the presence of carbon dots yielded the desired material. Photoluminescence studies showed a linear response to glucose concentrations up to  $20 \times 10^{-3}$  M, indicating suitability to function as a sensor within this range. After loading insulin into the material, its release at physiologically relevant conditions was studied. Cargo discharge was dependent on glucose concentration, in the absence of glucose  $\approx 15\%$  cumulative release was noted within 48 h, whereas in the presence of  $20 \times 10^{-3}$  M concentrations of glucose  $\approx 80\%$  of the retained insulin was released over the same time frame. Toxicity studies revealed good biocompatibility of the studied material incentivizing further studies.

Liu and co-workers aimed to address the problems of vascular diabetes complications as well as stabilise blood glucose through the use of a micelle-hydrogel hybrid glucose-responsive system.<sup>[138]</sup> The authors envisioned a system capable of delivering both insulin nattoxinase, a thrombolytic agent capable of reducing vascular diabetes complications.<sup>[139,140]</sup> The authors derivatised starch dialdehyde by transforming it into a polymerisation macroinitiator through partial esterification with 2-bromoisobutryl bromide, followed by single electron transfer living radical polymerisation with 4-vinylphenyl boronic acid. The obtained material was further reacted with a 3-aminopropanesulphonic acid derived zwitterionic alkylating agent, yielding a material capable of forming micelles. Assembly

of micelles in insulin solution yielded cargo-loaded particles that were then introduced into a solution chitosan and nattoxinase. Cargo release properties of the obtained hybrid systems were tested under physiological conditions in the presence of glucose at  $0 \times 10^{-3}$ ,  $5.5 \times 10^{-3}$  M and  $16.6 \times 10^{-3}$  M concentrations. For both insulin and nattoxinase, burst release was observed in the initial stage. The cumulative release of nattoxinase was similar for each glucose concentration, ( $\approx 80\%$  after 50 h); however, the release of insulin was shown to be more glucose dependent. At  $0 \times 10^{-3}$  M glucose up to 20% of loaded insulin was released after 72 h, while for 5.5 and  $16.6 \times 10^{-3}$  M glucose  $\approx 35\%$  and 50% of loaded insulin was released, respectively over the same timeframe. The authors also undertook thrombolytic tests using their synergistic dual delivery therapy system and blood clots were successfully dissolved.

A micelle-hydrogel hybrid formulation was identified by Ma and co-workers as a suitable platform for dual-mode insulin delivery, offering gradual sustained release that could be increased with increasing glucose concentrations.<sup>[141]</sup> This composite material was designed in such way that both components, the micelles and the hydrogel, were endowed with glucose responsiveness, though originally only micelles were loaded with insulin. Moreover, boronic acid moieties in the micelles (derived from 3-aminophenylboronic acid **24**) were of lower acidity than boronic acid moieties in the hydrogel (derived from 3-fluoro-4-carboxyphenylboronic acid). It is noteworthy that the binding partner diols both in micelles and hydrogels were polypeptides functionalised with D-aminogalactose. The authors reasoned that the diol-binding capabilities the two types of boronic acid in the hydrogel and micelle parts of their system will permit a tuned glucose response across ranges of glucose concentration regimens. Therefore, under hyperglycemic conditions both the hydrogel and micelles should be primed to deliver cargo resulting in rapid insulin release. While under normoglycemic states the micelles could still release insulin but entrance to the bloodstream would be controlled by the hydrogel matrix in which boronate crosslinks would be formed again, slowing the release. Both micelles and hydrogel were individually studied for glucose induced insulin release under physiological conditions (pH 7.4 and 37 °C) at glucose concentrations of 0, 5.5,  $11.1 \times 10^{-3}$  and  $27.7 \times 10^{-3}$  M. Insulin release profiles for the two systems were significantly different, for the hydrogel cumulative release of insulin after 45 h at 5.5 and  $11.1 \times 10^{-3}$  M glucose was about 5%, while for micelles it was close to 30% over the same range. This divergence in insulin release potential across these glucose concentrations was further emphasised to 40% under equivalent conditions for a hybrid material containing both micelles and hydrogel. The authors confirmed that release rate could be modulated by switching glucose concentration between  $5.5 \times 10^{-3}$  and  $27.7 \times 10^{-3}$  M. CD spectroscopic analysis of the released insulin confirmed its integrity. STZ-induced type 1 diabetic mice were used for in vivo testing of the insulin-loaded hybrid material, which showed the tested material to be able to maintain healthy glucose level for up to 24 h. In a separate experiment it was also proven that blood glucose level can be stabilised after injections of glucose, a critical stress test of the system akin to a diabetic patient eating a meal. The hydrogel and micelles alone were not as effective; in the case of the hydrogel hypoglycemia was detected, which could be attributed to the large pore size of hydrogel allowing for insulin to

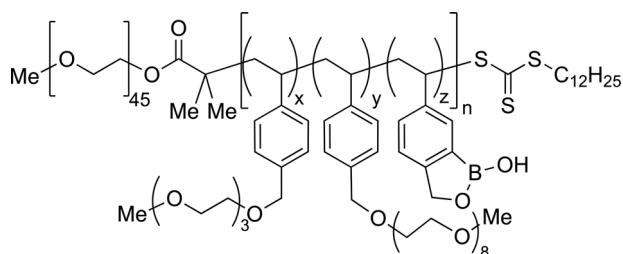


**Figure 13.** Jeong et al.'s<sup>[143]</sup> block copolymers of polyethylene monomethyl ether and copolymeric blocks derived from styreneboroxole and oligo(ethylene glycol)-functionalised styrene, capable of forming vesicles able to release insulin in response to glucose.

be released freely rather than modulated by glucose concentration fluctuations.<sup>[141]</sup>

## 10. Micelles and Vesicles

Micelles and vesicles are structures assembled from amphiphilic compounds. Micelles are particles with a core-shell structure with amphiphile fragments of the same polarity grouping together either inside of a sphere or at its surface, while vesicles are bilayer hollow spheres.<sup>[142]</sup>

Jeong et al. utilised RAFT to obtain a series of block copolymers with polyethylene monomethyl ether block and copolymeric blocks derived from styreneboroxole and oligo(ethylene glycol)-functionalised styrenes (**Figure 13**).<sup>[143]</sup> The amphiphilic polymers that were obtained could self-assemble into vesicles that were analyzed by TEM and DLS. The authors successfully encapsulated insulin into the assemblies, and performed an experiment demonstrating glucose responsive release of the protein in the absence and presence ( $100 \times 10^{-3}$  M) of glucose.

A micellar insulin delivery system integrating glucose- and UV-responsiveness has been developed by Jiang and co-workers.<sup>[144]</sup> The authors synthesised an amphiphilic copolymer with one block derived from acrylamide or poly(ethylene glycol) monomethyl ether amine, and the other based on **13** and 2-nitrobenzylacrylate monomers, endowing the resulting material with glucose- and UV-responsive properties, respectively. To improve the stability of the resultant micelles a small quantity of *N,N'*-bis(acryloyl)cystamine was used. Insulin could be loaded into micelles during polymerisation process with a capacity of 25.6%. The authors demonstrated that UV irradiation ( $\lambda_{\text{max}} = 365$  nm,  $75$  mW  $\text{cm}^{-2}$ ) could cause near quantitative release of insulin within 30 min, as a result of photo-induced micelle degradation brought about by ester cleavage. During these investigations negligible insulin discharge was observed (about 5%) in the absence of glucose, however in  $5 \times 10^{-3}$  M glucose solutions  $\approx 50\%$  cumulative insulin release was observed, reaching 93% release at  $25 \times 10^{-3}$  M glucose, characterised by burst release in the initial stages. CD spectroscopic analysis confirmed the integrity of the released insulin.

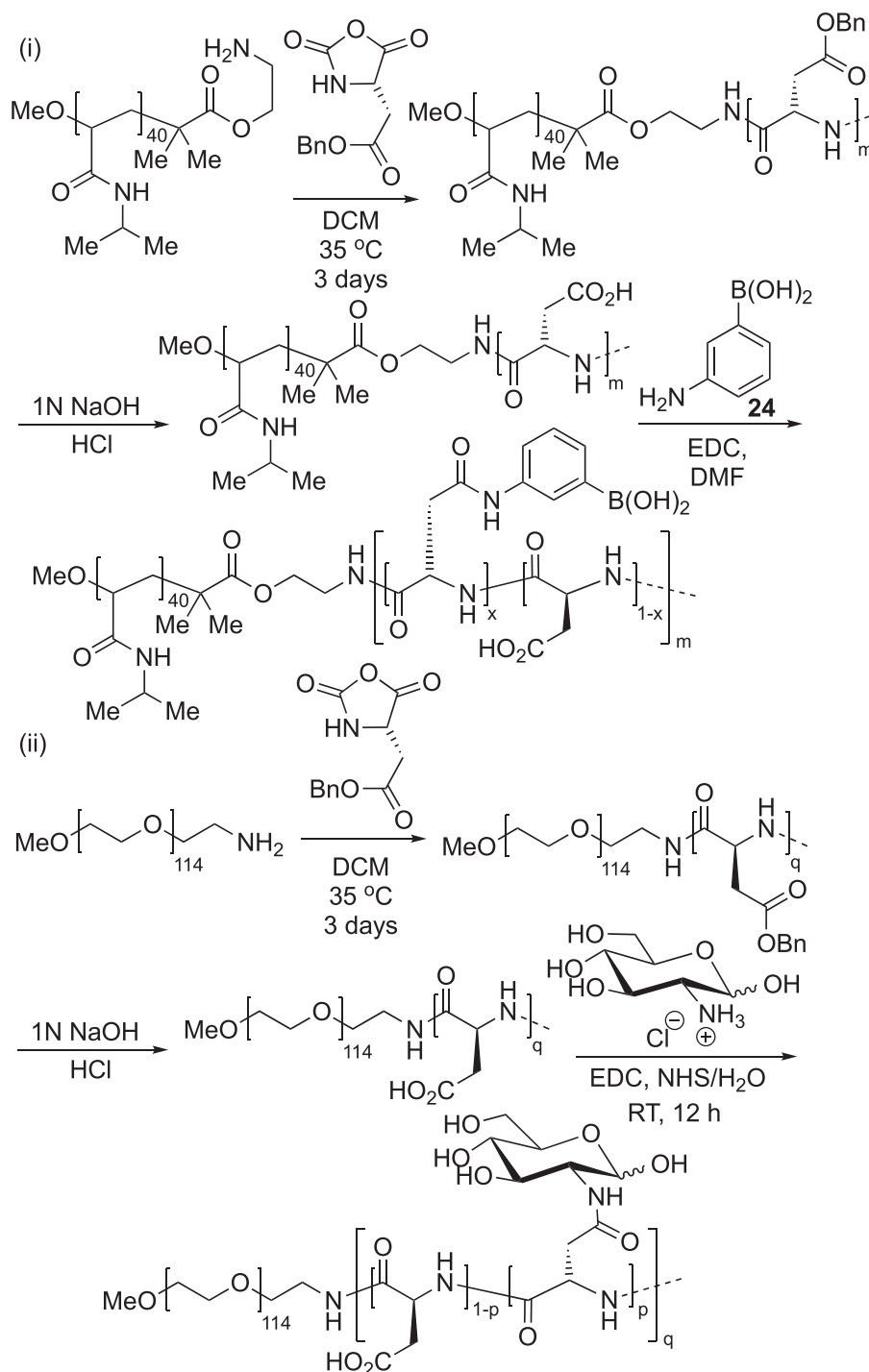
Continuing their efforts to develop micellar insulin delivery platforms, Jiang and co-workers created systems based on random copolymers of **13** and PEG monomethyl ether methacrylate.<sup>[145]</sup> These monomers were polymerised in a radical process using 3-phenylpyruvic acid as a photo-initiator, at

which point insulin could be loaded into the micelles. The authors found that insulin release was temperature dependent, with increased temperature causing increased release. The glucose sensitivity of the system was also investigated; within 24 h in the absence of glucose about 20% of insulin was released. This value rose significantly, accompanied by burst release, to 60% for  $5.5 \times 10^{-3}$  M glucose concentration and to  $\approx 75\%$  and 80% cargo release for  $11.1 \times 10^{-3}$  and  $27.7 \times 10^{-3}$  M glucose concentrations, respectively.

In a following contribution, Jiang and co-workers used photopolymerisation combined with enzymatic transesterification to obtain a micelle-forming random copolymer capable of insulin encapsulation and glucose-responsive release.<sup>[146]</sup> The authors used 4-vinylphenylboronic acid, trifluoroethyl methacrylate and 9-anthracenylmethyl methacrylate as monomers. Trifluoroethyl groups were substituted with poly(ethylene glycol) chains in enzymatic transesterification catalyzed by *Candida antarctica* lipase B enzyme. The resulting polymer could form micelles, as demonstrated by DLS analysis and TEM imaging. The anthracene moieties within the assemblies imbued them with inherent fluorescence. Insulin was successfully loaded into the micelles post-polymerisation and its release in response to glucose was studied in PBS solution, pH 7.4. Regardless of glucose concentration burst discharge was observed in initial stages; in the absence of glucose  $\approx 25\%$  of loaded insulin was released within 24 h. At  $11.1 \times 10^{-3}$  M glucose almost 50% of loaded insulin was released, while for  $27.7 \times 10^{-3}$  M glucose 80% of loaded insulin was discharged. Cell viability studies proved good biocompatibility of the studied material.

A combination of controlled polymerisation techniques and click chemistry<sup>[147]</sup> allowed Yang and co-workers to obtain an amphiphilic brush copolymer, able to form micelles with thermo- and glucose-responsive properties.<sup>[148]</sup> The authors used atom transfer radical polymerisation (ATRP) to obtain an alkyne-terminated polymer comprising of boronate-containing units derived from (2-phenylboronic esters-1,3-dioxane-5-ethyl) methacrylate. Next, RAFT and nucleophilic substitution were used to obtain a block copolymer containing benzyl azide and mixed oligo(ethylene glycol) monomethyl ether units. CuAAC was employed to graft the boronate-containing polymer to the alkyne terminated polymer chain by a formed triazole linkage. The obtained polymer was capable of self-organizing into micelles in water, with a boronate-rich core and oligo(ethylene glycol) monomethyl chains segments in its corona. The presence of glucose caused swelling of the micelle core, while a temperature rise the lower critical solution temperature (LCST) of the hydrophilic block ( $38$  °C) resulted in shrinkage of the micelle outer layer. Both phenomena impacted insulin release, with the influence of glucose being more pronounced. At in the absence of glucose at  $37$  °C and pH 7.4  $\approx 30\%$  of loaded insulin was released over 70 h. Under normoglycemic conditions ( $5.5 \times 10^{-3}$  M glucose)  $\approx 40\%$  of loaded insulin was released, while under hyperglycemic ( $11.1 \times 10^{-3}$  M glucose) this value increased to 60% release. The authors also demonstrated the "on-off" release capability of this material by alternating glucose concentrations between  $5.5$  and  $27.7 \times 10^{-3}$  M.

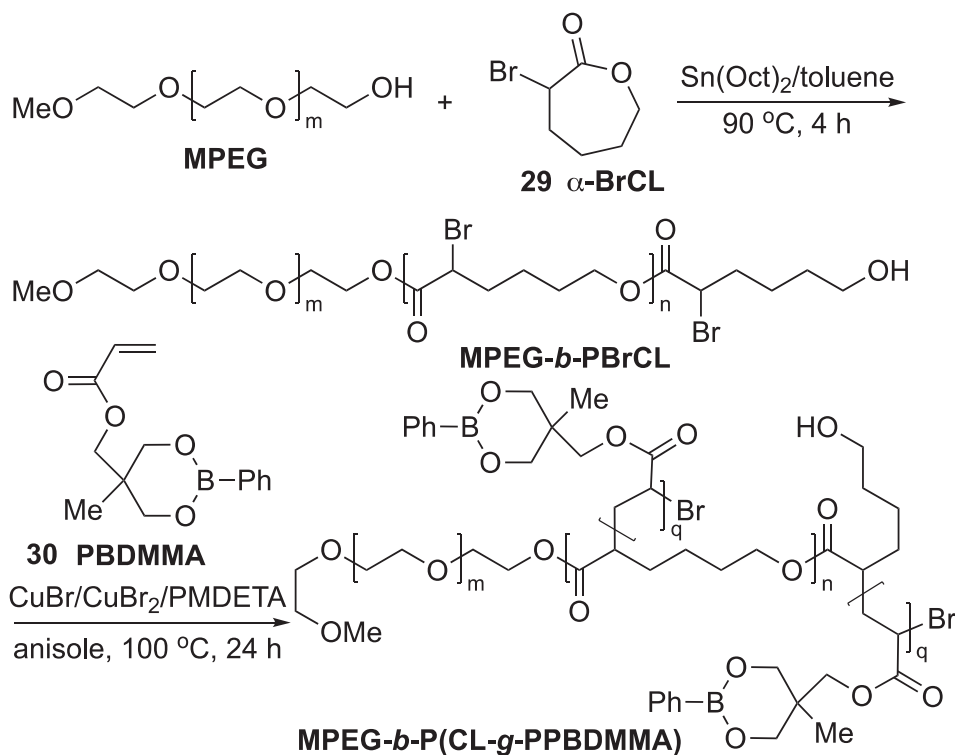
An interesting approach was taken by Shi and co-workers, who prepared a vesicular insulin delivery system obtained from complex micelles with a thermo-responsive core.<sup>[65b]</sup>



**Scheme 18.** The synthetic route toward the polymer used by Shi and co-workers to produce temperature and glucose responsive vesicles.<sup>[65b]</sup> i) an L-aspartic acid block is copolymerised onto a PNIPAM block, and subsequently reacted with **24** to imbue glucose sensitivity. ii) A PEG block is copolymerised onto a PNIPAM block, and subsequently reacted with **24** to imbue glucose sensitivity.

The authors first synthesised a block copolymer consisting of a poly(*N*-isopropylacrylamide) (PNIPAM) block, offering thermo-sensitive properties, and an L-aspartic acid derived block, functionalised by partial amide formation with **24** (Scheme 18). This polymer was able to form micelles capable of insulin en-

capsulation in aqueous medium at 45 °C. The obtained micelles were further transformed by covering them with a hydrophilic copolymer that contained glucosamine units. Crosslinking between the boronic acids and the glucosamine diol groups of the two polymers resulted in the formation of complex



**Scheme 19.** The synthesis of poly( $\epsilon$ -caprolactone) derived polymer described by Yang and co-workers.<sup>[149]</sup> PEG monoether was reacted with **29** to form a block copolymer. Through ATRP (2-phenylboronic esters-1,3-dioxane-5-ethyl) methacrylate (**30**) side chains are then bound to the poly( $\epsilon$ -caprolactone) backbone.

core-shell-corona micelles. Storing these constructs below the LCST of PNIPAM core (34.5 °C) resulted in transformation of these complex micelles into vesicles. In this study two types of complex micelles were obtained by using different ratios of boronic acid- and glucosamine-containing copolymers, namely 1:0.8 and 1:1.5. The authors noted that complex micelles could not be produced if the glucosamine-containing copolymer was used in less than a 0.8 weight ratio in relation to the boronic acid-containing copolymer. Micelles with a 1:0.8 copolymer ratio were further transformed into vesicles. DLS measurements and TEM imaging revealed that complex micelle to vesicle transition is accompanied with size expansion, ascribed by authors to water absorption. These techniques were also employed to demonstrate vesicle swelling upon treatment with glucose. Insulin release was investigated at physiologically relevant conditions (37 °C, pH 7.4) and glucose dependent behavior was demonstrated. In all cases burst discharge was observed in the initial stages; in the absence of glucose cumulative insulin release was below 15%, while at  $27.7 \times 10^{-3}$  M glucose this value reached 40% after 70 h, which increased to 80% at  $111 \times 10^{-3}$  M glucose over the same period. The authors also demonstrated that the system they developed is capable of “on-off” cargo release.

Yang and co-workers worked toward developing degradable micelles that exhibit glucose-sensitivity.<sup>[149]</sup> The authors envisioned that incorporating poly( $\epsilon$ -caprolactone) would endow a material with good degradability properties. Therefore, they prepared a block copolymer by ring opening polymerisation using  $\alpha$ -bromo- $\epsilon$ -caprolactone (**29**) and poly(ethylene glycol) monomethyl ether as an initiator. Next, ATRP was employed to

graft (2-phenylboronic esters-1,3-dioxane-5-ethyl) methacrylate (**30**) derived sidechains onto the poly( $\epsilon$ -caprolactone) backbone (**Scheme 19**). The authors prepared a series of three copolymers differing in length of the boronate-containing block, yielding polymers capable of forming micelles that could encapsulate insulin. The encapsulation process was more effective with higher boronate content (up to 74%), while the loading capacity was essentially the same for all studied materials (about 17%). Three types of polymeric micelles were studied for insulin release under physiologically relevant conditions 0, 5.5, and  $16.6 \times 10^{-3}$  M glucose concentrations. Remarkably, no burst release was observed in any case and no insulin release was observed over 30 h from any material. In the absence of glucose 10% of loaded insulin was released at 70 h, at  $5.5 \times 10^{-3}$  M glucose  $\approx$ 30% of loaded insulin was released and up to 100% of loaded insulin was released at  $16.6 \times 10^{-3}$  M glucose over the same timeframe. Importantly, the insulin release profiles of the three tested materials differed little under no or low ( $5.5 \times 10^{-3}$  M) glucose concentrations; however, at higher glucose concentrations the impact of the material's boron content was manifest, i.e., increased boronate content renders insulin release less efficient. CD spectroscopy confirmed the integrity of the released insulin, and good biocompatibility was confirmed via cell toxicity assays. The authors studied the degradability of their material by monitoring the release of insulin from drug loaded micelles in the presence of Novozym 435 lipase. Without the enzyme less than 10% of insulin was discharged over 50 h, while in presence of lipase quantitative cargo delivery was realised within that time. Gel permeation chromatography (GPC) analysis of

decomposition products revealed hydrolysis of the poly( $\epsilon$ -caprolactone) backbone.

In a subsequent contribution Yang and co-workers, guided by the intention of improving salt-tolerance, developed another complex nanoparticle carrier for glucose-responsive insulin delivery.<sup>[150]</sup> The authors sought to take advantage of stabilising effect of hydrogen bonding in polyamides and developed a platform that consisted of two block copolymers, both containing a poly(ethylene glycol) block, with the second block being either a polymer chain derived from 30 or poly( $\gamma$ -benzyl-L-glutamate). These two materials were combined in differing ratios to yield micellar assemblies. These micelles were analyzed with CD spectroscopy and structural composition assigned, showing an increased ratio of  $\alpha$ -helix structures with increasing size of the poly( $\gamma$ -benzyl-L-glutamate) block. This was accompanied by a reduction in the population of  $\beta$ -sheet structures. Next, the authors loaded insulin into their formulations and studied the stability of the assemblies against salt by monitoring cargo release. The best results were obtained for micelles composed of 75 wt% of polyamide-containing copolymer which released only 12% of loaded insulin within 12 h (0.15 M PBS). The structures of these best-performing micelles were studied by CD spectroscopy, and changes with time were observed, whereby the  $\alpha$ -helix content drops at as  $\beta$ -sheet content increases. Glucose-mediated insulin release was also studied (0.15 M PBS, pH 7.4 at 37 °C). In an observation similar to the previous contribution of Yang and co-workers burst release was not observed. Materials with a higher content of poly( $\gamma$ -benzyl-L-glutamate) showed high divergence in payload discharge between normo- and hyperglycemic conditions,  $\approx$ 20% versus 100% loaded insulin release within 90 h respectively. Cell toxicity assays of the investigated material yielded good results.

Yang and co-workers further explored their glucose responsive platform for insulin delivery in context of how the polyamide component's secondary structure influenced the payload discharge process.<sup>[151]</sup> The authors prepared equivalent sets of two block copolymers, with higher degrees of polymerisation in poly( $\gamma$ -benzyl-L-glutamate) block. Next, partial hydrolysis of benzyl esters was performed yielding two derivatives with ester to carboxylic acid ratios of 20:40 and 48:12 (Figure 14). The difference in free carboxylic acid content resulted in hydrogen bonding differences, leading to differences in secondary structure, as evidenced using CD spectroscopy. At physiological pH (7.4) the  $\alpha$ -helical form was the dominant structural motif for the copolymers with no carboxylic acid groups, while copolymers with 20:40 and 48:12 ester to carboxylic acid group ratios random coil and  $\beta$ -sheet structures predominated respectively. The incorporation of boronate units into the block copolymer did not disrupt the tertiary structure of these polyamides. Three types of assembly were obtained and TEM served to determine their morphology that varied from irregular nanopatterns with tentacles, through to willow leaf-like shapes, to nearly spherical micelles for assemblies made from the copolymer with no carboxylic acid groups. Insulin release and salt stability studies in the absence of glucose proved that these micellar assemblies show low cargo release (0.15 M PBS) over a prolonged period of time ( $\approx$ 10% cumulative loaded insulin release after 90 h). Under normoglycemic conditions ( $5.5 \times 10^{-3}$  M glucose)  $\approx$ 20% cumulative release of loaded insulin occurred after 90 h, while significant increases in insulin re-

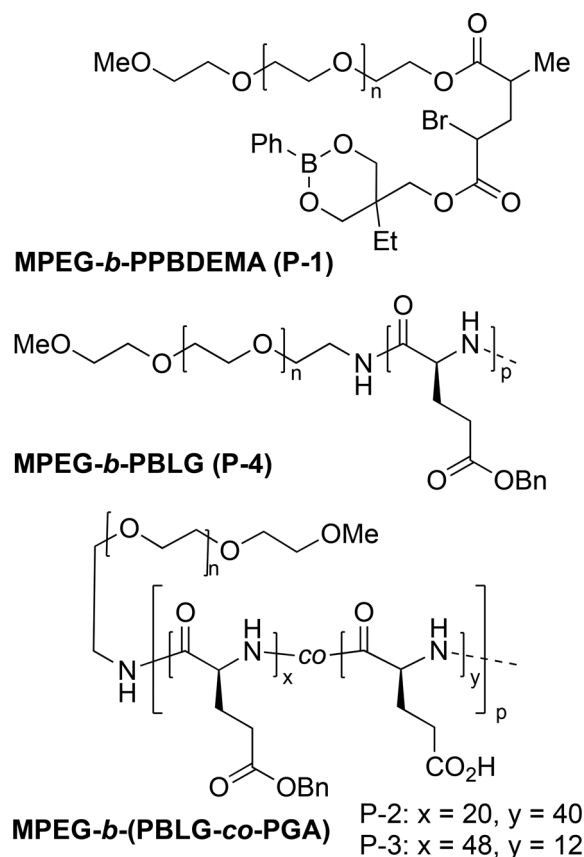
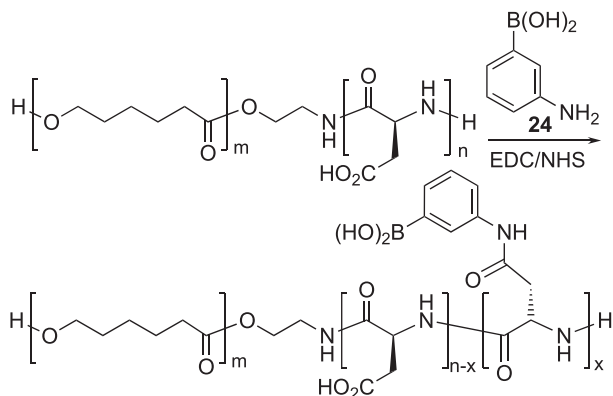


**Figure 14.** The structure of block copolymers **MPEG-b-PPBDEMA (P-1)**, **MPEG-b-PBLG (P-4)**, **MPEG-b-(PBLG-co-PGA) (P-2)**, and **MPEG-b-(PBLG-co-PGA) (P-3)** reported by Yang and co-workers.<sup>[151]</sup>

lease were observed under elevated glucose concentrations ( $11.1 \times 10^{-3}$  and  $16.6 \times 10^{-3}$  M) under the same conditions at the same time ( $\approx$ 75% and 90% cumulative loaded insulin release, respectively). The two other materials displayed inferior properties, in terms of both salt stability and insulin release discrimination for different glucose concentrations, attributed by the authors to the differences of secondary structures of polyamide components of the assemblies. Furthermore, blood compatibility of the best performing carrier was studied showing encouraging results which prompted in vivo experiments. The authors demonstrated that their delivery platform showed superior blood glucose level stabilisation in diabetic mice compared to administration of equivalent amounts of free insulin. For free insulin, 1 h post administration blood glucose dropped to hypoglycemic levels whereas glucose levels were maintained at more satisfactory levels when the studied assemblies were deployed. Moreover, in mice treated with free insulin blood glucose returned to a hyperglycemic level of  $16.6 \times 10^{-3}$  M after 4 h, while for studied material blood glucose levels reached  $11.1 \times 10^{-3}$  M over the same time frame. The authors also evidenced a low to no risk of hypoglycemia in healthy mice.

Boronic acid derivatives have been utilised by Ma and co-workers as synthetic chaperones in the form of glucose responsive mixed-shell (hydrophilic/hydrophobic) micellar assemblies for insulin protection and delivery.<sup>[152]</sup> In their approach



**Scheme 20.** The synthesis reported by Ma and co-workers<sup>[152]</sup> of copolymers containing poly( $\epsilon$ -caprolactone)-*b*-poly(ethylene glycol) and poly( $\epsilon$ -caprolactone)-*b*-poly(aspartic acid), functionalised with **24** post polymerisation to poly( $\epsilon$ -caprolactone)-*b*-poly(aspartic acid-*co*-aspartamidophenylboronic acid).

the authors drew inspiration from natural assisting proteins that support structural changes of other macromolecules, and were able to draw upon insights gained in previous experience of restoration of amyloid  $\beta$  homeostasis.<sup>[153]</sup> By developing synthetic nanochaperones capable of glucose-sensitive insulin delivery, they have sought to address potential issues with aggregation and fibrillation of insulin in the process of drug encapsulation, storage and release. The authors constructed their insulin delivery platforms as mixed-shell polymeric micelles with hydrophobic and hydrophilic domains on the surface. These particles were built of two copolymers poly( $\epsilon$ -caprolactone)-*b*-poly(ethylene glycol) and poly( $\epsilon$ -caprolactone)-*b*-poly(aspartic acid-*co*-aspartamidophenylboronic acid) (**Scheme 20**). The boronic acid-containing copolymer formed hydrophobic domains on the surface of the nanochaperones which were responsible for adsorbing partially unfolded insulin, while PEG chains from the other copolymer in surrounding hydrophilic domains formed a protective barrier for the adsorbed insulin, shielding it from enzymatic degradation. The potential of these nanochaperones for protecting insulin was studied. The authors demonstrated that the structure of insulin was practically undisturbed either after seven days of incubation at 37 °C or after 1 h at temperatures as high as 70 °C. Moreover, degradation assays showed that insulin adsorbed onto nanochaperones was shielded from proteinase K activity, displaying 4.6 times less degradation compared to a free insulin reference sample. The binding of glucose, resulting in boronate formation, inverts the polarity of the hydrophobic domains, making them hydrophilic. Thus, insulin was released, as the hydrophobic interactions keeping it adsorbed are broken. Glucose tolerance experiments, conducted at 37 °C (PBS, pH 7.4), showed the extent of insulin liberation to be proportional to glucose concentration. In the absence of glucose only 16% of loaded insulin was released after 60 h. At glucose concentrations of  $5.5 \times 10^{-3}$  M cumulative release of loaded insulin was 24% and for  $22.2 \times 10^{-3}$  M glucose 60% of loaded insulin was released under otherwise equivalent conditions. The authors also confirmed the capability of their platform to performing “on-off” release for varying glucose concentrations. In vivo studies on diabetic mice

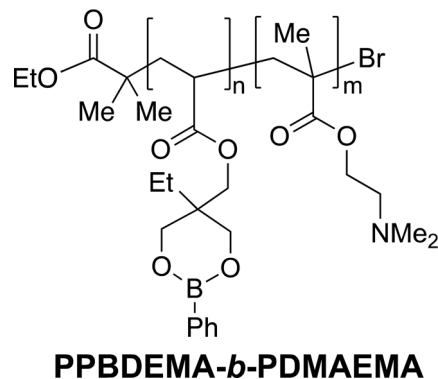
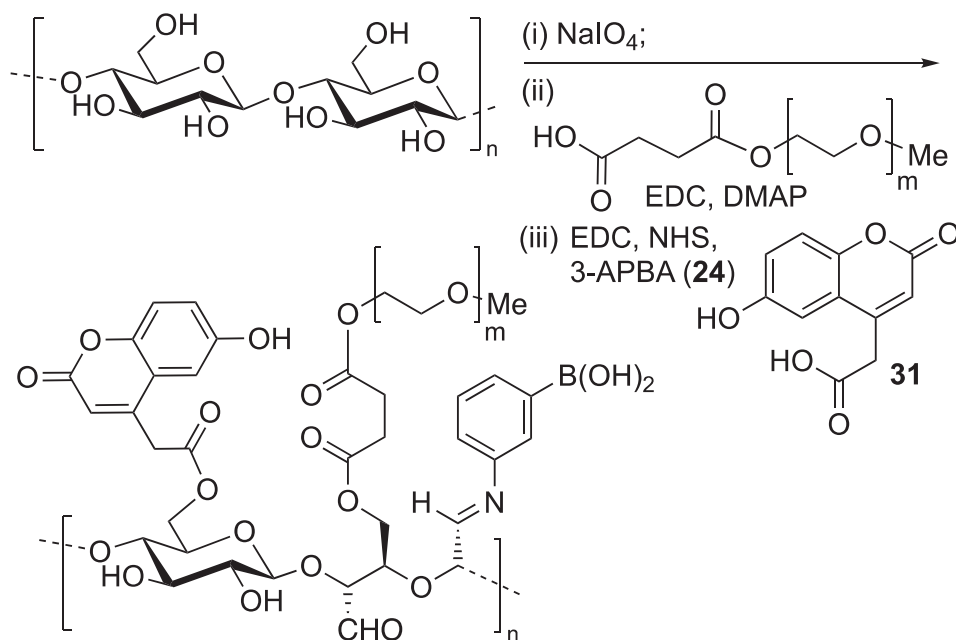


**Figure 15.** Block copolymer containing poly[2-(*N,N*-dimethylamino)ethyl methacrylate] and poly[(2-phenylboronic esters-1,3-dioxane-5-ethyl) methacrylate] as reported by Yuang and co-workers.<sup>[154]</sup>

showed that the investigated insulin delivery platform is capable of stabilising blood glucose levels in a normoglycemic range up to 5 h after administration, blood glucose levels returned to their original levels after 14 h. Moreover, hypoglycemia was avoided and nanochaperones treated with proteinase K or incubated for 7 days at 37 °C or for 1 h at 70 °C were still effective in the normalisation of blood glucose levels of diabetic mice. The authors also conducted an intraperitoneal glucose tolerance test; 1 h after administration of insulin or nanochaperones carrying insulin mice were intraperitoneally injected with  $1.5 \text{ g kg}^{-1}$  glucose. The nanochaperone platform provided very good blood glucose stabilisation, resembling the blood glucose profile obtained for control group of healthy mice within 2 h.

In their quest for multi-responsive drug delivery materials Yuan and co-workers developed a polymer based micelle-forming material capable of insulin release upon exposure to glucose, which also featured temperature and pH sensitivity (**Figure 15**).<sup>[154]</sup> The authors integrated dual thermo- and pH-responsive poly[2-(*N,N*-dimethylamino)ethyl methacrylate] structure with glucose-sensitive poly[(2-phenylboronic esters-1,3-dioxane-5-ethyl) methacrylate] by making a block copolymer using ATRP (**Scheme 21**). Thanks to the amphiphilic nature of the material, it could self-assemble in water, forming micelles with a hydrophobic core of the boronic acid ester block, and a hydrophilic amine appended shell with critical micelle concentration (CMC) as low as  $0.02 \text{ mg mL}^{-1}$ . Studies showed that when in contact with glucose the micelle core swelled significantly, while temperature increases resulted in shrinking of the micelle shell and the aggregation of particles. An increase in pH initially resulted in shell shrinkage and micellar aggregation, but after 48 h new micelles were formed in which the core and shell had swapped. That was explained in terms of differences between acid-base reactions taking place in both copolymer blocks. As deprotonation of (*N,N*-dimethylamino)ethyl causes an increase in hydrophobicity, the ionisation of boronic acid ester units increases hydrophilicity. When response to different stimuli was established, the authors demonstrated that their micelles were capable of entrapping insulin with an efficiency and loading capacity of 29% and 5.3%, respectively. Insulin release studies have shown that in the absence of a glucose stimuli 33.4% of loaded insulin is released after 70 h (pH 7.4, 37 °C), while 38%, 53%,



**Scheme 21.** Starch based polymer synthesis as reported by Lü and co-workers.<sup>[155]</sup> i) Starch was partially oxidised by sodium periodate. ii) The remaining free hydroxyl groups were then esterified with methoxypolyethyleneglycol succinic acid monoester and EDC with DMAP. iii) Imine formation with **24** and esterification with **31** was then performed using EDC/NHS.

and 71% of cumulative loaded insulin release was observed for glucose concentrations of  $5.5 \times 10^{-3}$ ,  $11.1 \times 10^{-3}$ , and  $27.7 \times 10^{-3}$  M, respectively. The authors have also shown “on-off” insulin release under alternating glucose concentration of 5.5 and  $27.7 \times 10^{-3}$  M.

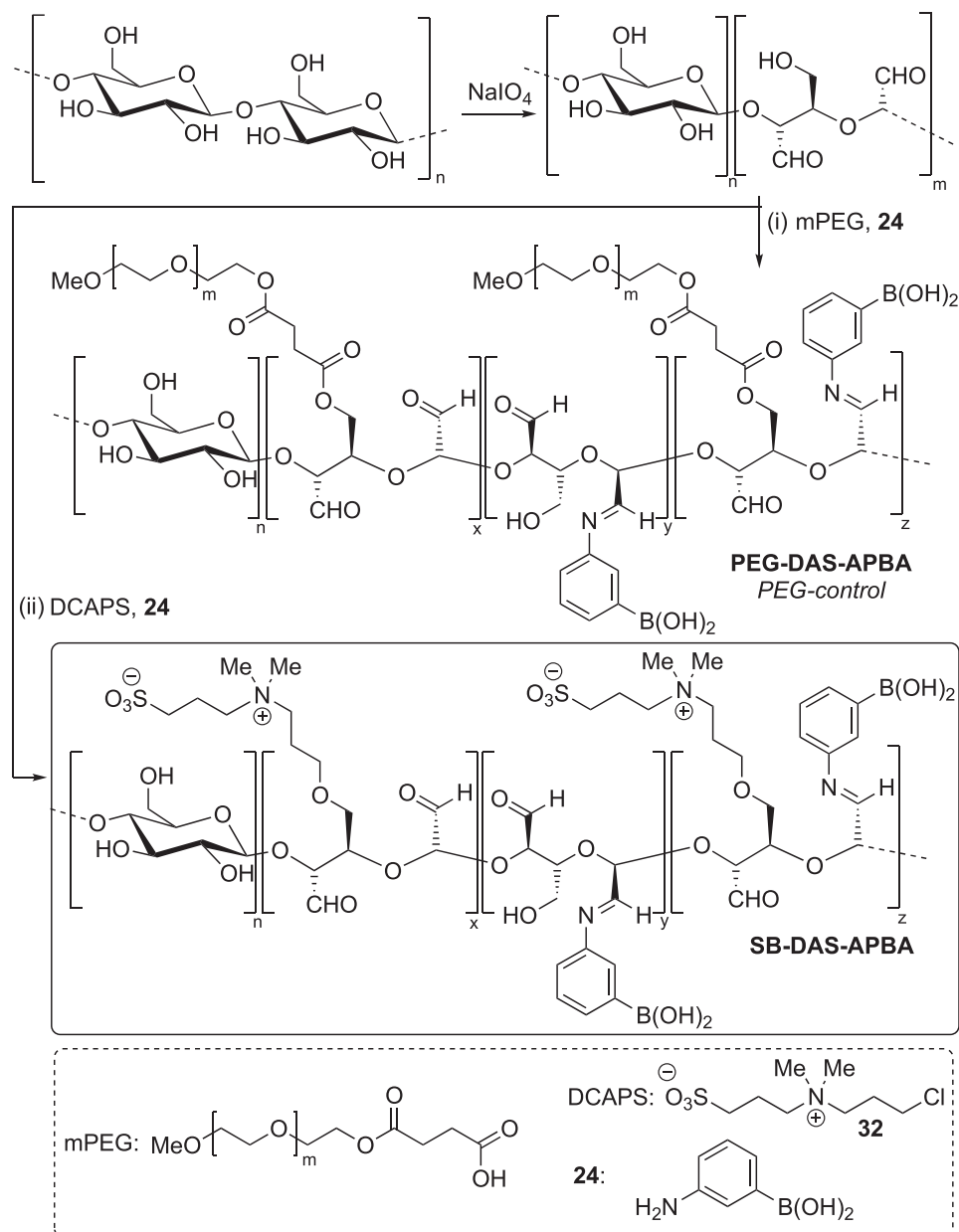
Lü and co-workers obtained micelles suitable for glucose-responsive insulin delivery from starch.<sup>[155]</sup> Hoping to develop a material with good biocompatibility and degradability they first was partially oxidised starch using sodium periodate to convert some of the 1,2-diol units to aldehydes. Next, the methoxypolyethyleneglycol monoester of succinic acid was used to partially esterify the remaining hydroxyl groups. This material was the subject of imine formation with 3-aminophenylboronic acid (**24**) and a second esterification step, this time with 7-hydroxycoumarinyl-4-acetic acid (**31**) (Scheme 21). The authors explained that they decided to introduce the coumarin moiety to lower the effective  $pK_a$  of arylboronic acid units. It was also determined that introducing coumarin unit resulted in significant lowering of CMC when compared to a corresponding material that did not include it, and that it contributed to increased micellar core hydrophobic stabilisation. The obtained materials formed micelles capable of encapsulating insulin. Cargo release studies were performed showing a glucose-dependent degree of discharge with a burst profile in the initial stages. Good results in hemolyses and cytotoxicity assays further supported authors' expectations.

Starch-based micelles were investigated further by Lü and co-workers in a subsequent contribution.<sup>[156]</sup> The authors decorated a starch derived material with zwitterionic moieties that had previously been shown to have a positive effect on stability and other properties (e.g., cell interactions) of nanoparticles.<sup>[157]</sup> Similarly, to their previous work, Lü and

co-workers partially oxidised starch by reaction with sodium periodate, and the resulting aldehyde groups were used to form imines with 3-aminophenylboronic acid **24**, and free hydroxyl groups were functionalised in reaction with 3-((3-chloropropyl)dimethylamino)propane-1-sulfonate (**32**), resulting in two materials differing in graft ratio (Scheme 22). The first having a 0.15 boronic acid graft ratio and a 0.25 graft ratio of zwitterionic units. The second material had lower content of boronic acid units and higher content of zwitterionic units as their graft ratio were 0.13 and 0.33, respectively. A PEG-functionalised reference material was also prepared, its boronic acid graft ratio was 0.15 and PEG graft ratio was 0.25. It was shown that starch-derived materials functionalised with boronic acids and zwitterionic betaine-derived groups were able to form micelles, with CMC reducing as betaine content increased. Insulin was effectively loaded into zwitterion functionalised starch bearing boronic acid units. Glucose-induced release capabilities were further studied under physiological conditions over 48 h. For the material with higher boronic acid graft ratio in the absence of glucose insulin release rates were slow, reaching  $\approx 22\%$  of loaded insulin release, while at  $5.5$  and  $16.6 \times 10^{-3}$  M glucose, insulin release profiles were almost identical ( $\approx 68\%$ ). The material with the lower boronic acid content was tested in the presence of  $16.6 \times 10^{-3}$  M glucose and showed insulin release of  $\approx 35\%$ . The integrity of released insulin was corroborated by CD spectroscopy. Hemolysis and cell viability studies showed good results for both tested materials. Phagocytosis test proved that micelles with zwitterionic groups were internalised by macrophage cells to far less extent than reference PEG-functionalised micelles.

The aforementioned concept of using zinc to increase insulin loading that was explored by Ma and co-workers in gels (Scheme 8)<sup>[110]</sup> was also applied by them in the formation





**Scheme 22.** Zwitterionic starch-based polymers as reported by Lü and co-workers.<sup>[156]</sup> The starch was partially oxidised by sodium periodate, before the aldehydes were reacted with i) mPEG and 3-aminophenylboronic acid **24** to produce **mPEG-DAS-APBA** or ii) **32** and **24** to produce **SB-DAS-APBA**.

of complex micelles for boron-mediated insulin delivery.<sup>[158]</sup> The authors fabricated complex micelles using two copolymers: poly(aspartic acid-co-aspartylglucosamine-co-aspartyl nitrilotriacetic acid) and poly(ethylene glycol)-*b*-poly(aspartic acid-co-aspartamidophenylboronic acid) (**Figure 16**). The process consisted of conditioning the copolymer with nitrilotriacetic acid units in a solution containing zinc ions, followed by the addition of insulin, and then subsequent complexation with the other copolymer containing boronic acid units. Four sets of complex micelles were obtained, varying in their ratio of boronic acid, glucosamine, and nitrilotriacetic acid units, with one blank with respect to the nitrilotriacetic acid units, to serve as a reference.

Insulin loading efficacy was shown to increase by about 40% for materials with zinc ions complexed by nitrilotriacetic acid units. Subsequent insulin release experiments showed confirmed a dependence on glucose concentration. Moreover, the authors demonstrated an “on-off” release profile for their complex micelles. Cell viability studies using MTT assays on NIH 3T3 mouse fibroblast cells proved studied materials to nontoxic by *tis* measure. This prompted authors to pursue *in vivo* tests using diabetic mice. The results showed that complex micelles with zinc assisted insulin loading were able to stabilise blood glucose significantly better than the material without zinc and were superior in this regard to injection of insulin.

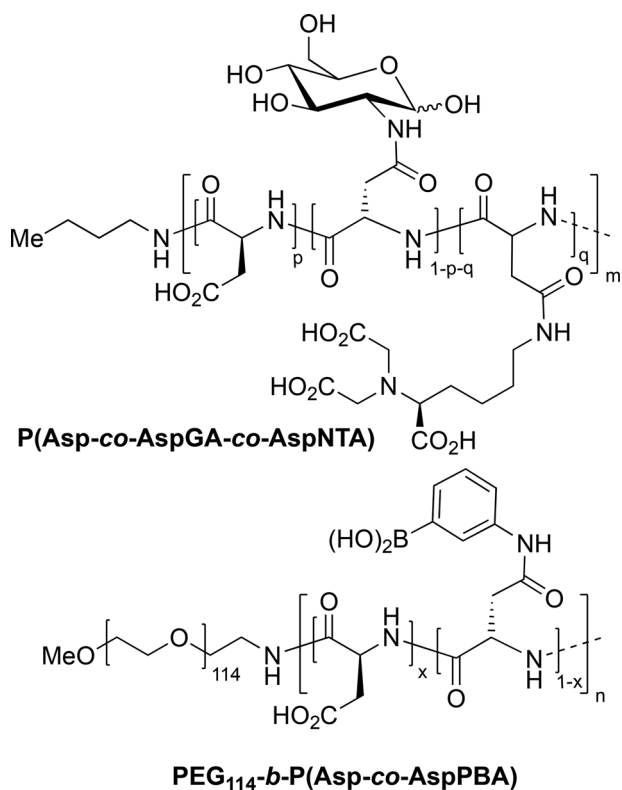


**Figure 16.** Block co-polymers capable of forming glucose responsive micelles as reported by Ma and co-workers,<sup>[158]</sup> boronic acid containing PEG-*b*-P(Asp-co-AspPBA) and glycopolymer containing P(Asp-co-AspGA-co-AspNTA).

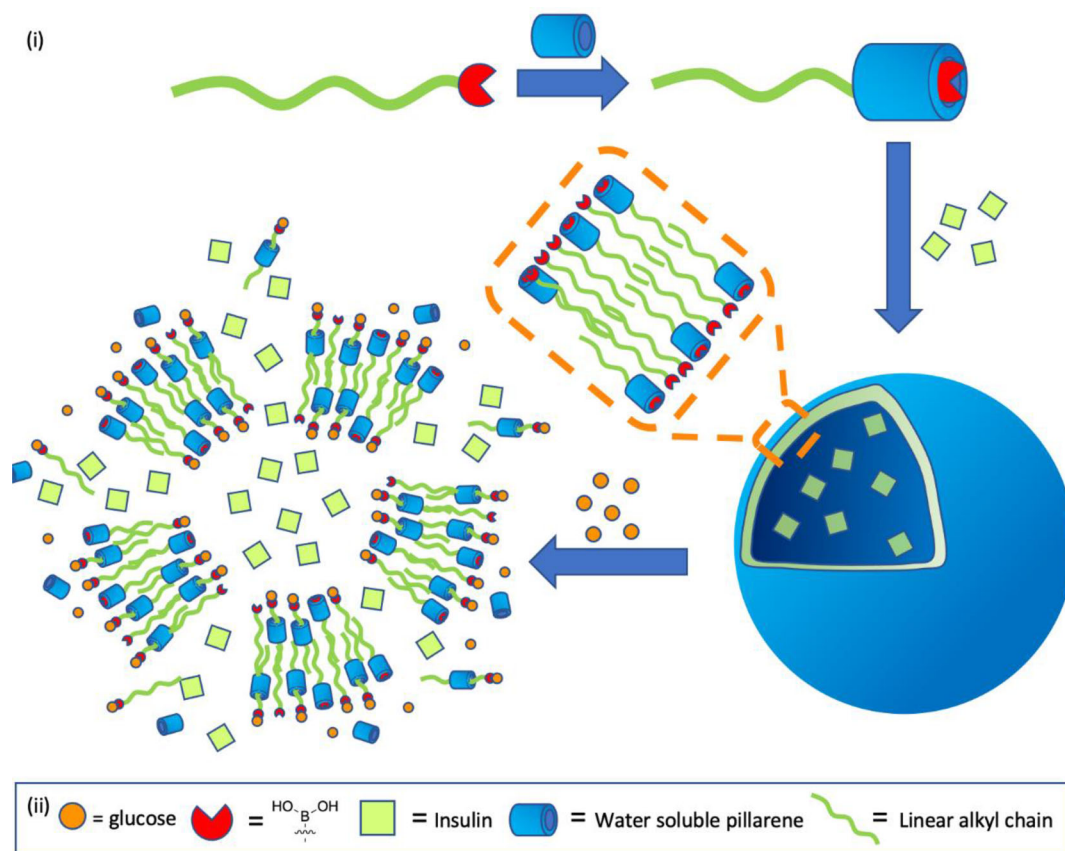
A unique vesicle insulin delivery platform built from supramolecular host–guest complexes of pillar[5]arene and pyridynyl boronic acid derivatives was constructed by Hu and co-workers (Scheme 23).<sup>[159]</sup> The authors sought to take advantage of the fact that pyridinium salts form stable inclusion complexes with water-soluble pillar[5]arene,<sup>[160]</sup> and use this phenomenon for functional supramolecular amphiphile formation (Scheme 15). Insulin-loaded vesicles were prepared by adding insulin to an aqueous solution of 4-borono-1-hexadecylpyridinium bromide and carboxylatopillar[5]arene decasodium salt (in a 1.5:1 molar ratio, respectively; with 1% of ethanol). Encapsulation efficiency was determined to be 64%. TEM and DLS analysis confirmed that insulin-loaded vesicles were much larger than their hollow analogs ( $\approx 320$  nm vs 132 nm). Insulin release studies were performed at pH 7.4 with a range of glucose concentrations. In the absence of glucose no insulin discharge was observed. Furthermore, the vesicles were able to differentiate between normo- and hyperglycemic conditions, as at  $5.5 \times 10^{-3}$  M glucose concentration  $\approx 20\%$  of loaded insulin was released while for  $11.1 \times 10^{-3}$  M glucose nearly 60% of insulin was released. However, strong burst release was observed, and discharge profiles reached a plateau after about 15 min. Cytocompatibility studies also gave good results.

Hu and co-workers took the concept of supramolecular vesicles for insulin release even further.<sup>[161]</sup> This time, instead of using pyridinium boronic acids with *N*-substituted long aliphatic

chains, the authors utilised a bis-boronic acid with an analogous structure to those synthesised by James and Shinkai for glucose sensing.<sup>[162]</sup> This bis-boronic acid used together with carboxylatopillar[5]arene decasodium salt was able to form vesicles. As demonstrated by the authors these assemblies were disrupted by glucose, as well as by hydrogen peroxide and by a drop in pH, as a result of GOx being incorporated alongside insulin. This was attributed to the oxidation of glucose to gluconic acid with  $H_2O_2$  being produced as a side product, and subsequent boronic acid oxidation furthering vesicle disruption and insulin release. The presence of gluconic acid caused a pH drop, resulting in the protonation of pillararene carboxylate groups, causing a decrease in water solubility.

Gu and co-workers noticed that orally administered materials for insulin delivery often lack in their ability to efficiently release insulin following meals. In response they designed insulin-loaded liposomes that targeted Fc receptor (FcRn), which were enclosed in a glucose sensitive shell made of hyaluronic acid modified with 2-aminophenylboronic acid.<sup>[163]</sup> FcRn facilitates protein transport across the intestinal epithelium as it binds Immunoglobulin G (IgG) and is expressed in the apical region of epithelial cells in the small intestine.<sup>[164]</sup> These liposomes were based on egg phosphatidylcholine, dioleoylphosphatidylethanolamine, cholesterol, 1,2-distearoyl-*sn*-glycero-3-phosphoethanolamine-*N*-[maleimide(polyethylene glycol)] and 1,2-distearoyl-*sn*-glycero-3-phosphoethanolamine-*N*-[carboxy(polyethylene glycol)] which they coupled with dopamine, a binder of boronic acid. After the preparation of insulin loaded liposomes through a lipid film hydration method, polyclonal IgG Fc fragments were modified with Traut's Reagent and conjugated to the PEG through maleimide-thiol bonds. These liposomes were then enclosed in a shell of hyaluronic acid coupled with 2-aminophenylboronic acid, and boronate formation between the dopamine catechol unit from the liposomal surface and boronic acid moieties integrated the two structures. This coating served to protect the liposomes until a postprandial increase of glucose concentration caused shell disruption due to competitive binding. When this occurred, Fc groups became exposed promoting intestinal absorption of insulin-loaded liposomes, leading to insulin release into the bloodstream and subsequent lowering of blood glucose concentration. That was confirmed by in vivo studies on STZ-induced type 1 diabetic mice which showed around a 40% decline in blood glucose levels 8 h after oral administration of the vesicles, while free insulin had no effect. Similarly, other reference materials (insulin-loaded liposomes without Fc groups on the surface and insulin-loaded liposomes with a chemically crosslinked shell of hyaluronic acid) showed no effect. Simulation of postprandial conditions showed the tested liposomes work effectively in reducing an initial increase and in further lowering blood glucose levels.

Another orally administered platform for insulin delivery was developed by Feng and co-workers.<sup>[165]</sup> This time authors designed an amphiphilic dendrimer branching out from an eight-armed poly(ethylene glycol) with hydrophobic blocks, terminated by benzoxaborole units (Scheme 24). This material proved able to self-assemble into micelles under aqueous conditions. Moreover, insulin encapsulation could be achieved by introducing the dendrimer to an insulin solution. In vitro experiments on insulin release in response to glucose showed that the studied micelles are



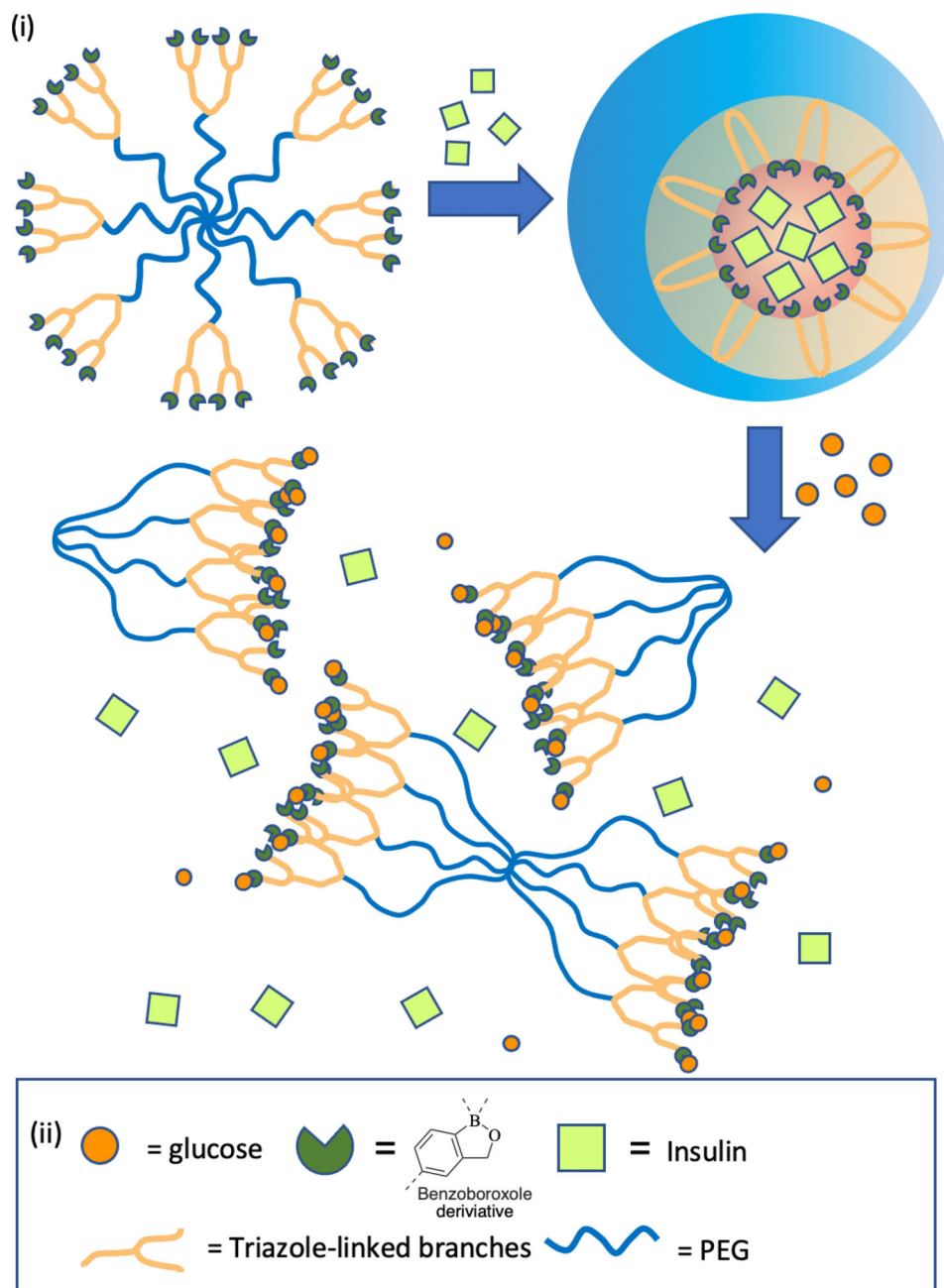
**Scheme 23.** The insulin delivery vehicle based on host-guest complexation, as reported by Hu and co-workers.<sup>[159]</sup> i) A pictographic representation of the inclusion of the water soluble pillar[5]ene complexation around the pyridinyl boronic acid derivative bound to a linear alkyl chain. This complex is then shown to form vesicles which may encapsulate insulin, with subsequent release on addition of glucose. ii) Key: Orange circles represent glucose. Red cut out circles represent boronic acid units. Pale green squares represent insulin. Blue hollow cylinders represent pillar[5]arenes. Green chains represent linear alkyl chains.

glucose sensitive, with concentration dependent payload release. This was attributed to the benzoxaborole units binding glucose, leading to a reduction of the hydrophobic nature of the core of the micelle structure, consequently leading to the rupture of the assembly and cargo liberation. Authors also noticed that at low pH ( $\text{pH} < 2$ ) spontaneous release of insulin from studied micelles is hampered, which is beneficial given that oral administration was intended for that material, and thus it must pass through the acidic stomach. Encouraging results of permeation experiments led to *in vivo* studies being undertaken on STZ-induced type 1 diabetic mice. Insulin loaded micelles, administered orally, showed prolonged stabilisation of blood glucose levels compared to subcutaneously injected insulin (10 h vs 4 h). Moreover, glucose tolerance tests proved that blood glucose levels of diabetic mice injected intraperitoneally with glucose 1 h after administration of insulin-loaded micelles closely resembled those for healthy mice after the same glucose intake. Moreover, none of the tested mice experienced hypoglycemia following the use of the orally administered system, while 75% of mice injected with subcutaneous insulin did.

Another type of vesicular assembly for glucose-responsive insulin release and delivery was prepared by Tong and co-workers.<sup>[166]</sup> The authors utilised RAFT polymerisation tech-

niques in order to obtain a well-defined triblock copolymer with boronic acid and boronate units (Figure 17). Tong and co-workers envisaged that the boronic acid groups would endow their material with glucose responsivity, while including boronate units would provide responsivity to  $\text{H}_2\text{O}_2$ . Further tests proved that the studied material is able to form vesicles and encapsulate insulin, which would be subsequently released on exposure to glucose or  $\text{H}_2\text{O}_2$ .  $\approx 20\%$  of loaded insulin was released in glucose free media, while  $\approx 50\%$  and  $70\%$  of cumulative release was obtained in  $11.1 \times 10^{-3}$  and  $22.2 \times 10^{-3}$  M glucose solutions, respectively. It is worth noting that the authors also found out that if glucose oxidase is co-loaded with insulin, it increases insulin release in response to glucose, resulting to over 90% cumulative loaded insulin release at  $22.2 \times 10^{-3}$  M glucose. Furthermore, the studied polymeric vesicles were shown to have good biocompatibility and the authors used them to prepare transcutaneous microneedle array patch devices. *In vivo* testing proved the potential of this invention to lower blood glucose levels.

Mandal and Das reported a glucose-responsive vesicular assembly based on a cholesterol derived boronic acid (33) (Figure 18).<sup>[167]</sup> The authors decided to utilise cholesterol, which is known to be beneficial for lipid vesicles formation, and build on it in order to construct a spherical drug-delivery platform.



**Scheme 24.** The orally administered insulin delivery platform developed by Feng and co-workers.<sup>[165]</sup> i) A pictographic representation of the benzoboroxole terminated branched amphiphilic dendrimer, and their encapsulation of insulin into micelles, with subsequent insulin release as the benzoboroxole units bind to glucose. ii) Key: Orange circles represent glucose. Green cut out circles represent benzoboroxole units. Pale green squares represent insulin. Yellow chains represent hydrophobic triazole linked branches. Blue chains represent PEG chains.

Electron microscopy techniques confirmed the formation of vesicular assemblies from the designed compound. The authors successfully entrapped insulin, which according to their observations localised itself in the bilayer of the assembly, and studied cargo was release upon glucose stimulation. UV-vis and fluorescence measurements served to determine the extent of insulin release. Glucose concentrations of  $0\text{--}30 \times 10^{-3} \text{ M}$  were tested with  $6 \times 10^{-3} \text{ M}$  increments, and a concentration dependent release of insulin, reaching a maximum of 66% release, was observed.

Shi and co-workers once more addressed the problem of enzymatic degradation of insulin in drug-delivery platforms by preparing complex micelles that could protect the insulin from this process.<sup>[168]</sup> The authors synthesised two types of polymeric materials. One being a block copolymer of poly(*N*-isopropylacrylamide)-*co*-poly(aspartic acid) with poly(aspartic acid) block functionalised with a nitrilotriacetic acid derivative and with glucosamine, the other being a block copolymer of PEG and poly(aspartic acid) functionalised with **24**. Using these two

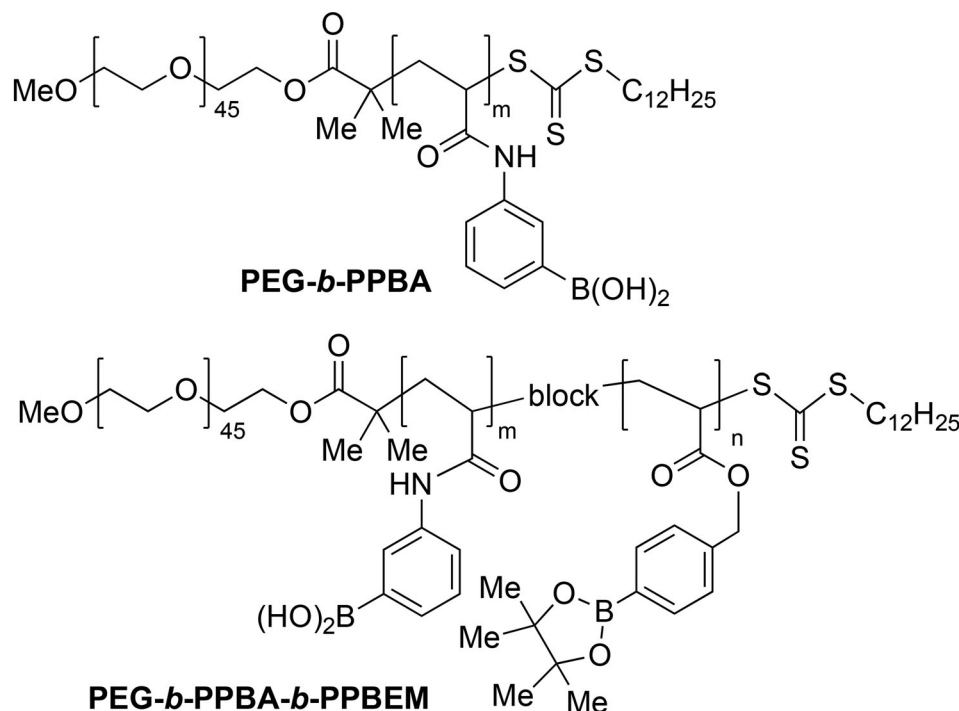


**Figure 17.** Di- and Tri-block copolymers **PEG-*b*-PPBA** and **PEG-*b*-PPBA-*b*-PPBEM** prepared by Tong and co-workers to develop a material for glucose responsive insulin delivery.<sup>[166]</sup>

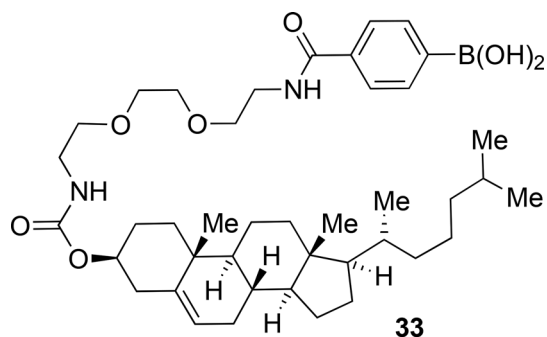


**Figure 18.** The cholesterol derived boronic acid derivative (**33**) utilised by Mandal and Das to develop a spherical glucose responsive insulin delivery system.<sup>[167]</sup>

materials the authors prepared a series of complex micelles with varying compositions. The PNIPAM block endowed the micelles with thermo-responsive properties, with an LCST of 37 °C. This collapse of the PNIPAM fraction was how the authors intended to protect insulin against degradation. To increase the insulin loading efficiency Zn<sup>2+</sup> ions were chelated by nitrilotriacetic acid domains. Stimuli-induced cargo discharge experiments were conducted under physiological conditions using glucose solutions with a concentration of 0 × 10<sup>-3</sup>, 11.1 × 10<sup>-3</sup>, and 27.7 × 10<sup>-3</sup> M giving cumulative release after 60 h of 19%, 53%, and 71%, respectively. Moreover, “on-off” release of insulin was demonstrated when the complex micelles were exposed to alternating 0 × 10<sup>-3</sup> and 27.7 × 10<sup>-3</sup> M glucose concentrations. Next, the degradation of the encapsulated insulin was measured on exposure to

proteinase K, and results showed that the developed material significantly reduces degradation compared to analogous micelles lacking PNIPAM blocks or free insulin. Moreover, this protection is increased by raising the temperature from 25 °C to 37 °C. After proving the biocompatibility of their material the authors undertook in vivo studies. STZ-induced diabetic mice were treated with insulin loaded complex micelles and two controls: free insulin and insulin loaded micelles without PNIPAM blocks. Only the use of complex micelles prevented hypoglycemia following injection, and this material also exerted the longest blood glucose level stabilisation effect (16 h), compared to the other micelles (10 h) and free insulin (5 h). The micelles were also shown to stabilise blood-glucose levels following glucose injection, simulating a meal.

Gaballa and Theato employed RAFT to prepare block copolymers that they transformed into glucose-responsive micelle-forming materials.<sup>[169]</sup> The authors installed diol moieties (D-(+)-glucosamine, (±)-3-aminopropane-1,2-diol) or boronic acid residues by aminolysis of the corresponding pentafluorophenyl ester in a block derived from the appropriate acrylate (**Figure 19i-iii**), respectively. After studying the assembly of pairs of block copolymers into micelles, glucose-responsive insulin release was also investigated. Cargo discharge investigations were performed under physiological conditions (pH 7.4, 37 °C). The micelles formed from the glucosamine copolymer offered the same cumulative release of insulin for 5.5 × 10<sup>-3</sup> and 11.1 × 10<sup>-3</sup> M glucose concentration, ≈90% and 95% loaded insulin release after 24 h, respectively. The discrimination of payload liberation was much more pronounced for micelles incorporating 3-aminopropane-1,2-diol. In this case

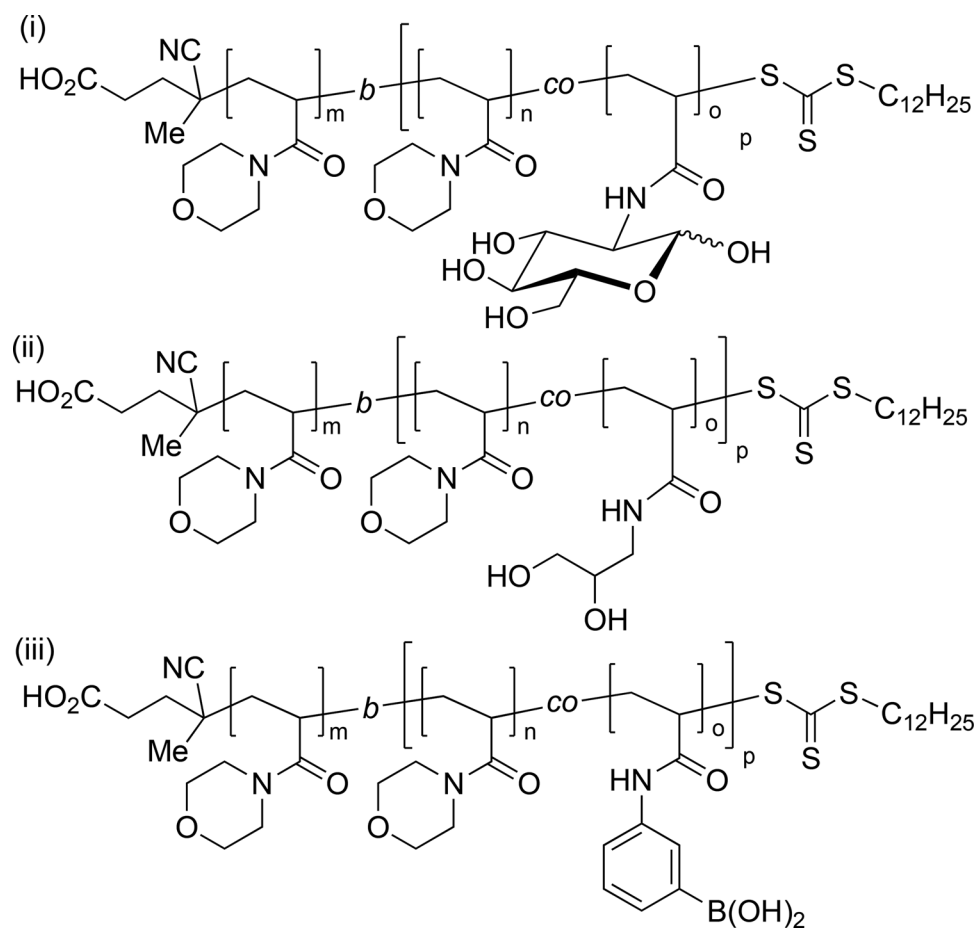


**Figure 19.** Block co-polymer prepared by Gaballa and Theato<sup>[169]</sup> prepared by aminolysis pentafluorophenyl esters, through reaction with i) boronic acid derivative (**24**); ii) diol moieties (D-(+)-glucosamine; or iii) (±)-3-aminopropane-1,2-diol).

cumulative loaded insulin release after 24 h for  $5.5 \times 10^{-3}$  M of glucose was about 30% while for  $11.1 \times 10^{-3}$  M it was close to 90%.

## 11. Capsules

Chen and co-workers explored glucose-concentration controlled insulin release from polymeric capsules prepared by a layer-by-layer (LbL) technique.<sup>[170]</sup> The authors sought to address issues that are common with such assemblies including low degradability, low biocompatibility, and poor glucose-responsive release profiles. They anticipated that using poly( $\gamma$ -glutamic acid) and chitosan, well known biological polyelectrolytes, might alleviate these disadvantages.<sup>[170a]</sup> In order to endow resulting capsules with the desired properties these bio-derived materials were further modified; poly( $\gamma$ -glutamic acid) was grafted with 3-aminophenylboronic acid (**24**) by amide formation and similar transformation was employed to functionalise chitosan with lactobionic acid (**34**) (Figure 20).

Boronic acid moieties were added to ensure glucose-responsivity, while lactobionic acid was introduced to provide 1,2-diols to improve the binding between these two polymers. To form the capsules, the authors utilised LbL techniques with amino-functionalised SiO<sub>2</sub> particles as a template. Insulin load-

ing was performed prior to the LbL process. The final capsule had ten alternating layers on a SiO<sub>2</sub> core, before the SiO<sub>2</sub> was removed using an NH<sub>4</sub>F/HF mixture. The resulting particles exhibited significant swelling in glucose containing media, even breaking in more concentrated solutions. Studying capsules with poly( $\gamma$ -glutamic acid) functionalised to a different degree showed that increasing the boronic acid content increased the stability of the capsules in glucose solutions. Insulin release monitoring led to the conclusion that boronic acid content also has an influence on the cargo discharge process. The higher the boron content, the smaller the observed cumulative release and the slower initial discharge for a given glucose concentration. The authors also showed that these particles were also capable of “on-off” release. Biocompatibility studies gave good results at reasonably high concentrations, leading to the conclusion that these capsules have potential to be applied in diabetes treatment.

In their following contribution on glucose-responsive capsules for insulin delivery, Chen and co-workers aimed to limit polymer dissociation from the capsules in order to better control cargo discharge processes, and to minimise the burden on the kidney involved in clearance processes.<sup>[170b]</sup> They sought to accomplish this by reinforcing the capsules via crosslinking in their walls. Alginate was chosen for this purpose, as it is known that calcium ions cause the formation of crosslinked networks in this material.

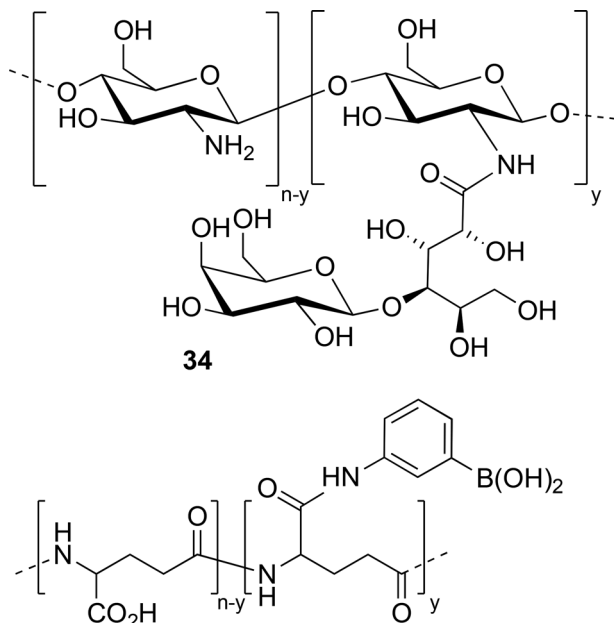
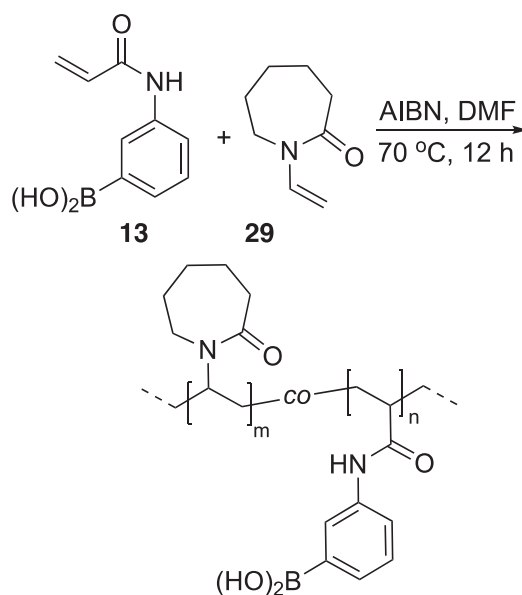


**Figure 20.** The two polymers utilised by Chen and co-workers<sup>[170]</sup> to develop glucose responsive capsules; chitosan functionalised with lactobionic acid (**34**) and poly( $\gamma$ -glutamic acid) functionalised with 3-aminophenylboronic acid (**24**).

The second component for capsule formation was chitosan modified via amide coupling with 3-carboxyphenylboronic acid. The fabrication of these capsules and the subsequent insulin loading were performed similarly as in previous report.<sup>[170]</sup> The authors obtained a series of capsules differing in degree of chitosan functionalisation and number of layers. TEM analysis revealed that the addition of calcium ions resulted in a slight increase of capsules size and a significant thickening of their shell. Calcium ions were also shown to influence the glucose-responsive swelling behavior of the studied capsules making it less pronounced with increased calcium content. This was translated to the insulin release process as capsules with calcium ions were slightly less active in cargo discharge at a given glucose concentration. Secondary structure of released insulin was investigated by CD spectroscopy showing no significant changes when compared with standards. Irrespective of the inclusion of the calcium ions and alginate, the capsules maintained good biocompatibility.

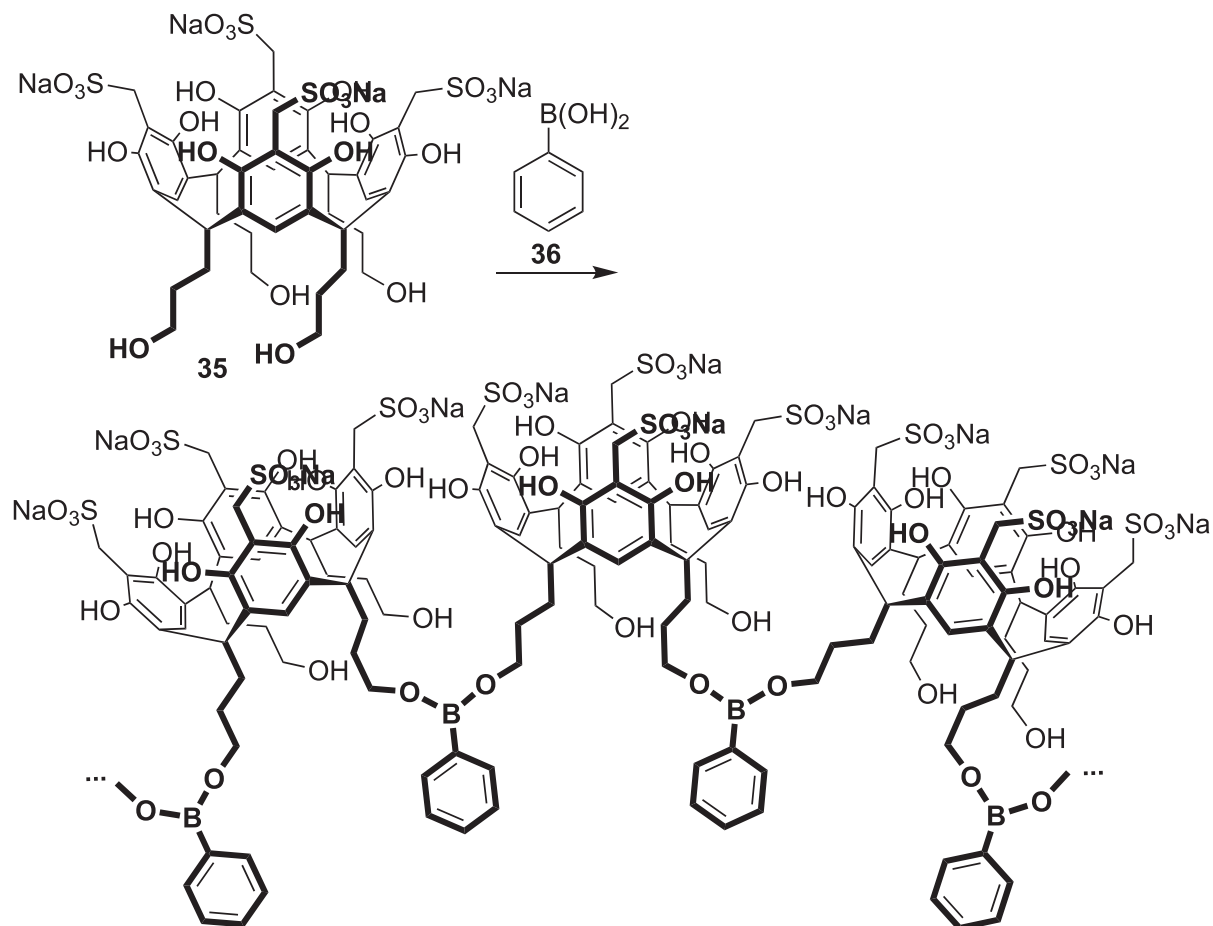
The LbL approach was also utilised by Li and co-workers who developed microspheres based on poly(lactic-co-glycolic acid) and a copolymer of **13** and *N*-vinyl- $\epsilon$ -caprolactam, (**29**) (Scheme 25).<sup>[171]</sup> These vehicles were capable of sustained insulin release over 25 days and displayed marked glucose-dependence, increasing discharge rates with increased glucose concentrations. CD spectroscopy corroborated the integrity of the released insulin. Furthermore, cell and animal toxicity studies of the microspheres confirmed good biocompatibility. The authors performed *in vivo* studies of their material on diabetic mice, which showed that after single administration it can keep blood glucose level the same as in healthy control group for 16 days; a further seven days were required for blood glucose to rise over  $10 \times 10^{-3}$  M.



**Scheme 25.** Radical initiated polymerisation of **13** and *N*-vinyl- $\epsilon$ -caprolactam (**29**) to form a polymer capable of forming a glucose responsive insulin delivery system, as reported by Li and co-workers.<sup>[171]</sup>

Multilayer capsules with glucose responsiveness for insulin release were also prepared by Belbekhouche and co-workers.<sup>[172]</sup> The authors prepared modified alginate by amide formation using 3-aminophenylboronic acid, (**24**) and deposited this material in alternating layers with polyvinylpyrrolidone using  $\text{CaCO}_3$  microparticles as a sacrificial templates, later removed by action of EDTA upon completion of the LbL assembly process. Insulin loading was performed utilizing the porous nature of  $\text{CaCO}_3$  before deposition of the first layer. As a proof of concept, the authors performed studies on a surface. Analysis of LbL by quartz crystal microbalance (QCM) first gave evidence for formation of consecutive polymer layers. Subsequent studies using QCM determined the impact of glucose solutions at different pHs (pH 2 and 8) on the multilayer assembly. The authors found that at pH 2 the material remains intact regardless of glucose concentration (up to  $27.7 \times 10^{-3}$  M). At pH 8, glucose concentrations up to  $2.76 \times 10^{-3}$  M caused minor decomposition of the multilayer assembly,  $5.5 \times 10^{-3}$  M glucose caused a significantly higher degree of decomposition. The insulin loaded capsules behaved in a similar way. No cargo release was observed upon treatment with  $5.5 \times 10^{-3}$  M glucose at pH 2, while for the same glucose concentration at pH 8 cumulative loaded insulin release was about 95% after 10 min. It is worth noting that these capsules did not release any insulin at pH 8 without glucose present. Their stability at a range of pHs was attributed to hydrogen bonding that was preserved even at elevated pH, thanks to the presence of boronic acid groups serving as hydrogen bond donors to polyvinylpyrrolidone while carboxylic groups of alginate are deprotonated.

Ziganshina and co-workers sought to improve the properties of their sulfonated resorcinarene-phenylboronate polymer nanospheres in such way that they would become stable in normoglycemic glucose concentrations with no insulin release.<sup>[173]</sup> The authors hypothesised that this could be achieved through



**Scheme 26.** Sulfonated resorcinarene nanosphere formation through boronate complexation using phenyl boronic acid **36**, as reported by Ziganshina and co-workers.<sup>[173]</sup>

optimisation of the sulfonated resorcinarene (**35**) to phenylboronic acid (**36**) ratio during the preparation of their nanoparticles (**Scheme 26**).<sup>[174]</sup> Experiments proved this hypothesis to be true, with a 6:5 molar ratio of sulfonated resorcinarene to phenylboronic acid proving to be optimal. Nanospheres of that composition were capable of insulin encapsulation with 76% efficiency, and their loading capacity was determined to be 8.5%. Insulin release experiments demonstrated that this material liberates only 7% of its cargo at  $5 \times 10^{-3}$  M glucose, while at 7.5 and  $10 \times 10^{-3}$  M glucose cumulative insulin release was 21% and 100%, respectively. In all cases the insulin release profiles plateau within 30 min of exposure to glucose under physiological conditions. CD spectroscopy corroborated the integrity of the released insulin.

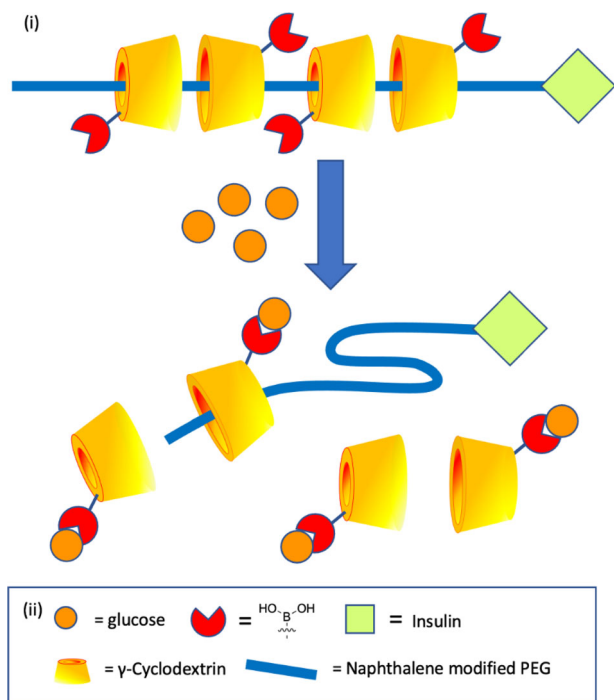
## 12. Cyclodextrin-Derived Materials

An interesting example of a molecular glucose-responsive capsule for insulin delivery was produced by Li and co-workers.<sup>[175]</sup> The authors sought to take advantage of cyclodextrin's potential to encapsulate proteins<sup>[176]</sup> and integrate this property with the glucose-sensitivity of boronic acids and their derivatives. This prompted them to *O*-alkylate  $\beta$ -cyclodextrin with (2-

phenylboronic esters-1,3-dioxane-5-ethyl) bromoacetate. Insulin complexation by functionalised  $\beta$ -cyclodextrin was evidenced by FTIR and a continuous variation method served to determine complex stoichiometry as 1:4  $\beta$ -cyclodextrin derivative:insulin. The mechanism for insulin release was based on competitive displacement of the diol unit in by glucose forcing the insulin out of the  $\beta$ -cyclodextrin cavity by the freed boronic acid derivative. This behavior was confirmed by the authors, the integrity of the released insulin was corroborated by CD spectroscopy. Cytotoxicity studies showed that the insulin complex has better properties than  $\beta$ -cyclodextrin derivative itself, which is used already in a range of medical applications.<sup>[177]</sup>

PEG functionalised insulin has been shown to form pseudopolyrotaxanes with cyclodextrins, in which cyclodextrin rings are threaded by a polymer chain and these systems were studied for sustained release.<sup>[178]</sup> Egawa and co-workers endowed such pseudopolyrotaxanes with glucose-sensitivity by using  $\gamma$ -cyclodextrins functionalised with arylboronic acid (**Scheme 27**).<sup>[179]</sup> The authors prepared two  $\gamma$ -cyclodextrin derivatives in form of esters with 4-carboxyphenylboronic acid or 3-carboxy-5-nitrophenylboronic acid. Pseudopolyrotaxanes with PEG functionalised insulin have been obtained for these derivatives. Structural studies of pseudopolyrotaxanes by powder





**Scheme 27.** Glucose responsive pseudopolyrotaxanes as reported by Egawa and co-workers. i) A pictographic representation of PEG-derivatised insulin threaded with  $\gamma$ -cyclodextrins functionalised with boronic acids, and the subsequent glucose responsive discharge of the  $\gamma$ -cyclodextrin. ii) Key: Orange circles represent glucose. Red cut out circles represent boronic acid units. Pale green squares represent insulin. Golden hollow cones represent  $\gamma$ -cyclodextrin. Blue chains represent naphthalene modified PEG chains.<sup>[179b]</sup>

X-ray diffraction indicated that the cyclodextrin rings with nitro-boronic acids are arranged in a head-to-head and tail-to-tail fashion, while the other material presents a head-to-tail arrangement. Further analysis of the materials by 2D NMR and CD spectroscopic techniques, in conjunction with density functional calculations gave insight into the orientations of the boronic acid moieties in both types of pseudopolyrotaxanes. The nitro-boronic acid groups were localised as protruding from the pseudopolyrotaxane string, while boronic acid groups in the other material were mostly situated inside a cavity of a neighboring cyclodextrin derivative along the string. Glucose-responsiveness tests were performed on both materials at pH 7.4 and 37 °C using 0, 30, and  $100 \times 10^{-3}$  M glucose solutions. The obtained results showed that the pseudopolyrotaxane with nitro-boronic acid moieties displays a much higher sensitivity for glucose, resulting in a cumulative release of about 70% (compared to  $\approx 45\%$  for the other material), at a concentration of  $100 \times 10^{-3}$  M glucose after 24 h. Authors attribute this effect to easier accessibility of nitro-boronic acid moieties protruding from the pseudopolyrotaxane string.

### 13. Membranes

Building on their experience with (2-phenylboronic esters-1,3-dioxane-5-ethyl)methyl appended block copolymers for insulin releasing micelles,<sup>[154]</sup> Yuan and co-workers constructed a membrane material capable of glucose responsive behavior.<sup>[180]</sup> The

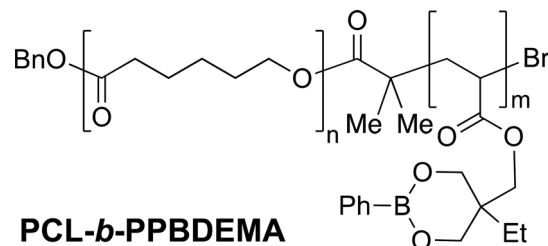


**Figure 21.** Boronic acid appended block copolymer **PCL-*b*-PPBDEMA**, used by Yuan and co-workers to form a glucose responsive membrane material.<sup>[180]</sup>

authors noted that membranes have an advantage over self-assemblies like micelles, and are often characterised with better encapsulation efficiency and loading capacity. Deciding on a copolymer structure, Yuan and co-workers picked poly( $\epsilon$ -caprolactone) as it is both biodegradable and biocompatible. As for the glucose responsive part poly[(2-phenylboronic esters-1,3-dioxane-5-ethyl)methylacrylate] was selected (**Figure 21**). The block copolymer was synthesised by combination of ROP and ATRP. Polarised optical microscopy (POM) and DSC studies revealed that presence of poly[(2-phenylboronic esters-1,3-dioxane-5-ethyl)methylacrylate] block reduced the crystallinity of poly( $\epsilon$ -caprolactone) segments, thus making the whole material more plastic. A solution casting method was used to load the membrane with insulin. The encapsulation efficiency and loading capacity values of insulin for the prepared membrane material were 71% and 7.1%, respectively. Such an insulin-loaded membrane was proven to hold its cargo well when stored in PBS buffer (pH 7.4) at 37 °C, as cumulative insulin release after 72 h was about 20%. For a glucose concentration of  $5.5 \times 10^{-3}$  M the observed insulin release was only negligibly higher, while for a hyperglycemic glucose concentration ( $11.1 \times 10^{-3}$  M) over 55% of loaded insulin was released. A glucose concentration of  $44.4 \times 10^{-3}$  M caused a cumulative 95% insulin release after 72 h. Further studies showed that the membrane material exhibited modulating insulin release rate proportional to changes in glucose concentration.

### 14. Films

The first example of a porous functional film for glucose-responsive insulin release was presented recently by Wu and co-workers.<sup>[181]</sup> The authors utilised a method similar in principle to breath figure<sup>[182]</sup> that consisted of preparation of a microemulsion of water in polystyrene/dichloromethane with dodecylamine as surfactant-stabiliser. After casting this mixture on a surface and allowing for the evaporation of the organic solvent, water droplets served as template for pore formation. Due to the amphiphilic nature of dodecylamine its amino groups localised mainly on the cavity surface after evaporation of water. This was further taken advantage of in following functionalisation. Poly(acrylic acid) was deposited into cavities thanks to interaction between amino- and carboxylic acid groups. Carboxylic acid groups on the poly(acrylic acid) surface were used to introduce 3-aminophenylboronic acid (**24**) to the cavities via amide formation. Next, the authors utilised the affinity of boronic acids toward 1,2-diols to cover the pores with a negatively

charged alginate layer. Finally, positively charged insulin aggregates were deposited in cavities thanks to electrostatic charge attraction. The authors demonstrated that the obtained material is capable of releasing insulin, and that this process is glucose concentration dependent. However, in each case strong burst discharge was observed.

Egawa and co-workers used PVA and boronic acid appended insulin, which served as a linker, to prepare multi-layer glucose-responsive films by a LbL method.<sup>[183]</sup> The authors started by modifying insulin by amide coupling with 4-carboxyphenylboronic acid or 3-fluoro-4-carboxyphenylboronic acid. According to HPLC traces the materials obtained were mixtures of insulin derivatives in each case, which resulted from a statistical reaction outcome. These were further tested for their hypoglycemic activity. Both had impeded activity, in case of 4-carbamoylphenylboronic acid appended insulin this drop was roughly 50%, but for fluoro-analog loss of activity was much more significant. Five-layer films were prepared with both types of insulin derivative and their degradation in glucose containing media was studied. Unfortunately, regardless of “crosslinker” used, film degradation upon stimulation with glucose at physiological pH was only marginal and comparable to a glucose-free scenario. However, fructose, which binds to monoboronic acid motifs more effectively than glucose was effective at inducing film degradation.

## 15. Conclusions

The boronic acid/boronate based materials for glucose-responsive insulin delivery presented in this review cover a wide variety of formats, nevertheless all are utilizing the same fundamental property of boronic acids to reversibly bind diols. Dynamic chemistry of boronic acids and boronates is now well understood, enabling the next steps to be taken in the development of evermore effective functional materials. Indeed, analysis of recent results in the field leads to the conclusion that current research is focused more on gaining a deeper understanding and fine-tuning properties that are not strictly related to payload discharge, e.g., salt stability or thermo-responsiveness. Nonetheless, exciting new approaches, such as developments in the use of supramolecular vesicles, are still being introduced. Reversible boronic ester formation with glucose has also been incorporated into insulin derivatives, offering potential for new strategies toward artificial pancreas development.<sup>[184]</sup> Researchers are also developing boronate based materials for insulin delivery with additional functions to strengthen potential therapeutic effect (additional type of cargo) or/and allow for better glucose monitoring, which may soon see the realisation of multicomponent systems. One of the key advantage of enzymes over man-made materials is their specificity whereas wholly synthetic systems offer superior shelf lives and may be processed, transported and stored under nonambient or nonrefrigerated conditions; while the problem of glucose selectivity over fructose in the context of insulin delivery platforms has been tackled, huge improvements are still to be made to match the exquisite specificity of nature's tools.

Alongside developments within the field of boronic acid based insulin delivery, so too have great advances been made in boronic acid based molecular sensors in diagnostic systems.<sup>[15]</sup> In efforts

to develop ever more selective sensors, synthetic chemists have begun to utilise a diverse range of boronic acid derivatives, and incorporate a range on functionalities and broadening the sensors' reporting capabilities. Conversely, the materials reported for use in insulin delivery, and thus reported in this review, tend to be constructed from building blocks that draw upon a smaller, simpler subset of compounds.<sup>[185]</sup> It is our belief that the application of the ever-expanding synthetic chemical toolbox bolstered by the developments in the boron-containing chemical sensors arena could bolster the chemical diversity and capabilities on offer in the boron-mediated insulin delivery domain and incorporation of more diverse derivatives into drug-delivery materials presents a great source of untapped potential within this field.<sup>[186]</sup>

The release of multiple agents in addition to insulin from these materials can further increase therapeutic benefit in control of diabetes. While it is primarily pancreatic  $\beta$ -cells that are considered in diabetes, there is also evidence that the  $\alpha$ -cells may also become damaged, preventing the release of glucagon.<sup>[187]</sup> This is another hormone essential to blood glucose control, which converts glycogen into glucose in hypoglycemic conditions. One of the key problem areas in the development of artificial pancreas materials is the delay in the “turn off” of release. Dual release systems that are also capable of releasing this important secondary hormone, which can help to prevent hypoglycemia due to excessive insulin release have also been the subject of some important studies.<sup>[188]</sup> We envisage that dual hormone release protocols will become more important as this research translates toward clinical serving to present a more useful artificial pancreas.

Looking toward a material as a potential clinical candidate for diabetes management, those materials that display “on-off” release kinetic profiles are undeniably superior; since in the absence of a clear “off” characteristic, resolving high blood glucose only for a patient to potentially become hypoglycemic offers little advantage compared to current treatments. The capacity for encapsulating insulin also varies greatly across the reviewed materials, with the most effective materials reaching over 90% loading efficiency. While this is an important metric to consider, the maximum reported loading capacity of the reviewed materials was 35.6% with many failing to reach even half of this level. It may perhaps be concluded that this value should be improved in order prevent the requirement for large volumes of material to be ultimately clinically administered. The glucose concentration range over which these materials are effective is also of great importance; normal blood sugar levels are between  $4 \times 10^{-3}$  and  $11 \times 10^{-3}$  M, however a number of the tested systems use much higher concentrations to trigger release. It is imperative moving forward in this field that materials are developed that are capable of responding to these smaller fluctuations. While the shelf life of materials is impacted by glucose-free insulin leaching it is important to recognise that the absence of glucose is not a physiologically relevant scenario and clinically accessible extremes of blood glucose offer a tighter test regime by which to benchmark controlled release materials to for translation. Many of these materials exhibit “burst release” responses, which while important for immediate control of blood sugar, must be limited in scale to prevent hypoglycemia. An accompanying slow release of insulin may also serve to help maintain basal insulin levels; optimum release factors and rates are yet to be defined, and will be crucial moving forward in the development of these materials. Many

authors noted that other sugars, fructose in particular, may interfere with the insulin release. This may not however be an issue, owing to the low concentration of other sugars within the body, though to test against nonglucose specific release at their physiological concentrations would help to alleviate these concerns. Other common interferents and drugs are also meritorious control compounds that could be considered at the in vitro efficacy testing stage. As in many of the reported works, the use of CD spectroscopy to determine the integrity of the released insulin, and thus activity, is essential. While there are no instances within this review of the insulin being adversely effective by encapsulation and release, it is imperative to determine that this is the case before proceeding toward in vivo studies. Indeed, unless successful results across the a range of rigorous in vitro experiments are obtained the use of animal models should not be pursued.<sup>[189]</sup>

One of the largest barriers to the translation of materials to a clinical setting is that of in vivo testing, and it gives us great reassurance in this approach to see how many of the reviewed works offer no negative side effects and prolonged delivery characteristics. As injectable/implantable devices, such materials are defined within the EU as a class III medical device.<sup>[190]</sup> This necessitate that not only does the device gain approval through regulatory authorities, but there are regulations that must be adhered to when considering the sourcing and manufacture of associated materials; this may guide the choice of materials from which future systems are developed.

## Acknowledgements

All the authors thank the University of Birmingham for support. Ł.B. also thanks Adam Mickiewicz University in Poznań. Cancer Research UK (CRUK Pioneer Award 26212), the Juvenile Diabetes Research Foundation (JDRF 2-SRA-2016-267-A-N), and Medical Research Council (MRC Confidence in Concepts 7.1-07F) grants supported research of the authors of this review which informed the scope and direction of the details contained within this manuscript. Members of the research group are thanked for helpful comments during the preparation of this manuscript.

## Conflict of Interest

The authors declare no conflict of interest.

## Author Contributions

All authors critically assessed the literature in constructing this review. All authors prepared figures, co-wrote text, and commented upon all aspects of the manuscript.

## Keywords

boronic acid, controlled release, diabetes mellitus, glucose, insulin

Received: May 18, 2021

Revised: July 7, 2021

Published online: August 15, 2021

[1] a) A. American Diabetes, *Diabetes Care* **2013**, *36*, S67; b) A. American Diabetes, *Diabetes Care* **2014**, *37*, S81; c) *IDF Diabetes Atlas*, 9th ed., Brussels, Belgium, **2019**.

- [2] a) D. Daneman, *Lancet* **2006**, *367*, 847; b) E. M. Benjamin, *Clin. Diabetes* **2002**, *20*, 45.
- [3] A. Zambanini, R. B. Newson, M. Maisey, M. D. Feher, *Diabetes Res. Clin. Pract.* **1999**, *46*, 239.
- [4] a) W. Wu, S. Zhou, *Macromol. Biosci.* **2013**, *13*, 1464; b) S. M. Marshall, *Diabetologia* **2021**, *64*, 944; c) C. K. Boughton, R. Hovorka, *Diabetologia* **2021**, *64*, 1007.
- [5] M. A. Jarosinski, B. Dhayalan, N. Rege, D. Chatterjee, M. A. Weiss, *Diabetologia* **2021**, *64*, 1016.
- [6] a) M. W. Tibbitt, J. E. Dahlman, R. Langer, *J. Am. Chem. Soc.* **2016**, *138*, 704; b) A. S. Hoffman, *J. Controlled Release* **2008**, *132*, 153.
- [7] a) P. T. Wong, S. K. Choi, *Chem. Rev.* **2015**, *115*, 3388; b) G.-H. Son, B.-J. Lee, C.-W. Cho, *J. Pharm. Invest.* **2017**, *47*, 287.
- [8] T. M. Allen, P. R. Cullis, *Science* **2004**, *303*, 1818.
- [9] D. Liu, F. Yang, F. Xiong, N. Gu, *Theranostics* **2016**, *6*, 1306.
- [10] J. Siepmann, F. Siepmann, *Int. J. Pharm.* **2008**, *364*, 328.
- [11] P. Raskin, R. A. Guthrie, L. Leiter, A. Riis, L. Jovanovic, *Diabetes Care* **2000**, *23*, 583.
- [12] *IDF Diabetes Atlas*, 7th ed., Brussels, Belgium, **2015**.
- [13] E. Boland, T. Monsod, M. Delucia, C. A. Brandt, S. Fernando, W. V. Tamborlane, *Diabetes Care* **2001**, *24*, 1858.
- [14] a) H. G. Kuivila, A. H. Keough, E. J. Soboczenski, *J. Org. Chem.* **1954**, *19*, 780; b) J. P. Lorand, J. O. Edwards, *J. Org. Chem.* **1959**, *24*, 769.
- [15] G. T. Williams, J. L. Kedge, J. S. Fossey, *ACS Sens.* **2021**, *6*, 1508.
- [16] W. L. A. Brooks, B. S. Sumerlin, *Chem. Rev.* **2016**, *116*, 1375.
- [17] a) G. Wulff, *Pure Appl. Chem.* **1982**, *54*, 2093; b) G. Wulff, M. Lauer, H. Böhnke, *Angew. Chem., Int. Ed.* **1984**, *23*, 741.
- [18] D. Li, Q. Li, S. Wang, J. Ye, H. Nie, Z. Liu, *J. Chromatogr. A* **2014**, *1339*, 103.
- [19] a) W. Zhai, L. Male, J. S. Fossey, *Chem. Commun.* **2017**, *53*, 2218; b) X. Sun, W. Zhai, J. S. Fossey, T. D. James, *Chem. Commun.* **2016**, *52*, 3456; c) W. Zhai, X. Sun, T. D. James, J. S. Fossey, *Chem.-Asian J.* **2015**, *10*, 1836.
- [20] L. Zhao, C. Xiao, L. Wang, G. Gai, J. Ding, *Chem. Commun.* **2016**, *52*, 7633.
- [21] a) H. Schellekens, *Clin. Ther.* **2002**, *24*, 1720; b) S. Hermeling, D. J. Crommelin, H. Schellekens, W. Jiskoot, *Pharm. Res.* **2004**, *21*, 897; c) A. J. Chirino, M. L. Ary, S. A. Marshall, *Drug Discovery Today* **2004**, *9*, 82; d) A. S. De Groot, D. W. Scott, *Trends Immunol.* **2007**, *28*, 482.
- [22] a) E. P. Gillis, M. D. Burke, *J. Am. Chem. Soc.* **2008**, *130*, 14084; b) D. M. Knapp, E. P. Gillis, M. D. Burke, *J. Am. Chem. Soc.* **2009**, *131*, 6961; c) J. W. B. Fyfe, A. J. B. Watson, *Chem* **2017**, *3*, 31.
- [23] a) D. G. Hall, *Boronic Acids* **2011**; b) D. G. Hall, *Boronic Acids*, Wiley-VCH, Weinheim, **2005**.
- [24] A. American Diabetes, *Diabetes Care* **2012**, *35*, S11.
- [25] K. Ogurtsova, J. D. da Rocha Fernandes, Y. Huang, U. Linnenkamp, L. Guariguata, N. H. Cho, D. Cavan, J. E. Shaw, L. E. Makaroff, *Diabetes Res. Clin. Pract.* **2017**, *128*, 40.
- [26] *Diabetes Care* **2013**, *37*, S81.
- [27] a) F. G. Banting, C. H. Best, *J. Lab. Clin. Med.* **1922**, *7*, 251; b) F. G. Banting, C. H. Best, *J. Lab. Clin. Med.* **1922**, *7*, 464; c) F. G. Banting, C. H. Best, J. B. Collip, W. R. Campbell, A. A. Fletcher, *Can. Med. Assoc. J.* **1922**, *12*, 141.
- [28] a) U. Derewenda, Z. Derewenda, G. G. Dodson, R. E. Hubbard, F. Korber, *Br. Med. Bull.* **1989**, *45*, 4; b) G. Bentley, E. Dodson, G. U. Y. Dodson, D. Hodgkin, D. A. N. Mercola, *Nature* **1976**, *261*, 166; c) M. F. Dunn, *BioMetals* **2005**, *18*, 295; d) E. Ciszak, G. D. Smith, *Biochemistry* **1994**, *33*, 1512.
- [29] D. Mathis, L. Vence, C. Benoist, *Nature* **2001**, *414*, 792.
- [30] a) A. Alvestrand, J. Wahren, D. Smith, R. A. DeFronzo, *Am. J. Physiol.* **1984**, *246*, E174; b) A. K. Gupta, R. V. Clark, K. A. Kirchner, *Hypertension* **1992**, *19*, 178; c) P. Puigserver, J. Rhee, J. Donovan, C. J. Walkey, J. C. Yoon, F. Oriente, Y. Kitamura, J. Altomonte, H. Dong, D. Accili,

- B. M. Spiegelman, *Nature* **2003**, 423, 550; d) H.-Y. Liu, J. Han, S. Y. Cao, T. Hong, D. Zhuo, J. Shi, Z. Liu, W. Cao, *J. Biol. Chem.* **2009**, 284, 31484.
- [31] a) A. K. Niazi, S. K. Niazi, *Indian J. Endocrinol. Metab.* **2012**, 16, 57; b) J. M. Benni, P. A. Patil, *J. Basic Clin. Physiol. Pharmacol.* **2016**, 27, 445.
- [32] a) R. A. DeFronzo, E. Jacot, E. Jequier, E. Maeder, J. Wahren, J. P. Felber, *Diabetes* **1981**, 30, 1000; b) M. P. Czech, *Annu. Rev. Physiol.* **1985**, 47, 357; c) S. R. Hubbard, L. Wei, L. Ellis, W. A. Hendrickson, *Nature* **1994**, 372, 746; d) N. J. Bryant, R. Govers, D. E. James, *Nat. Rev. Mol. Cell Biol.* **2002**, 3, 267.
- [33] W. C. Knowler, E. Barrett-Connor, S. E. Fowler, R. F. Hamman, J. M. Lachin, E. A. Walker, D. M. Nathan, Diabetes Prevention Program Research Group, *N. Engl. J. Med.* **2002**, 346, 393.
- [34] M. de Veciana, C. A. Major, M. A. Morgan, T. Asrat, J. S. Toohey, J. M. Lien, A. T. Evans, *N. Engl. J. Med.* **1995**, 333, 1237.
- [35] J. W. Baynes, *Diabetes* **1991**, 40, 405.
- [36] D. E. DeWitt, I. B. Hirsch, *J. Am. Med. Assoc.* **2003**, 289, 2254.
- [37] a) T. Deckert, *Diabetes Care* **1980**, 3, 623; b) P. Home, *Expert Opin. Investig. Drugs* **1999**, 8, 307; c) M. Lepore, S. Pampanelli, C. Fanelli, F. Porcellati, L. Bartocci, A. Di Vincenzo, C. Cordoni, E. Costa, P. Brunetti, G. B. Bolli, *Diabetes* **2000**, 49, 2142; d) M. C. Riddle, J. Rosenstock, J. Gerich, *Diabetes Care* **2003**, 26, 3080; e) S. Havelund, A. Plum, U. Ribel, I. Jonassen, A. Volund, J. Markussen, P. Kurtzhals, *Pharm. Res.* **2004**, 21, 1498; f) K. Raslova, M. Bogoev, I. Raz, G. Leth, M. A. Gall, N. Hancu, *Diabetes Res. Clin. Pract.* **2004**, 66, 193; g) S. K. Garg, S. L. Ellis, H. Ulrich, *Expert Opin. Pharmacother.* **2005**, 6, 643; h) R. J. Heine, L. F. Van Gaal, D. Johns, M. J. Mihm, M. H. Widell, R. G. Brodows, G. S. Group, *Ann. Intern. Med.* **2005**, 143, 559; i) R. H. Becker, A. D. Frick, *Clin. Pharmacokinet.* **2008**, 47, 7; j) M. Oak, J. Singh, *J. Controlled Release* **2012**, 163, 145.
- [38] M. Peyrot, A. H. Barnett, L. F. Meneghini, P. M. Schumm-Draeger, *Diabet. Med.* **2012**, 29, 682.
- [39] R. G. McCoy, H. K. Van Houten, J. Y. Ziegenfuss, N. D. Shah, R. A. Wermers, S. A. Smith, *Diabetes Care* **2012**, 35, 1897.
- [40] a) P. Kurtzhals, B. Kiehr, A. R. Sørensen, *J. Pharm. Sci.* **1995**, 84, 1164; b) P. Kurtzhals, S. Havelund, I. Jonassen, B. Kiehr, U. D. Larsen, U. Ribel, J. Markussen, *Biochem. J.* **1995**, 312, 725; c) I. Jonassen, S. Havelund, U. Ribel, A. Plum, M. Loftager, T. Hoeg-Jensen, A. Volund, J. Markussen, *Pharm. Res.* **2006**, 23, 49; d) L. Malik, J. Nygaard, R. Hoiberg-Nielsen, L. Arleth, T. Hoeg-Jensen, K. J. Jensen, *Langmuir* **2012**, 28, 593; e) I. Jonassen, S. Havelund, T. Hoeg-Jensen, D. B. Steensgaard, P. O. Wahlund, U. Ribel, *Pharm. Res.* **2012**, 29, 2104.
- [41] a) B. J. Wheeler, K. Heels, K. C. Donaghue, D. M. Reith, G. R. Ambler, *Diabetes Technol. Ther.* **2014**, 16, 558; b) A. L. Brorsson, G. Viklund, E. Ortqvist, A. Lindholm Olander, *Pediatr. Diabetes* **2015**, 16, 546.
- [42] J. C. Pickup, *N. Engl. J. Med.* **2012**, 366, 1616.
- [43] a) J. C. Pickup, N. Yemane, A. Brackenridge, S. Pender, *Diabetes Technol. Ther.* **2013**, 16, 145; b) M. Peyrot, D. Dreon, V. Zraick, B. Cross, M. H. Tan, *Diabetes Ther.* **2018**, 9, 297.
- [44] a) A. C. Sintov, H. V. Levy, S. Botner, *J. Controlled Release* **2010**, 148, 168; b) L. Illum, *J. Controlled Release* **2012**, 161, 254.
- [45] a) H. Iyer, A. Khedkar, M. Verma, *Diabetes Obes. Metab.* **2010**, 12, 179; b) S. H. Bakhr, S. Furtado, A. P. Morello, E. Mathiowitz, *Adv. Drug Delivery Rev.* **2013**, 65, 811.
- [46] a) F. Andrade, M. Videira, D. Ferreira, B. Sarmiento, *Nanomedicine* **2011**, 6, 123; b) F. Fang, Y. Lu, Y. Liang, J. Zhu, J. He, J. Zheng, N. Li, Y. Tang, J. Zhu, X. Chen, *Pharmazie* **2012**, 67, 706.
- [47] a) Y. Tahara, S. Honda, N. Kamiya, M. Goto, *MedChemComm* **2012**, 3, 1496; b) Y. Ito, T. Nakahigashi, N. Yoshimoto, Y. Ueda, N. Hamasaki, K. Takada, *Diabetes Technol. Ther.* **2012**, 14, 891; c) A. Azagury, L. Khoury, G. Enden, J. Kost, *Adv. Drug Delivery Rev.* **2014**, 72, 127.
- [48] a) D. Eek, M. Krohe, I. Mazar, A. Horsfield, F. Pompilus, R. Friebe, A. L. Shields, *Patient Prefer. Adherence* **2016**, 10, 1609; b) *J. Oncol. Pract.* **2008**, 4, 175.
- [49] D. K. Chellappan, Y. Yenese, C. C. Wei, J. Chellian, G. Gupta, *J. Environ. Pathol. Toxicol. Oncol.* **2017**, 36, 283.
- [50] a) E. Bosi, P. Choudhary, H. W. de Valk, S. Lablanche, J. Castañeda, S. de Portu, J. Da Silva, R. Ré, L. Vorrink-de Groot, J. Shin, F. R. Kaufman, O. Cohen, A. Laurenzi, A. Caretto, D. Slatlerly, M. Henderson-Wilson, S. J. Weisnagel, M.-C. Dubé, V.-É. Julien, R. Trevisan, G. Lepore, L. Bellante, I. Hramiik, T. Spaic, M. Driscoll, S. Borot, A. Clergeot, L. Khiat, P. Hammond, S. Ray, L. Dinning, G. Tonolo, A. Manconi, M. S. Ledda, W. de Ranitz, B. Silvius, A. Wojtuszczyk, A. Farret, T. Vriesendorp, F. Immecker-de Jong, J. van der Linden, H. S. Brink, M. Alkemade, P. Schaepeylnck-Belicar, S. Galie, C. Trégliia, P.-Y. Benhamou, M. Haddouche, R. Hoogma, L. Leelarathna, A. Shaju, L. James, *Lancet Diabetes Endocrinol.* **2019**, 7, 462; b) S. K. Garg, S. A. Weinzimer, W. V. Tamborlane, B. A. Buckingham, B. W. Bode, T. S. Bailey, R. L. Brazg, J. Ilany, R. H. Slover, S. M. Anderson, R. M. Bergenstal, B. Grosman, A. Roy, T. L. Cordero, J. Shin, S. W. Lee, F. R. Kaufman, *Diabetes Technol. Ther.* **2017**, 19, 155.
- [51] G. P. Forlenza, O. Pinhas-Hamiel, D. R. Liljenquist, D. I. Shulman, T. S. Bailey, B. W. Bode, M. A. Wood, B. A. Buckingham, K. B. Kaiserman, J. Shin, S. Huang, S. W. Lee, F. R. Kaufman, *Diabetes Technol. Ther.* **2018**, 21, 11.
- [52] a) D. Lewis, *J. Diabetes Sci. Technol.* **2018**, 13, 790; b) A. Gawrecki, D. Zozulinska-Ziolkiewicz, M. A. Michalak, A. Adamska, M. Michalak, U. Frackowiak, J. Flotyńska, M. Pietrzak, S. Czaplak, B. Gehr, A. Araszkiwicz, *PLoS One* **2021**, 16, e0248965.
- [53] M. Brownlee, A. Cerami, *Science* **1979**, 206, 1190.
- [54] R. A. Insel, D. C. Deecher, J. Brewer, *Diabetes* **2012**, 61, 30.
- [55] a) C. M. Wong, K. H. Wong, X. D. Chen, *Appl. Microbiol. Biotechnol.* **2008**, 78, 927; b) S. B. Bankar, M. V. Bule, R. S. Singhal, L. Ananthanarayan, *Biotechnol. Adv.* **2009**, 27, 489; c) L. A. Klumb, T. A. Horbett, *J. Controlled Release* **1992**, 18, 59.
- [56] a) W. Zhao, H. Zhang, Q. He, Y. Li, J. Gu, L. Li, H. Li, J. Shi, *Chem. Commun.* **2011**, 47, 9459; b) J. Luo, S. Cao, X. Chen, S. Liu, H. Tan, W. Wu, J. Li, *Biomaterials* **2012**, 33, 8733; c) R. Luo, H. Li, *Soft Mater.* **2013**, 11, 69; d) P. Diez, A. Sanchez, M. Gamella, P. Martinez-Ruiz, E. Aznar, C. de la Torre, J. R. Murguía, R. Martinez-Manez, R. Villalonga, J. M. Pingarron, *J. Am. Chem. Soc.* **2014**, 136, 9116.
- [57] a) Z. Gu, T. T. Dang, M. Ma, B. C. Tang, H. Cheng, S. Jiang, Y. Dong, Y. Zhang, D. G. Anderson, *ACS Nano* **2013**, 7, 6758; b) M. Y. Kim, J. Kim, *ACS Biomater. Sci. Eng.* **2017**, 3, 572; c) C. R. Gordijo, A. J. Shuhendler, X. Y. Wu, *Adv. Funct. Mater.* **2010**, 20, 1404.
- [58] J. Yu, Y. Zhang, Y. Ye, R. DiSanto, W. Sun, D. Ranson, F. S. Ligler, J. B. Buse, Z. Gu, *Proc. Natl. Acad. Sci. USA* **2015**, 112, 8260.
- [59] N. Sharon, H. Lis, *Science* **1972**, 177, 949.
- [60] a) M. J. Taylor, S. Tanna, T. S. Sahota, B. Voermans, *Eur. J. Pharm. Biopharm.* **2006**, 62, 94; b) S. Tanna, T. S. Sahota, K. Sawicka, M. J. Taylor, *Biomaterials* **2006**, 27, 4498; c) K. Yoshida, Y. Hasebe, S. Takahashi, K. Sato, J. Anzai, *Mater. Sci. Eng., C* **2014**, 34, 384; d) R. Yin, Z. Tong, D. Yang, J. Nie, *Int. J. Biol. Macromol.* **2011**, 49, 1137.
- [61] a) R. Ballerstadt, C. Evans, R. McNichols, A. Gowda, *Biosens. Bioelectron.* **2006**, 22, 275; b) W. A. Broom, C. E. Coulthard, M. R. Gurd, M. E. Sharpe, *Br. J. Pharmacol. Chemother.* **1946**, 1, 225.
- [62] a) R. Mo, T. Jiang, J. Di, W. Tai, Z. Gu, *Chem. Soc. Rev.* **2014**, 43, 3595; b) V. Ravaine, C. Ancla, B. Catargi, *J. Controlled Release* **2008**, 132, 2; c) O. Veisheh, B. C. Tang, K. A. Whitehead, D. G. Anderson, R. Langer, *Nat. Rev. Drug Discovery* **2015**, 14, 45; d) J. Yang, Z. Cao, *J. Controlled Release* **2017**, 263, 231; e) J. Wang, Z. Wang, J. Yu, A. R. Kahkoska, J. B. Buse, Z. Gu, *Adv. Mater.* **2020**, 32, 1902004.

- [63] a) D. Roy, J. N. Cambre, B. S. Sumerlin, *Prog. Polym. Sci.* **2010**, *35*, 278; b) Y. Guan, Y. Zhang, *Chem. Soc. Rev.* **2013**, *42*, 8106; c) R. Ma, L. Shi, *Polym. Chem.* **2014**, *5*, 1503; d) T. Elshaarani, H. Yu, L. Wang, Z.-u.-A. Zain-ul-Abdin, R. S. Ullah, M. Haroon, R. U. Khan, S. Fahad, A. Khan, A. Nazir, M. Usman, K.-u.-R. Naveed, *J. Mater. Chem. B* **2018**, *6*, 3831.
- [64] a) A. D. Drozdov, J. D. Christiansen, *J. Mech. Behav. Biomed. Mater.* **2017**, *65*, 533; b) K. Sarkar, P. Dastidar, *Langmuir* **2018**, *34*, 685.
- [65] a) H. Yang, C. Zhang, C. Li, Y. Liu, Y. An, R. Ma, L. Shi, *Biomacromolecules* **2015**, *16*, 1372; b) H. Yang, R. Ma, J. Yue, C. Li, Y. Liu, Y. An, L. Shi, *Polym. Chem.* **2015**, *6*, 3837.
- [66] a) X. Jin, X. Zhang, Z. Wu, D. Teng, X. Zhang, Y. Wang, Z. Wang, C. Li, *Biomacromolecules* **2009**, *10*, 1337; b) Q. Guo, T. Zhang, J. An, Z. Wu, Y. Zhao, X. Dai, X. Zhang, C. Li, *Biomacromolecules* **2015**, *16*, 3345.
- [67] a) R. Ma, H. Yang, Z. Li, G. Liu, X. Sun, X. Liu, Y. An, L. Shi, *Biomacromolecules* **2012**, *13*, 3409; b) X. Zhang, S. Lu, C. Gao, C. Chen, X. Zhang, M. Liu, *Nanoscale* **2013**, *5*, 6498; c) L. Zhao, C. Xiao, J. Ding, P. He, Z. Tang, X. Pang, X. Zhuang, X. Chen, *Acta Biomater.* **2013**, *9*, 6535; d) G. Liu, R. Ma, J. Ren, Z. Li, H. Zhang, Z. Zhang, Y. An, L. Shi, *Soft Matter* **2013**, *9*, 1636; e) Y. N. Zhao, Q. Yuan, C. Li, Y. Guan, Y. Zhang, *Biomacromolecules* **2015**, *16*, 2032; f) Y. Gao, K. Y. Wong, A. Ahiabu, M. J. Serpe, *J. Mater. Chem. B* **2016**, *4*, 5144; g) W. L. A. Brooks, G. Vancoillie, C. P. Kabb, R. Hoogenboom, B. S. Sumerlin, *J. Polym. Sci. Pol. Chem.* **2017**, *55*, 2309.
- [68] S. Kitano, K. Kataoka, Y. Koyama, T. Okano, Y. Sakurai, *Makromol. Chem. Rapid Commun.* **1991**, *12*, 227.
- [69] a) S. Kitano, Y. Koyama, K. Kataoka, T. Okano, Y. Sakurai, *J. Controlled Release* **1992**, *19*, 161; b) C. Young Kweon, J. Seo Young, K. Young Ha, *Int. J. Pharm.* **1992**, *80*, 9.
- [70] A. Matsumoto, T. Ishii, J. Nishida, H. Matsumoto, K. Kataoka, Y. Miyahara, *Angew. Chem., Int. Ed.* **2012**, *51*, 2124.
- [71] V. Lapeyre, C. Ancla, B. Catargi, V. Ravaine, *J. Colloid Interface Sci.* **2008**, *327*, 316.
- [72] a) Y. Li, W. Xiao, K. Xiao, L. Berti, J. Luo, H. P. Tseng, G. Fung, K. S. Lam, *Angew. Chem.* **2012**, *51*, 2864; b) Y. Zhao, B. G. Trewyn, I. I. Slowing, V. S. Lin, *J. Am. Chem. Soc.* **2009**, *131*, 8398; c) W. Wu, N. Mitra, E. C. Y. Yan, S. Zhou, *ACS Nano* **2010**, *4*, 4831; d) X. Zhang, Y. Guan, Y. Zhang, *J. Mater. Chem.* **2012**, *22*, 16299.
- [73] a) F. Tietze, G. E. Mortimore, N. R. Lornax, *Biochim. Biophys. Acta* **1962**, *59*, 336; b) D. Shiino, Y. Murata, K. Kataoka, Y. Koyama, M. Yokoyama, T. Okano, Y. Sakurai, *Biomaterials* **1994**, *15*, 121.
- [74] a) S. W. Kim, Y. H. Bae, T. Okano, *Pharm. Res.* **1992**, *9*, 283; b) N. A. Peppas, P. Bures, W. Leobandung, H. Ichikawa, *Eur. J. Pharm. Biopharm.* **2000**, *50*, 27.
- [75] a) S. Correa, A. K. Grosskopf, H. L. Hernandez, D. Chan, A. C. Yu, L. M. Stapleton, E. A. Appel, *Chem. Rev.* **2021**, <https://doi.org/10.1021/acs.chemrev.0c01177>; b) E. Caló, V. V. Khutoryanskiy, *Eur. Polym. J.* **2015**, *65*, 252.
- [76] D. Mandal, S. K. Mandal, M. Ghosh, P. K. Das, *Chemistry (Easton)* **2015**, *21*, 12042.
- [77] D. J. Abdallah, R. G. Weiss, *Adv. Mater.* **2000**, *12*, 1237.
- [78] V. Yesilyurt, M. J. Webber, E. A. Appel, C. Godwin, R. Langer, D. G. Anderson, *Adv. Mater.* **2016**, *28*, 86.
- [79] a) A. Matsumoto, M. Yuasa, H. Matsumoto, M. Sanjo, M. Tabata, T. Goda, T. Hoshi, T. Aoyagi, Y. Miyahara, *Chem. Lett.* **2016**, *45*, 460; b) A. Matsumoto, M. Tanaka, H. Matsumoto, K. Ochi, Y. Moro-oka, H. Kuwata, H. Yamada, I. Shirakawa, T. Miyazawa, H. Ishii, K. Kataoka, Y. Ogawa, Y. Miyahara, T. Suganami, *Sci. Adv.* **2017**, *3*, eaaq0723b.
- [80] R. Yoshida, K. Sakai, T. Okano, Y. Sakurai, *Adv. Drug Delivery Rev.* **1993**, *11*, 85.
- [81] S. Chen, H. Matsumoto, Y. Moro-oka, M. Tanaka, Y. Miyahara, T. Suganami, A. Matsumoto, *Adv. Funct. Mater.* **2019**, *29*, 1807369.
- [82] S. Chen, H. Matsumoto, Y. Moro-oka, M. Tanaka, Y. Miyahara, T. Suganami, A. Matsumoto, *ACS Biomater. Sci. Eng.* **2019**, *5*, 5781.
- [83] S. Chen, T. Miyazaki, M. Itoh, H. Matsumoto, Y. Moro-oka, M. Tanaka, Y. Miyahara, T. Suganami, A. Matsumoto, *ACS Appl. Polym. Mater.* **2020**, *2*, 2781.
- [84] A. Matsumoto, H. Kuwata, S. Kimura, H. Matsumoto, K. Ochi, Y. Moro-oka, A. Watanabe, H. Yamada, H. Ishii, T. Miyazawa, S. Chen, T. Baba, H. Yoshida, T. Nakamura, H. Inoue, Y. Ogawa, M. Tanaka, Y. Miyahara, T. Suganami, *Commun. Biol.* **2020**, *3*, 313.
- [85] J. Yu, J. Wang, Y. Zhang, G. Chen, W. Mao, Y. Ye, A. R. Kahkoska, J. B. Buse, R. Langer, Z. Gu, *Nat. Biomed. Eng.* **2020**, *4*, 499.
- [86] B. Cai, Y. Luo, Q. Guo, X. Zhang, Z. Wu, *Carbohydr. Res.* **2017**, *445*, 32.
- [87] H. Peng, X. Ning, G. Wei, S. Wang, G. Dai, A. Ju, *Carbohydr. Polym.* **2018**, *195*, 349.
- [88] J. Lee, J. H. Ko, K. M. Mansfield, P. C. Nauka, E. Bat, H. D. Maynard, *Macromol. Biosci.* **2018**, *18*, 1700372.
- [89] X. Zhi, C. Zheng, J. Xiong, J. Li, C. Zhao, L. Shi, Z. Zhang, *Langmuir* **2018**, *34*, 12914.
- [90] S. Gu, L. Yang, S. Li, J. Yang, B. Zhang, J. Yang, *Polym. Int.* **2018**, *67*, 1256.
- [91] L. Zhao, L. Niu, H. Liang, H. Tan, C. Liu, F. Zhu, *ACS Appl. Mater. Interfaces* **2017**, *9*, 37563.
- [92] T. Elshaarani, H. Yu, L. Wang, J. Feng, C. Li, W. Zhou, A. Khan, M. Usman, B. U. Amin, R. Khan, *Int. J. Biol. Macromol.* **2020**, *161*, 109.
- [93] M. Q. Tong, L. Z. Luo, P. P. Xue, Y. H. Han, L. F. Wang, D. L. Zhuge, Q. Yao, B. Chen, Y. Z. Zhao, H. L. Xu, *Acta Biomater.* **2021**, *122*, 111.
- [94] E. Roduner, *Chem. Soc. Rev.* **2006**, *35*, 583.
- [95] a) C. Quillet, H. F. Eicke, *J. Phys. Chem.* **1987**, *91*, 4211; b) A. E. Ekkelenkamp, M. R. Elzes, J. F. J. Engbersen, J. M. J. Paulusse, *J. Mater. Chem. B* **2018**, *6*, 210.
- [96] a) T. Tanaka, D. J. Fillmore, *J. Chem. Phys.* **1979**, *70*, 1214; b) J. Wang, D. Gan, L. A. Lyon, M. A. El-Sayed, *J. Am. Chem. Soc.* **2001**, *123*, 11284; c) C. E. Reese, A. V. Mikhonin, M. Kamenjicki, A. Tikhonov, S. A. Asher, *J. Am. Chem. Soc.* **2004**, *126*, 1493.
- [97] L. Zhao, C. S. Xiao, J. X. Ding, X. L. Zhuang, G. Q. Gai, L. Y. Wang, X. S. Chen, *Polym. Chem.* **2015**, *6*, 3807.
- [98] D. Lee, K. Choe, Y. Jeong, J. Yoo, S. M. Lee, J.-H. Park, P. Kim, Y.-C. Kim, *RSC Adv.* **2015**, *5*, 14482.
- [99] Q. Guo, X. Zhang, *J. Biomater. Sci., Polym. Ed.* **2019**, *30*, 815.
- [100] S. Yuan, X. Li, X. Shi, X. Lu, *Colloid. Polym. Sci.* **2019**, *297*, 613.
- [101] C. Li, X. Liu, Y. Liu, F. Huang, G. Wu, Y. Liu, Z. Zhang, Y. Ding, J. Lv, R. Ma, Y. An, L. Shi, *Nanoscale* **2019**, *11*, 9163.
- [102] N. A. Siddiqui, N. Billa, C. J. Roberts, Y. Asantewaa Osei, *Pharmaceuticals* **2016**, *8*, 30.
- [103] Y. Wang, F. Huang, Y. Sun, M. Gao, Z. Chai, *J. Biomater. Sci., Polym. Ed.* **2017**, *28*, 93.
- [104] L. Li, G. Jiang, W. Yu, D. Liu, H. Chen, Y. Liu, Z. Tong, X. Kong, J. Yao, *Mater. Sci. Eng. C* **2017**, *70*, 278.
- [105] G. Springsteen, B. Wang, *Tetrahedron* **2002**, *58*, 5291.
- [106] X. Wu, Z. Li, X.-X. Chen, J. S. Fossey, T. D. James, Y.-B. Jiang, *Chem. Soc. Rev.* **2013**, *42*, 8032.
- [107] N. A. Siddiqui, N. Billa, C. J. Roberts, *J. Biomater. Sci., Polym. Ed.* **2017**, *28*, 781.
- [108] X. Zhou, A. Lin, X. Yuan, H. Li, D. Ma, W. Xue, *J. Appl. Polym. Sci.* **2016**, *133*, 43504.
- [109] a) D. A. Scott, *Biochem. J.* **1934**, *28*, 1592; b) J. Goldman, F. H. Carpenter, *Biochemistry* **1974**, *13*, 4566.
- [110] C. Li, G. Wu, R. Ma, Y. Liu, Y. Liu, J. Lv, Y. An, L. Shi, *ACS Biomater. Sci. Eng.* **2018**, *4*, 2007.
- [111] a) J. Z. Wu, D. H. Bremner, H. Y. Li, S. W. Niu, S. D. Li, L. M. Zhu, *Mater. Sci. Eng. C* **2017**, *76*, 845; b) J. Z. Wu, G. R. Williams, H. Y.

- Li, D. Wang, H. Wu, S. D. Li, L. M. Zhu, *Int. J. Nanomed.* **2017**, *12*, 4037.
- [112] Y. Zhong, B. Song, D. He, Z. Xia, P. Wang, J. Wu, Y. Li, *Nanotechnology* **2020**, *31*, 395601.
- [113] H. H. Hsieh, L. C. Ho, H. T. Chang, *Anal. Bioanal. Chem.* **2016**, *408*, 6557.
- [114] J. Liu, S. Z. Qiao, H. Liu, J. Chen, A. Orpe, D. Zhao, G. Q. Lu, *Angew. Chem., Int. Ed.* **2011**, *50*, 5947.
- [115] J. Z. Wu, D. H. Bremner, H. Y. Li, X. Z. Sun, L. M. Zhu, *Mater. Sci. Eng., C* **2016**, *69*, 1026.
- [116] J. Z. Wu, Y. Yang, S. Li, A. Shi, B. Song, S. Niu, W. Chen, Z. Yao, *Int. J. Nanomed.* **2019**, *14*, 8059.
- [117] H. Guo, H. Li, J. Gao, G. Zhao, L. Ling, B. Wang, Q. Guo, Y. Gu, C. Li, *Polym. Chem.* **2016**, *7*, 3189.
- [118] Z. Chai, L. Ma, Y. Wang, X. Ren, *J. Biomater. Sci., Polym. Ed.* **2016**, *27*, 599.
- [119] W. Wang, L. Liao, X. Zhang, F. Lei, Y. Zhang, G. Liu, W. Xie, *Molecules* **2018**, *23*, 2945.
- [120] C. M. Hu, L. Zhang, *Biochem. Pharmacol.* **2012**, *83*, 1104.
- [121] Y. H. Zhang, Y. M. Zhang, Q. H. Zhao, Y. Liu, *Sci. Rep.* **2016**, *6*, 22654.
- [122] a) B. A. Deore, M. S. Freund, *Macromolecules* **2009**, *42*, 164; b) M. Sanjoh, D. Iizuka, A. Matsumoto, Y. Miyahara, *Org. Lett.* **2015**, *17*, 588.
- [123] a) Y. Zhang, M. Wu, W. Dai, Y. Li, X. Wang, D. Tan, Z. Yang, S. Liu, L. Xue, Y. Lei, *Nanoscale* **2019**, *11*, 6471; b) Y. Zhang, M. Wu, W. Dai, M. Chen, Z. Guo, X. Wang, D. Tan, K. Shi, L. Xue, S. Liu, Y. Lei, *J. Nanobiotechnol.* **2019**, *17*, 74.
- [124] a) Y. Lei, L. Tang, Y. Xie, Y. Xianyu, L. Zhang, P. Wang, Y. Hamada, K. Jiang, W. Zheng, X. Jiang, *Nat. Commun.* **2017**, *8*, 15130; b) Y. Xie, Y. Xianyu, N. Wang, Z. Yan, Y. Liu, K. Zhu, N. S. Hatzakis, X. Jiang, *Adv. Funct. Mater.* **2018**, *28*, 1702026; c) Y. Xie, Y. Liu, J. Yang, Y. Liu, F. Hu, K. Zhu, X. Jiang, *Angew. Chem., Int. Ed.* **2018**, *57*, 3958.
- [125] Y. Zhang, M. Wu, D. Tan, Q. Liu, R. Xia, M. Chen, Y. Liu, L. Xue, Y. Lei, *J. Mater. Chem. B* **2021**, *9*, 648.
- [126] J. Wang, J. Yu, Y. Zhang, X. Zhang, A. R. Kahkoska, G. Chen, Z. Wang, W. Sun, L. Cai, Z. Chen, C. Qian, Q. Shen, A. Khademhosseini, J. B. Buse, Z. Gu, *Sci. Adv.* **2019**, *5*, eaaw4357.
- [127] J. Wang, Z. Wang, G. Chen, Y. Wang, T. Ci, H. Li, X. Liu, D. Zhou, A. R. Kahkoska, Z. Zhou, H. Meng, J. B. Buse, Z. Gu, *ACS Nano* **2021**, *15*, 4294.
- [128] X. Wei, X. Duan, Y. Zhang, Z. Ma, C. Li, X. Zhang, *ACS Appl. Bio Mater.* **2020**, *3*, 2132.
- [129] H. Li, J. He, M. Zhang, J. Liu, P. Ni, *ACS Biomater. Sci. Eng.* **2020**, *6*, 1553.
- [130] a) Y. Cao, J. He, J. Liu, M. Zhang, P. Ni, *ACS Appl. Mater. Interfaces* **2018**, *10*, 7811; b) J. Liu, J. He, M. Zhang, G. Xu, P. Ni, *J. Mater. Chem. B* **2018**, *6*, 3262; c) G. Ma, J. Liu, J. He, M. Zhang, P. Ni, *ACS Biomater. Sci. Eng.* **2018**, *4*, 2443.
- [131] Z. Zou, D. He, L. Cai, X. He, K. Wang, X. Yang, L. Li, S. Li, X. Su, *ACS Appl. Mater. Interfaces* **2016**, *8*, 8358.
- [132] L. Hou, Y. Zheng, Y. Wang, Y. Hu, J. Shi, Q. Liu, H. Zhang, Z. Zhang, *ACS Appl. Mater. Interfaces* **2018**, *10*, 21927.
- [133] a) E. C. Cho, J.-W. Kim, A. Fernández-Nieves, D. A. Weitz, *Nano Lett.* **2008**, *8*, 168; b) M. D. Baumann, C. E. Kang, J. C. Stanwick, Y. Wang, H. Kim, Y. Lapitsky, M. S. Shoichet, *J. Controlled Release* **2009**, *138*, 205; c) L. W. Xia, R. Xie, X. J. Ju, W. Wang, Q. Chen, L. Y. Chu, *Nat. Commun.* **2013**, *4*, 2226; d) A. K. Gaharwar, N. A. Peppas, A. Khademhosseini, *Biotechnol. Appl. Biochem.* **2014**, *111*, 441; e) F. Zhao, D. Yao, R. Guo, L. Deng, A. Dong, J. Zhang, *Nanomaterials* **2015**, *5*, 2054; f) E. A. Appel, M. W. Tibbitt, M. J. Webber, B. A. Mat-tix, O. Veisoh, R. Langer, *Nat. Commun.* **2015**, *6*, 6295; g) Y. Zheng, Y. Cheng, J. Chen, J. Ding, M. Li, C. Li, J. C. Wang, X. Chen, *ACS Appl. Mater. Interfaces* **2017**, *9*, 3487.
- [134] L. Li, G. Jiang, W. Yu, D. Liu, H. Chen, Y. Liu, Q. Huang, Z. Tong, J. Yao, X. Kong, *Mater. Sci. Eng., C* **2016**, *69*, 37.
- [135] F. Zhao, D. Wu, D. Yao, R. Guo, W. Wang, A. Dong, D. Kong, J. Zhang, *Acta Biomater.* **2017**, *64*, 334.
- [136] J. Lee, Y. J. Oh, S. K. Lee, K. Y. Lee, *J. Controlled Release* **2010**, *146*, 61.
- [137] H. Wang, J. Yi, Y. Yu, S. Zhou, *Nanoscale* **2017**, *9*, 509.
- [138] N. Wen, S. Lu, X. Xu, P. Ning, Z. Wang, Z. Zhang, C. Gao, Y. Liu, M. Liu, *Mater. Sci. Eng., C* **2019**, *100*, 94.
- [139] Y. Weng, J. Yao, S. Sparks, K. Y. Wang, *Int. J. Mol. Sci.* **2017**, *18*, 523.
- [140] Y. Kurosawa, S. Nirengi, T. Homma, K. Esaki, M. Ohta, J. F. Clark, T. Hamaoka, *Sci. Rep.* **2015**, *5*, 11601.
- [141] J. Lv, G. Wu, Y. Liu, C. Li, F. Huang, Y. Zhang, J. Liu, Y. An, R. Ma, L. Shi, *Sci. China Chem.* **2019**, *62*, 637.
- [142] A. Blanzas, S. P. Armes, A. J. Ryan, *Makromol. Chem. Rapid Commun.* **2009**, *30*, 267.
- [143] E. S. Jeong, C. Park, K. T. Kim, *Polym. Chem.* **2015**, *6*, 4080.
- [144] G. Jiang, T. Jiang, H. Chen, L. Li, Y. Liu, H. Zhou, Y. Feng, J. Zhou, *Colloid Polym. Sci.* **2015**, *293*, 209.
- [145] X. Du, G. Jiang, L. Li, Y. Liu, H. Chen, Q. Huang, *Colloid Polym. Sci.* **2015**, *293*, 2129.
- [146] X. Du, G. Jiang, L. Li, W. Yang, H. Chen, Y. Liu, Q. Huang, *J. Appl. Polym. Sci.* **2016**, *133*, 43026.
- [147] a) M. G. Finn, H. C. Kolb, V. V. Fokin, K. B. Sharpless, *Pro. Chem.* **2008**, *20*, 1; b) H. C. Kolb, M. G. Finn, K. B. Sharpless, *Angew. Chem., Int. Ed.* **2001**, *40*, 2004.
- [148] W. Yuan, L. Li, H. Zou, *RSC Adv.* **2015**, *5*, 80264.
- [149] X. Zhang, L. Zhao, J. Yang, J. Yang, *RSC Adv.* **2016**, *6*, 21486.
- [150] Y. Li, Y. Zhang, J. Yang, J. Yang, *RSC Adv.* **2017**, *7*, 14088.
- [151] L. Yang, J. Lv, Y. Li, J. Yang, B. Zhang, S. Li, J. Yang, *ACS Appl. Bio Mater.* **2018**, *1*, 328.
- [152] C. Li, X. Liu, Y. Zhang, J. Lv, F. Huang, G. Wu, Y. Liu, R. Ma, Y. An, L. Shi, *Nano Lett.* **2020**, *20*, 1755.
- [153] a) H. Yang, X. Li, L. Zhu, X. Wu, S. Zhang, F. Huang, X. Feng, L. Shi, *Adv. Sci.* **2019**, *6*, 1901844; b) F. Huang, J. Wang, A. Qu, L. Shen, J. Liu, J. Liu, Z. Zhang, Y. An, L. Shi, *Angew. Chem., Int. Ed.* **2014**, *53*, 8985.
- [154] H. Zou, C. Wang, W. Yuan, S. Wang, M. Li, *Polym. Chem.* **2017**, *8*, 4869.
- [155] N. Wen, C. Gao, S. Lü, X. Xu, X. Bai, C. Wu, P. Ning, S. Zhang, M. Liu, *RSC Adv.* **2017**, *7*, 45978.
- [156] N. Wen, S. Lü, C. Gao, X. Xu, X. Bai, C. Wu, P. Ning, M. Liu, *Chem. Eng. J.* **2018**, *335*, 52.
- [157] a) J. Park, J. Nam, N. Won, H. Jin, S. Jung, S. Jung, S.-H. Cho, S. Kim, *Adv. Funct. Mater.* **2011**, *21*, 1558; b) E. Muro, A. Fragola, T. Pons, N. Lequeux, A. Ioannou, P. Skourides, B. Dubertret, *Small* **2012**, *8*, 1029.
- [158] C. Li, F. Huang, Y. Liu, J. Lv, G. Wu, Y. Liu, R. Ma, Y. An, L. Shi, *Lang-muir* **2018**, *34*, 12116.
- [159] L. Gao, T. Wang, K. Jia, X. Wu, C. Yao, W. Shao, D. Zhang, X. Y. Hu, L. Wang, *Chem. - Eur. J.* **2017**, *23*, 6605.
- [160] a) C. Li, Q. Xu, J. Li, Y. Feina, X. Jia, *Org. Biomol. Chem.* **2010**, *8*, 1568; b) C. Li, X. Shu, J. Li, S. Chen, K. Han, M. Xu, B. Hu, Y. Yu, X. Jia, *J. Org. Chem.* **2011**, *76*, 8458; c) H. Li, D. X. Chen, Y. L. Sun, Y. B. Zheng, L. L. Tan, P. S. Weiss, Y. W. Yang, *J. Am. Chem. Soc.* **2013**, *135*, 1570.
- [161] M. Zuo, W. Qian, Z. Xu, W. Shao, X. Y. Hu, D. Zhang, J. Jiang, X. Sun, L. Wang, *Small* **2018**, *14*, 1801942.
- [162] a) K. R. A. S. Sandanayake, T. D. James, S. Shinkai, *Chem. Lett.* **1995**, *24*, 503; b) S. Arimori, K. A. Frimat, T. D. James, M. L. Bell, C. S. Oh, *Chem. Commun.* **2001**, 1836.
- [163] J. Yu, Y. Zhang, J. Wang, D. Wen, A. R. Kahkoska, J. B. Buse, Z. Gu, *Nano Res.* **2019**, *12*, 1539.

- [164] M. Raghavan, L. N. Gastinel, P. J. Bjorkman, *Biochemistry* **1993**, *32*, 8654.
- [165] Z. Zeng, D. Qi, L. Yang, J. Liu, Y. Tang, H. Chen, X. Feng, *J. Controlled Release* **2019**, *315*, 206.
- [166] Z. Tong, J. Zhou, J. Zhong, Q. Tang, Z. Lei, H. Luo, P. Ma, X. Liu, *ACS Appl. Mater. Interfaces* **2018**, *10*, 20014.
- [167] D. Mandal, S. Das, *New J. Chem.* **2019**, *43*, 7855.
- [168] G. Wu, C. Li, X. Liu, J. Lv, Y. Ding, Y. Liu, Y. Liu, F. Huang, L. Shi, Y. An, R. Ma, *Colloids Surf., B* **2019**, *180*, 376.
- [169] H. Gaballa, P. Theato, *Biomacromolecules* **2019**, *20*, 871.
- [170] a) D. Shi, M. Ran, L. Zhang, H. Huang, X. Li, M. Chen, M. Akashi, *ACS Appl. Mater. Interfaces* **2016**, *8*, 13688; b) D. Shi, M. Ran, H. Huang, L. Zhang, X. Li, M. Chen, M. Akashi, *Polym. Chem.* **2016**, *7*, 6779.
- [171] J. Z. Wu, G. R. Williams, H. Y. Li, D. X. Wang, S. D. Li, L. M. Zhu, *Drug Delivery* **2017**, *24*, 1513.
- [172] S. Belbekhouche, S. Charaabi, B. Carbonnier, *Colloids Surf., B* **2019**, *177*, 416.
- [173] T. Y. Sergeeva, R. K. Mukhitova, I. R. Nizameev, M. K. Kadirov, P. D. Klypina, A. Y. Ziganshina, A. I. Kononov, *Beilstein J. Nanotechnol.* **2018**, *9*, 1594.
- [174] T. Y. Sergeeva, R. K. Mukhitova, I. R. Nizameev, M. K. Kadirov, A. S. Sapunova, A. D. Voloshina, T. A. Mukhametzyanov, A. Y. Ziganshina, I. S. Antipin, *ChemPlusChem* **2019**, *84*, 1560.
- [175] X. Xu, H. Shang, T. Zhang, P. Shu, Y. Liu, J. Xie, D. Zhang, H. Tan, J. Li, *Int. J. Pharm.* **2018**, *548*, 649.
- [176] a) D. L. Dick, T. V. S. Rao, D. Sukumaran, D. S. Lawrence, *J. Am. Chem. Soc.* **1992**, *114*, 2664; b) H. Gao, Y. N. Wang, Y. G. Fan, J. B. Ma, *J. Controlled Release* **2005**, *107*, 158; c) S. Sajeesh, C. P. Sharma, *Int. J. Pharm.* **2006**, *325*, 147.
- [177] a) M. E. Davis, M. E. Brewster, *Nat. Rev. Drug Discovery* **2004**, *3*, 1023; b) N. Morin-Crini, S. Fourmentin, É. Fenyvesi, E. Lichtfouse, G. Torri, M. Fourmentin, G. Crini, *Environ. Chem. Lett.* **2021**, *19*, 2581.
- [178] a) T. Higashi, F. Hirayama, H. Arima, K. Uekama, *Bioorg. Med. Chem. Lett.* **2007**, *17*, 1871; b) T. Higashi, F. Hirayama, S. Misumi, H. Arima, K. Uekama, *Biomaterials* **2008**, *29*, 3866; c) T. Higashi, F. Hirayama, S. Misumi, K. Motoyama, H. Arima, K. Uekama, *Chem. Pharm. Bull.* **2009**, *57*, 541.
- [179] a) T. Seki, K. Abe, K. Nakamura, Y. Egawa, R. Miki, K. Juni, T. Seki, *J. Incl. Phenom. Macrocycl. Chem.* **2015**, *82*, 417; b) T. Seki, K. Abe, Y. Egawa, R. Miki, K. Juni, T. Seki, *Mol. Pharmaceutics* **2016**, *13*, 3807.
- [180] Y. Shen, Z. Xu, L. Li, W. Yuan, M. Luo, X. Xie, *New J. Chem.* **2019**, *43*, 7822.
- [181] J. Liang, Y. Ma, S. Sims, L. Wu, *J. Mater. Chem. B* **2015**, *3*, 1281.
- [182] A. Zhang, H. Bai, L. Li, *Chem. Rev.* **2015**, *115*, 9801.
- [183] C. Takei, Y. Ohno, T. Seki, R. Miki, T. Seki, Y. Egawa, *Chem. Pharm. Bull.* **2018**, *66*, 368.
- [184] D. H.-C. Chou, M. J. Webber, B. C. Tang, A. B. Lin, L. S. Thapa, D. Deng, J. V. Truong, A. B. Cortinas, R. Langer, D. G. Anderson, *Proc. Natl. Acad. Sci. USA* **2015**, *112*, 2401.
- [185] F. D'Hooge, D. Rogalle, M. J. Thatcher, S. P. Perera, J. M. H. van den Elsen, A. T. A. Jenkins, T. D. James, J. S. Fossey, *Polymer* **2008**, *49*, 3362.
- [186] a) D. K. Scrafton, J. E. Taylor, M. F. Mahon, J. S. Fossey, T. D. James, *J. Org. Chem.* **2008**, *73*, 2871; b) W. Zhai, B. M. Chapin, A. Yoshizawa, H.-C. Wang, S. A. Hodge, T. D. James, E. V. Anslyn, J. S. Fossey, *Org. Chem. Front.* **2016**, *3*, 918; c) X. Wu, X.-X. Chen, Y.-B. Jiang, *Analyst* **2017**, *142*, 1403; d) G. Fang, H. Wang, Z. Bian, J. Sun, A. Liu, H. Fang, B. Liu, Q. Yao, Z. Wu, *RSC Adv.* **2018**, *8*, 29400; e) J. Ramos-Soriano, S. Benitez-Benitez, A. Davis, M. C. Galan, *Angew. Chem., Int. Ed.* **2021**, *60*, 16880.
- [187] J. Gromada, P. Chabosseau, G. A. Rutter, *Nat. Rev. Endocrinol.* **2018**, *14*, 694.
- [188] a) A. Haidar, L. Legault, M. Dallaire, A. Alkhateeb, A. Coriati, V. Messier, P. Cheng, M. Millette, B. Boulet, R. Rabasa-Lhoret, *Can. Med. Assoc. J.* **2013**, *185*, 297; b) Z. Wang, J. Wang, H. Li, J. Yu, G. Chen, A. R. Kahkoska, V. Wu, Y. Zeng, D. Wen, J. R. Miedema, J. B. Buse, Z. Gu, *Proc. Natl. Acad. Sci. USA* **2020**, *117*, 29512.
- [189] UK Government legislation: <http://www.legislation.gov.uk/ukpga/1986/14/contents> (accessed: May 2021).
- [190] a) M. C. Catoira, J. González-Payo, L. Fusaro, M. Ramella, F. Boccafoschi, *J. Mater. Sci. Mater. Med.* **2020**, *31*, 64; b) Commission Implementing Decision (EU): [http://data.europa.eu/eli/dec\\_impl/2020/437/oj](http://data.europa.eu/eli/dec_impl/2020/437/oj) (accessed May 2021).



**Łukasz Banach** obtained Eng. and M. Eng. degrees in Chemical Technology (2011 and 2012) under supervision of Prof. D. Gryko. He gained a Ph.D. in Chemistry from Warsaw University of Technology (2016) under the supervision of Prof. W. Buchowicz. Later in 2016, he joined group of Prof. K. Grela at the University of Warsaw as a postdoctoral researcher. In 2017, he moved to the University of Birmingham, where he conducted research on glucose-responsive materials based on boronic acids with Prof. John S. Fossey. Since 2019, he has been working at the Adam Mickiewicz University in Poznań as an assistant professor.



**George T. Williams** obtained undergraduate and postgraduate degrees from the University of Bath working with Prof. A. Toby A. Jenkins and Dr Mark Sutton (Public Health England) towards his Ph.D. (2020). After postdoctoral research at the University of Kent, working with Dr Jennifer Hiscock, he moved to the University of Birmingham where he now works on the development of boronic-containing sensors and materials for biomedical applications, with Prof. John S. Fossey. His research interests are focused on sensing and drug delivery at the interface between supramolecular chemistry and medicine.



**John S. Fossey** obtained an M. Sci. degree from Cardiff University of Wales (2000) and a Ph.D. (under the supervision of Dr C. J. Richards) from Queen Mary University of London (2004). After a JSPS postdoctoral fellowship (with Prof. S. Kobayashi) at the University of Tokyo he joined the University of Bath. In 2008, he joined the University of Birmingham and became a professor of synthetic chemistry ten years later. He serves as the equality diversity and inclusion (EDI) lead for the School of Chemistry and his research interests span asymmetric synthesis and catalysis, molecular sensors, and recognition and medicinal chemistry.